

**PROCESSING AND CHARACTERIZATION  
OF INCONEL 625-SiC METAL MATRIX  
COMPOSITES BY DIRECT METAL LASER  
SINTERING**

Thesis

Submitted in partial fulfillment of the requirements for the degree of

**DOCTOR OF PHILOSOPHY**

by

**SATEESH N H**



**DEPARTMENT OF MECHANICAL ENGINEERING  
NATIONAL INSTITUTE OF TECHNOLOGY KARNATAKA,  
SURATHKAL, MANGALORE – 575025**

**October, 2015**

## DECLARATION

I hereby declare that the Research Thesis entitled “**PROCESSING AND CHARACTERIZATION OF INCONEL 625–SiC METAL MATRIX COMPOSITES BY DIRECT METAL LASER SINTERING**” which is being submitted to the **National Institute of Technology Karnataka, Surathkal** in partial fulfillment of the requirements for the award of the Degree of **Doctor of Philosophy in Mechanical Engineering** is a *bonafide report of the research work carried out by me*. The material contained in this Research Thesis has not been submitted to any other Universities or Institutes for the award of any degree.

Register Number: **100770ME10F09**

Name of the Research Scholar: **SATEESH N H**

Signature of the Research Scholar:

Department of Mechanical Engineering

Place: NITK-Surathkal

Date:

## **CERTIFICATE**

This is to certify that the Research Thesis entitled “**PROCESSING AND CHARACTERIZATION OF INCONEL 625–SiC METAL MATRIX COMPOSITES BY DIRECT METAL LASER SINTERING**” submitted by **Mr. SATEESH N H (Register Number: 100770ME10F09)** as the record of the research work carried out by him, *is accepted as the Research Thesis submission* in partial fulfillment of the requirements for the award of the Degree of **Doctor of Philosophy**.

**Prof. G C Mohan Kumar**

Research Guide

Date:

**Prof. Prasad Krishna**

Research Guide

Date:

**Prof. K V Gangadharan**

Chairman-DRPC

Date:

**DEDICATED TO**

**MY**

**BELOVED PARENTS AND TEACHERS**

## ACKNOWLEDGEMENT

Gratitude takes three forms, “A feeling from the heart, an expression in words and a giving in return”. I take this opportunity to express my heartfelt feelings to a number of people for their support and encouragement in the successful completion of this work.

At the outset, I wish to express my profound sense of gratitude and indebtedness to my guides **Prof. G. C. Mohan Kumar**, and **Prof. Prasad Krishna** for their invaluable guidance and supervision during the course of this research work. Their constant encouragement, discussions and constructive criticism are responsible for completion of this work. It was their valuable comments and suggestions which helped me to enhance the quality of work. It was their constant care and guidance which helped me to make necessary improvements.

I am thankful to Dr. K.V. Gangadharan, Professor and Head, Department of Mechanical Engineering for his wholehearted support. I would also like to thank the QIP-POLY Coordinators Prof.A.Mahesha, Applied Mechanics Department and Prof. Jagannath Nayak, Materials and Metallurgical Department, for their kind support and encouragement.

I thank the members of my Research Progress Assessment Committee: Prof.M. K. Nagaraj, Applied Mechanics Department and Prof. Vijay Desai, Mechanical Engineering Department, for their support, comments and suggestions. I also express my sincere thanks to Dr. Sathyabhama, Secretary, Department Research Progress Assessment Committee, for her kind help and constant cooperation.

I wish to express my deep sense of gratitude to Dr. C. K. Srinivasa, Head, Ultra Precision Engineering and Mr. A.R.Vinod, Scientist B, Rapid Product Development Centre, CMTI, Bangalore, for providing research facilities to carry out the experiments.

I extend my sincere thanks to Mr.Satish, of CMTI, Bangalore and Mr. Pradeep, and Mr. Ramchandra, of NITK, Surathkal, for their kind help in carrying out the experiments.

I am very much thankful to Mr. Krishnappa Naik, Product Manager, Saint Gobain Grindwell Norton Limited, Bangalore and Mr. Scott Ostholthoff, Powder Alloy Corporation, USA, for supplying the research material for my present work. I am very much grateful to Mr. Lakshmikantha and Mr. Raja Manikyam, GTTC, Bangalore for their kind help in machining of test specimens. I extend my sincere gratitude to my brothers Mr. Kumar Nijagal, USA and Dr. Swamy Nijagal, for their kind support with fruitful discussions and suggestions during my research work.

I am thankful to my fellow research scholars Mr. Saravanan Bavan, Kamal Babu, Rajashekar Lalbondre, Ragavendra, Manjunath Patel, Muralidhar Avvari, Manjaiah, Arun Kumar Shettigar, Riessom, Veeresh, Vignesh, Shivaprasad, and Parashuram, for their help and cooperation during my research work.

I am very much indebted to the Director, Department of Technical Education, Bangalore, Principal, and Staff of Mechanical Engineering Department, Karnataka Polytechnic, Mangalore, for permitting me to pursue research at NITK, Surathkal.

To my family, I am grateful to my parents for their support, and blessings. I greatly acknowledge the patience, motivation of my wife Smt.Suma and son Master Tejas throughout my research work. I thank all those people who have directly or indirectly helped me to achieve this objective.

Finally, my greatest submission to the Almighty for bestowing upon me the courage to face the complexities of life and complete this work successfully.

**Sateesh N H**

## ABSTRACT

Metal Matrix Composites (MMCs) are gaining wide spread popularity because of their superior mechanical properties such as high mechanical strength; wear resistance, excellent thermal conductivity and ability to retain strength at high temperature. Most of the work on MMCs till date is focused on development of aluminium, copper, magnesium, and titanium based MMCs. Lot of interest is shown now-a-days on aerospace and high temperature materials such as Inconel 625 superalloy which finds an application in important sectors like gas turbines, air craft engine components and electronic parts like cathode ray tube spiders, and springs. Also, excellent resistance to corrosion in purity water environment led to its use in the construction of control rods in nuclear reactors. Most of MMCs are developed by various methods like powder metallurgy, conventional casting, and very few researchers have reported about the processing of MMCs by different laser based additive manufacturing processes.

In the present thesis work, Nickel based Inconel-625 (IN625) metal matrix composites were processed using “Direct Metal Laser Sintering” (DMLS) additive manufacturing process. Silicon carbide (SiC) particles, coated with NiP and IN625 particles are premixed using hexagonal double cone blender for homogeneity of particulates. MMCs are developed in DMLS under nitrogen atmosphere using CO<sub>2</sub> laser and deposition of IN625 with addition of 1, 3, 5 weight percentage of NiP coated SiC particles was done using laser additive manufacturing process. The physical and mechanical behaviour of the MMCs were thoroughly examined. The micro-structure, density, micro-hardness, tensile properties, corrosion properties and machinability of the developed composites were studied. The distribution of SiC particles and micro-structures were characterized by using optical and scanning electron micrographs.

The results of the experiments were clearly reveal that the interface integrity between the SiC particles and the IN625 matrix, the mixed particulates flowability, the SiC ceramic particles and laser beam interaction, and the mechanical and physical

properties of the developed MMCs were improved effectively by the use of NiP coated SiC particles.

The results reveal that the NiP coated SiC particles can be used to reinforce IN625 using laser additive DMLS process. The micro-structure of IN625 matrix become more refined with the addition of more SiC particles, and the shape of the grains switched over from columnar dendrite to cellular equi-axed form. There is an increment in hardness by 33 % above the base IN625 material because of rarefaction in micro-structure with more addition of NiP coated SiC particulates. Lower density and hardness, at higher scan speed, due to increased porosity and higher density and hardness, due to high dislocation density and also because of excellent bonding between matrix and reinforcement was observed. Significant improvements in the tensile properties are observed and are due to micro-structure refinement and strengthening effect by addition of NiP coated SiC particles. With the addition of 3 weight percentage of NiP coated SiC, the UTS and YS increases by 12 % and 10 % respectively, compared to laser deposited IN625. The addition of NiP coated SiC particles into IN625 matrix beyond 3 weight percentage resulted in drastic reduction in UTS, YS and elongation because of increase in thermal cracking and due to large stress concentration around the reinforcement. This will lead to premature failure during straining of composites.

Further the corrosion studies indicate that the rate of corrosion increases with increase in laser scan speed because of increased porosity. The corrosion rate decreases with the increase in weight percentage of reinforcement because of effective laser absorption by NiP coated SiC particles. The machinability studies was carried out using Wire Electrical Discharge Machine (WEDM), and the results shows that the discharge current and weight percentage of NiP coated SiC have profound effect on machining time and surface roughness of developed composites.

**Key words:** *Metal Matrix Composites (MMCs), Additive Manufacturing (AM), Direct Metal Laser Sintering (DMLS), Inconel-625 (IN625), SiC, NiP Coating, Double Cone Blender, Wire Electrical Discharge Machine (WEDM) and Characterization.*



## CONTENTS

Title	Page No.
ACKNOWLEDGEMENT	i
ABSTRACT	iii
CONTENTS	v
LIST OF FIGURES	xi
LIST OF TABLES	xiv
LIST OF APPENDICES	x
NOTATIONS	xv
ABBREVIATIONS	xvi
<b>CHAPTER 1 INTRODUCTION</b>	<b>1</b>
1.1 COMPOSITES	1
1.1.1 History of Composites	1
1.1.2 Importance to Composites	2
1.1.3 Classification of Composites	2
1.1.4 Metal Matrix Composites (MMCs)	3
1.2 RAPID PROTOTYPING (RP)	4
1.2.1 Rapid Prototyping Technology	6
1.2.2 Additive Manufacturing	8
1.2.3 Rapid Manufacturing	9
1.3 ORGANIZATION OF THESIS	10
<b>CHAPTER 2 REVIEW OF LITERATURE</b>	<b>11</b>
2.1 COMPOSITES	11
2.1.1 Selection of Material for Composites	11
2.2 FABRICATION METHODS OF MMCs	12
2.3 SINTERING	13
2.3.1 Sintering Mechanism	13
2.3.2 Sintering Stages	15
2.4 CHALLENGES IN PROCESSING OF MMCs	16
2.5 RAPID PROTOTYPING	17

2.5.1	Principle of Layer Manufacturing	17
2.5.2	Classification of Layer Manufacturing	19
2.6	SINTERING MECHANISM USING LASER	20
2.6.1	Solid State Sintering	20
2.6.2	Liquid Phase Sintering	20
2.6.3	Partial Melting	21
2.6.4	Full Melting	21
2.7	DIRECT METAL LASER SINTERING (DMLS)	21
2.7.1	Schematic Representation of DMLS Layer Manufacturing Machine	22
2.7.2	Parts Building Steps in DMLS Process	23
2.7.3	DMLS Process Parameters	26
2.7.4	Effect of DMLS Process Parameters	27
	2.7.4.1 Power of Laser and Scan Speed of Laser	27
	2.7.4.2 Powder Size and Morphology	27
	2.7.4.3 Build Direction	28
	2.7.4.4 Sintering Atmosphere	28
	2.7.4.5 Layer Thickness	29
	2.7.4.6 Hatch width and Hatch Spacing	29
2.8	MMCs BY DIRECT METAL LASER SINTERING PROCESS	30
2.8.1	Nickel Based MMCs	32
2.9	COATING ON REINFORCEMENTS	34
2.10	BLENDING OF MATRIX AND REINFORCEMENT PARTICLES	36
2.11	PHYSICAL PROPERTIES OF MMCs	37
2.11.1	Density and Surface Roughness	37
2.12	MECHANICAL PROPERTIES OF MMCs	38
2.12.1	Hardness and Strength	38
2.13	CORROSION BEHAVIOUR OF MMCs	40
2.14	MACHINABILITY STUDIES ON PROCESSED MMCs	42

<b>CHAPTER 3</b>	<b>SCOPE OF THE WORK</b>	46
<b>CHAPTER 4</b>	<b>EXPERIMENTATION</b>	49
4.1	INTRODUCTION	49
4.2	MATERIAL SELECTION	49
4.2.1	Matrix Material and Its Properties	49
4.2.2	Reinforcement Material and Its Properties	50
4.3	CHARACTERIZATION OF MATRIX AND REINFORCEMENT MATERIAL	50
4.3.1	Particle Size Analysis	50
4.3.2	Morphology	51
4.4	NiP COATING ON SiC PARTICLES	51
4.4.1	Experimental Procedure	51
4.4.2	Evaluation of Coating Deposit	53
4.4.2.1	Coating Deposit Calculations	53
4.5	FABRICATION OF IN625 TEST SPECIMENS BY DMLS PROCESS	53
4.5.1	Modelling of Test Specimens	53
4.5.2	DMLS Machine and Machine Setup	54
4.5.3	Optimization of Laser Sintering Parameters	54
4.5.4	Preparation of Test Specimens	54
4.5.4.1	Separation of Test Specimens from Base Plate	55
4.6	CHARACTERIZATION OF IN625 TEST SPECIMENS FOR DENSITY, TENSILE STRENGTH, AND MICRO-STRUCTURE	56
4.6.1	Density Studies	56
4.6.2	Tensile Studies	56
4.6.3	Micro-structure Studies	56
4.7	FABRICATION OF IN625-SiC (NiP-coated) COMPOSITES BY DMLS PROCESS	57
4.7.1	Studies on Blending of IN625 and SiC (NiP-coated) Particulates and Their Characterisation	57

4.7.2	Preparation of Test Specimens	58
4.8	CHARACTERIZATION OF IN625 AND IN625-SiC (NiP-coated) TEST SPECIMENS FOR MICRO-STRUCTURE, PHYSICAL PROPERTIES, MECHANICAL PROPERTIES, CORROSION BEHAVIOUR AND MACHINABILITY STUDIES OF PROCESSED MMCs USING WEDM	58
4.8.1	Micro-structure Studies	59
4.8.1.1	Optical Micrograph and Scanning Electron Micrograph Studies	59
4.8.2	Studies on Physical Properties	59
4.8.2.1	Density Studies	59
4.8.2.2	Surface Roughness Studies	60
4.8.3	Studies on Mechanical Properties	60
4.8.3.1	Micro-hardness Studies	60
4.8.3.2	Tensile Studies	60
4.8.4	Studies on Corrosion Behaviour of MMCs	61
4.8.5	Machinability Studies of Processed MMCs Using WEDM	63
<b>CHAPTER 5</b>	<b>RESULTS AND DISCUSSIONS</b>	64
5.1	PARTICLE SIZE AND MORPHOLOGY	64
5.1.1	IN625 and SiC Particles	64
5.2	STUDIES ON ELECTROLESS COATING	67
5.2.1	Nickel Phosphide (Ni-P) Coating on SiC	67
5.3	OPTIMISATION OF LASER SINTERING (PROCESSING) PARAMETERS	73
5.3.1	Density, Tensile Strength and Micro-structure Studies	74
5.4	STUDIES ON BLENDING OF IN625 AND SiC (NiP-Coated)	76
5.5	TEST SPECIMENS BY DMLS PROCESS	78
5.6	CHARACTERIZATION OF IN625-SiC(NiP-coated) COMPOSITE SPECIMENS FOR PHYSICAL	79

	PROPERTIES	
5.6.1	Density	79
5.6.2	Surface Roughness	81
	CHARACTERIZATION OF IN625-SiC(NiP-coated)	
5.7	COMPOSITE SPECIMENS FOR MECHANICAL PROPERTIES	84
5.7.1	Micro-hardness	84
5.7.2	Tensile Properties	85
5.8	MICRO-STRUCTURE ANALYSIS	87
5.9	CORROSION STUDIES	90
5.9.1	Effect of Laser Scan Speed	90
5.9.2	Effect of Reinforcement	91
5.9.3	Effect of Test Duration	92
5.10	MACHINABILITY STUDIES	92
5.10.1	Machining Time	93
	5.10.1.1 Effect of Discharge Current	93
	5.10.1.1 Effect of Scan Speed of Laser	93
	5.10.1.1 Effect of SiC (NiP-coated) Reinforcement	95
5.10.2	Surface Roughness (SR)	97
	5.10.2.1 Effect of Discharge Current	97
	5.10.2.2 Effect of Scan Speed of Laser	98
	5.10.2.3 Effect of SiC (NiP-coated) Reinforcement	99
<b>CHAPTER 6</b>	<b>CONCLUSIONS AND FUTURE SCOPE OF WORK</b>	102
6.1	PREAMBLE	102
6.2	CONCLUSIONS	102
6.2.1	Reinforcement Coating and Blending	102
6.2.2	Micro-structure	103
6.2.3	Physical Properties	103
6.2.4	Mechanical Properties	104
6.2.5	Corrosion Resistance	105
6.2.6	Machinability	105

6.3	SCOPE FOR FUTURE WORK	106
	<b>APPENDICES</b>	107
APPENDIX A	Properties and Chemical Composition of IN625 and SiC Laser-based Particle Size Counter, Scanning Electron	107
APPENDIX B	Microscope, Optical Microscope, X-ray Diffractometer and Their Salient Features	108
APPENDIX C	Bath Composition of Electroless Nickel Phosphide Encapsulation and Equipments for Electroless Coating	110
APPENDIX D	2D and 3D Drawings of Test Specimens	111
APPENDIX E	EOSINT M250 DMLS Machine and Its Salient Features	112
APPENDIX F	Preparation and Separation of Test Specimens from Base Plate using WEDM	114
APPENDIX G	Density Measurement using Archimedes Principle	115
APPENDIX H	INSTRON-5569 Tensile Testing Machine Loaded with Specimen and Its Salient Features	116
APPENDIX I	Double Cone Blender with Schematic Diagram of Conical Container	117
APPENDIX J	Machining and Surface Preparation of Test Specimens for Micro-structure Studies	119
APPENDIX K	Confocal Microscope and Micro-hardness Tester with Salient Features	121
APPENDIX L	Schaublin CNC Lathe for Machining of Tensile Test Specimens and Its Salient Features	122
APPENDIX M	Salt Spray Apparatus and Its Salient Features for Corrosion Testing	123
APPENDIX N	Wire Electrical Discharge Machine (WEDM) used for Machinability Studies and Its Salient Features	124
	<b>REFERENCES</b>	125
	<b>PUBLICATIONS</b>	140
	<b>ACADEMIC CURRICULUM VITAE</b>	141

## LIST OF FIGURES

<b>Figure No.</b>	<b>Title</b>	<b>Page No.</b>
1.1	Classification of Composites	3
1.2	Transformation of RP to RM	8
2.1	Surface Area Reduction during Sintering Process	14
2.2	Formation of Neck between Spherical Particles	14
2.3	Different Stages during Sintering Mechanism	15
2.4	Structural and Binder Material before and after Sintering Process	15
2.5	Movement of Laser Beam during Sintering Process	16
2.6	Principle of Layer Manufacturing Process	18
2.7	Classification of Layer Manufacturing Processes	19
2.8	Schematic Representation of DMLS Machine	22
2.9	DMLS Process Steps	24
2.10	Part Fabrication Order in DMLS Process	25
2.11	Schematic Representation of Scan Path of Laser in DMLS Process	26
2.12	Schematic Representation of Scan Path of Laser in a Layer	27
2.13	Relationship between Process Parameters and Resulting Properties	29
3.1	Schematic Representation of the Experimental Procedure and Studies Conducted under this Investigation	48
5.1	Particle Size Distribution of IN625 Particles	64
5.2	SEM Showing Shape and Size of IN625 Particles	65
5.3	Energy Dispersive Spectroscopy (EDS) of IN625 Particles	65
5.4	SEM Showing Shape and Size of IN625 Particles	66
5.5	X-ray Diffraction (XRD) Pattern of SiC Particles	66
5.6	EDS of SiC Particles	67
5.7	SEM of Palladium Coated SiC Particles	68

5.8	EDS of Palladium Coated SiC Particles	68
5.9	SEM of NiP Coated SiC Particles	69
5.10	EDS of NiP Coated SiC Particles	70
5.11	XRD Pattern of Coated SiC before Heat-treatment	71
5.12	XRD Pattern of NiP Coated SiC after Heat-treatment	71
5.13	Coating Time Effect on NiP Deposition	72
5.14	Laser Sintered IN625 Test Specimens	73
5.15	Effect of Laser Scan Speed on Density and Tensile Strength of IN625 Processed at Hatch Spacing of 0.3 mm and 0.4 mm	74
5.16	Optical Micrographs of Laser Processed IN625 at 0.3 and 0.4 mm Hatch Spacing	75
5.17	SEM of IN625-1 Weight Percentage SiC (Ni-P-coated) Particulate Mix	77
5.18	EDS of IN625-1 Weight Percentage SiC (Ni-P-coated) Particulate Mix	77
5.19	Test Specimens Produced by DMLS Process	78
5.20	Effect of Laser Scan Speed and Weight Percentage of Reinforcement on Density	80
5.21	Effect of Laser Scan Speed and Weight Percentage of Reinforcement on SR	81
5.22	Confocal Macrographs of IN625 & IN625-SiC (NiP-Coated) Composites	83
5.23	Effect of Laser Scan Speed and Weight Percentage of Reinforcement on Micro-hardness	84
5.24	Laser Processed IN625 Composite Specimens at 0.3 mm Hatch Spacing	85
5.25	Effect of Weight Percentage of Reinforcement on UTS, YS and % EL	86
5.26	Fractured Surfaces for IN625 and IN625-5 Weight Percentage SiC (NiP-coated)	87
5.27	Optical Micrographs of IN625 and IN625-5 Weight Percentage SiC (NiP-coated) at a Laser Scan Speeds of 2.5 mm/s and 10	88



	mm/s Respectively	
5.28	Scanning Electron Micrographs of IN625 and IN625-SiC (NiP-coated) Composites	89
5.29	Effect of Laser Scan Speed on Corrosion Rate for IN625 and IN625-3 Weight Percentage SiC (NiP-coated) Composites	90
5.30	Effect of SiC (NiP-coated) on Corrosion Rate for 96 Hours and 120 Hours Duration	91
5.31	Effect of Test Duration on Corrosion Rate for IN625 and IN625-SiC (NiP-coated) Composites for a Laser Scan Speed of 2.5 mm/s and 10 mm/s	92
5.32	Effect of Discharge Current on Machining Time for IN625 and IN625-SiC (NiP-coated) Composites	93
5.33	Effect of Laser Scan Speed on Machining Time for IN625 and IN625-SiC (NiP-coated) Composites	94
5.34	Effect of Weight Percentage of SiC (NiP-coated) Reinforcement on Machining Time for IN625 and IN625-SiC (NiP-coated) Composites	95
5.35	Optical Micrograph of WEDM Debris Showing Un-melt SiC particles and Solidified IN625	96
5.36	Interaction of Brass Wire with IN625-1 and 5 Weight Percentage SiC (NiP-coated) Composites	97
5.37	Effect of Discharge Current on SR for IN625 and IN625-SiC (NiP-coated) Composites	98
5.38	Effect of Laser Scan Speed on SR for IN625 and IN625-SiC (NiP-coated) Composites	99
5.39	Effect of Weight Percentage of SiC (NiP-coated) on SR of IN625 and IN625-SiC (NiP-coated) Composites	100
5.40	Optical Micrographs of Parts Sintered at a Laser Scan Speed of 2.5 mm/s	100
5.41	Scanning Electron Micrograph of WEDM IN625-SiC (NiP-coated) Composites at a Discharge Current of 20 A.	101

## LIST OF TABLES

<b>Table No.</b>	<b>Title</b>	<b>Page No.</b>
1.1	Events For RP Systems	7
2.1	Research Work in Development of MMCs by Laser Sintering Process	30
4.1	Process Parameters used for Laser Sintering of IN625	55
4.2	Blending Time for Different Weight Percentage of SiC (NiP-coated) Particles	57
4.3	Process Parameters used for Laser Sintering of IN625-SiC (NiP-coated) Composites	58

## NOTATIONS

$\mu\text{m}$	Micro-meter
$\rho$	Density
mg	milligram
g	gram
mm	millimeter
s	second
t	Time
d	Diameter
$\lambda$	Thermal Conductivity
min	Minute
$R_a$	Surface Roughness
W	Watts
$\text{J}/\text{mm}^2$	Energy Density

## ABBREVIATIONS

MMCs	Metal Matrix Composites
DMLS	Direct Metal Laser Sintering
RP	Rapid Prototyping
CAD	Computer Aided Design
CAM	Computer Aided Manufacturing
CNC	Computer Numeric Control
2D	Two Dimensional
3D	Three Dimensional
AM	Additive Manufacturing
RM	Rapid Manufacturing
PSW	Process Software
STL	Stereolithography
SLS	Selective Laser Sintering
IN625	Inconel 625
SiC (NiP-Coated)	Silicon Carbide (Nickel Phosphide Coated)
OM	Optical Microscopy
SEM	Scanning Electron Microscopy
EDS	Energy Dispersive Spectroscopy
XRD	X-Ray Diffraction
Wt. %	Weight Percentage
DCB	Double Cone Blender
SR	Surface Roughness
HV	Vickers Micro Hardness
UTS	Ultimate Tensile Strength
YS	Yield Strength
% EL	Percentage Elongation
CTE	Co-efficient of Thermal Expansion
WEDM	Wire Electrical Discharge Machine
ASTM	American Society for Testing of Materials

# CHAPTER 1

## INTRODUCTION

### 1.1 COMPOSITES

#### 1.1.1 History of Composites

The growth of engineering through the centuries was dependant on the finding and availability of new structural materials. At one time, wood was the most widely used engineering material because of a number of excellent properties. Human being for want of different materials continues to search materials that are tough, strong, and light. Historically it has been observed that composite materials have an integrated merit with high accomplishment in contrast with each discrete material. For more than 3000 years, mankind has been putting fibers into a binder or matrix body. During olden days people used plant fibers to increase the strength of bricks and pottery. Some of the swords were fabricated by putting several different steels to-gether in laminated layers. Superior structural members now-a-days are the results of strength of steel reinforcing bars and the rigidity of the concrete matrix. The demands made on modern materials are so harsh that individual material no longer function or have the desired properties, so it is customary to add different materials into a composite.

Higher efficiency, reduction in cost and prospective savings in weight of advanced composites lead to the development of matrices, reinforcement technology and composites fabrication. From the late 1960 onwards, the fields of transportation, construction, automobile and aerospace were in need of strong, stiff and lighter materials. Composite materials are the answer to such unrivalled demand for materials in different sectors. Composite materials have high strength to weight ratio compared to traditional engineering materials like metals. The in-depth studies about characteristics and structural properties of materials resulted in development of composite materials with better physical and mechanical properties. The high performance polymer matrix composites, ceramic matrix composites and metal matrix composites were also the part of the newly identified materials (Dhingra, 1986, Upadhya, 1992, and Clyne, 2000). The

diversified application of composites had led to development of more than 200 composite materials out of 1600 engineering materials available in the present market.

### **1.1.2 Importance to Composites**

The plastics, ceramics and fewer composites were the dominant materials used for last 30 years from everyday used product to high end applications. The present market is occupied by huge number of composite materials with wider applications in different fields of engineering. The property of light weight with shock and vibration absorption has made composite materials a perfect candidate for seismic resistant structures. Composite materials can be tailored for any distinct applications in engineering. The designer can vary the values of stiffness and thermal properties of composite materials.

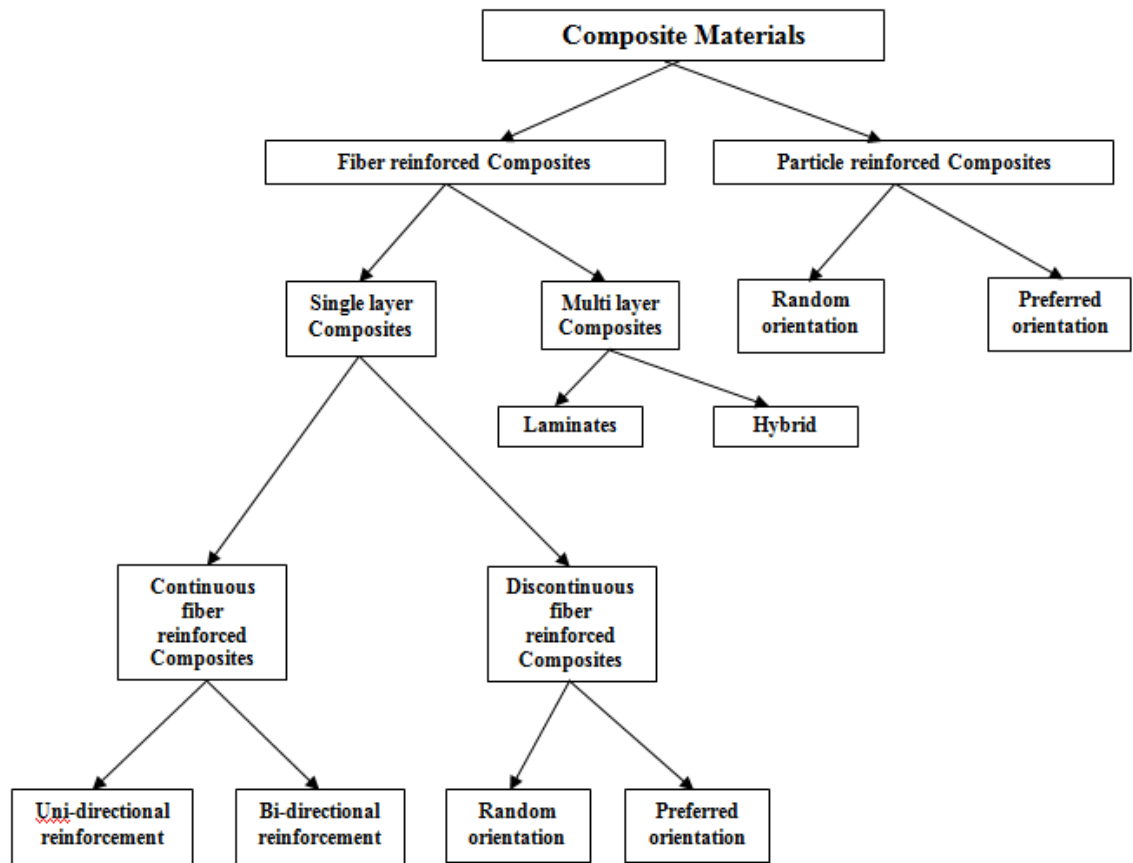
Even though the use of composites is the only choice in many cases but the best possible results can be obtained by using composites with traditional materials depending on the factors such as items requirement, complex nature of the product and savings in assembly costs.

### **1.1.3 Classification of Composites**

The classification of composite materials can be done in many ways (Agarwal, and Broutman, 1980). The geometry of the reinforcement which is accountable for better mechanical properties and high performance of the composites is taken as the basis for classification of composites. A symbolic classification of composites presented in the block diagram is shown in Figure 1.1.

The two main divisions of composites are particulate composites and fibrous composites.

In particulate composites, the particulate may be in different shape such as spherical, tetragonal, cubic, regular or irregular. Particulate reinforcement even though not able to improve the fracture resistance but can magnify the stiffness to some extent. To improve the machinability, increase the surface hardness, reduce the shrinkage, modify thermal and electrical conductivities, reduce friction, and improve the performance at higher temperatures particulate reinforcements are used in composite materials.



**Figure 1.1 Classification of Composites** (Agarwal, and Broutman, 1980).

In fibrous composites, the length is having higher value compared to cross sectional dimensions in case of fibrous composites. The property of the composite in this case depends on the dimensions of the reinforcement. The fracture resistance is good in fibers since they discourage the crack growth normal to the reinforcement. The smaller cross sectional of fibers made them unusable for direct engineering applications. So they are reinforced in matrix materials to form fibrous composites.

#### **1.1.4 Metal Matrix Composites (MMCs)**

Metal matrix composite consists of at least two components, one is the metal matrix and the other is reinforcement. The matrix is metal in almost all cases, but a pure metal is hardly used as the matrix. The matrix in general is an alloy. The reinforcement may be a

different metal or another material, such as a ceramic or organic compound. The matrix and the reinforcement are mixed together to obtain the composite.

The high stiffness and superior strength with better wear resistance when compared to wrought alloys resulted in the processing of MMCs at higher volumes in the recent years. The ductile matrix allows for reduction of cracks and stress concentrations by plastic deformation and makes the material to acquire improved fracture toughness.

Modern composites allow the introduction of any selected volume, shape and size of reinforcement into the matrix. Modern composites are considered as the non-equilibrium mixtures of metals and ceramics where there are no thermodynamic limitations on the respective volume percentages, size and shape of ceramic phases.

MMCs have the following advantages:

- Better wear resistance
- Lower coefficients of thermal expansion
- Higher stiffness-to-weight ratios
- Higher strength-to-weight ratios
- Better elevated temperature properties
  - Higher strength
  - Lower creep rate

## **1.2 RAPID PROTOTYPING**

Global competition, customer-driven product customization, fast product obsolescence and demand for cost saving are forcing industries to look for new technologies which can reduce the cost and product development cycle. Rapid Prototyping has emerged as a key empowered technology for fabrication of intricate and complex parts in lesser time, thereby reducing product design and development cycle.

Rapid Prototyping processes may be divided broadly into two groups:

- a) Subtractive.
- b) Additive.



The subtractive process involves removing of material from a solid mass to get the required shape. The additive process involves building of physical models, layer-by-layer, directly from computer aided design data base. The additive process is also called as layer manufacturing. This layer manufacturing is able to build parts from different materials such as polymers, metals and ceramics to full density. The concept of layer manufacturing was evolved during 1890 by Blather for making moulds for topographical relief maps (Pham, and Dimov, 2001).

The first commercially available RP system was introduced in the late 1980's. This new technique of producing customised 3D part in one step has evolved rapidly towards the realization of rapid manufacturing processes. There are numerous RP systems; Stereolithography (SLA), Selective laser sintering (SLS), Fused deposition modeling (FDM) (Anna Belini & Selcuk Guceri, 2003), 3D printing, Laminated object manufacturing (LOM) (Paul, and Voorakarnam, 2001), Laser Engineered Net Shaping (LENS). Early findings have shown that, RP systems significantly reduce the lead time by 54% in producing appearance models. The success of the RP process marked a revolution in product development and manufacturing. RP systems as their name advocates are used for production of prototype models. It is progressing quickly from prototyping towards the manufacturing of end user functional products.

Selective laser sintering technique is the leading Rapid Manufacturing (RM) system due to its capability to sinter a huge variety of materials. The interaction between the laser beam and the powder particles through an intricate thermo-mechanical process fusing the selected powders at the powder bed layer by layer until a 2D solid pattern is created. The sintered layer is lowered to a certain height and then a thin layer of new powder is deposited. Studies show that an extensive use of this technique is successful production of fully dense metal parts in one step. The capability of producing metal parts up to 99.8% density with fine microstructure and excellent mechanical properties are the main reason behind it. With full part densities achieved, the fabricated parts will have good mechanical properties. Therefore, a greater detail in understanding of this process is required to control the specific process parameters in order to get a desired microstructure

and good mechanical properties. This includes the effects of laser energy, spot size of laser beam, layer thickness, scan spacing, and scan speed (Williams, and Deckard, 1998).

Industries still need to be convinced that RM machines can reduce their manufacturing cost. Ruffo, et al., (2007), studied the manufacture of mixed components simultaneously using selective laser sintering to highlight the potential of cost reduction. A comparative study was also done. Attempts have also been made to integrate RM with other techniques in order to reduce manufacturing cost and time (Kim, and Oh, 2008). Fouchal, and Dickens, (2007), demonstrated the feasibility of RM system for high volumes production. Besides time and cost, the accuracy and repeatability of RM systems have also been heavily investigated (Kim, and Oh, 2008). The parts with required micro-structure and better mechanical properties are obtained with better knowledge of laser and powder interaction. An alternative way of fabrication of parts using pre-alloyed particles is shown by direct laser sintering machine through laser sintering process. The parts produced by this process have better mechanical properties such as strength and hardness in comparison to forged parts but with moderate elongation (Shellabear, and Nyrhila, 2007).

The advantages of rapid prototyping technology are:

- Parts with complex geometry can be produced from CAD data without the aid of jig, fixture or tooling.
- Drastic reduction in product design and development time.
- Errors in product design can be identified and corrected in early stage of design.
- Tooling for plastic injection moulding, die casting, metal forming and rubber-moulding processes can be fabricated in a short time.
- RP parts can be used for form, fit and functional tests.

### **1.2.1 Rapid Prototyping Technology**

Rapid Prototyping which is also known as additive freeform fabrication was introduced in the late 80's with the SLA machine. Since then, there are tremendously various machines using similar concepts which have been deposited and patented (Levy, et al.,

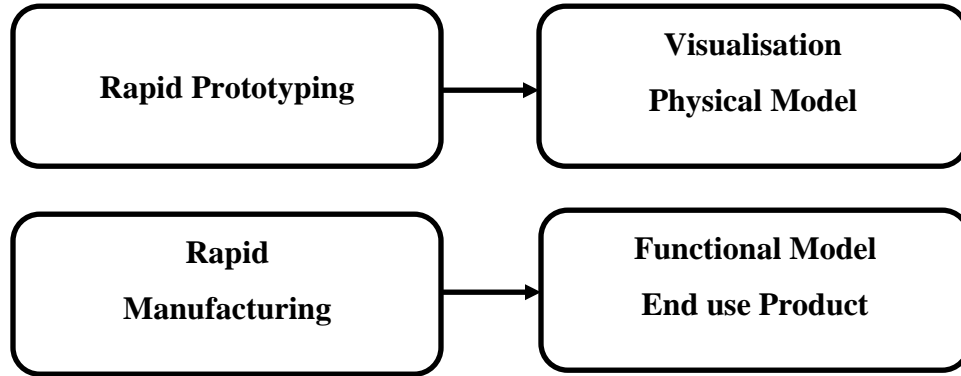
2003). Layer manufacturing technologies at this time are often known as rapid prototyping technologies due to their main objective of having a design prototype. Indeed, RP involves designing physical model using digitally driven, additive processes. RP systems manufacture models and prototype parts at a faster rate from three dimensional CAD data or data from 3D digitizing systems. Through the additive process, RP technology joins particles in liquid form to objects in physical form, layer by layer. RP machines are able to process plastics, ceramics, metals and different composites from horizontal thin cross sections of a computer model (Kruth, et al., 2007). The different RP machines developed over the years are given in Table 1.1.

**Table 1.1 Events for RP Systems** (Levy, et al., 2003)

<b>Name</b>	<b>Acronyms</b>	<b>Years of Development</b>
Stereolithography	SLA	1986-1988
Solid Ground Curing	SGC	1986-1988
Laminated Object Manufacturing	LOM	1985-1991
Fused Deposition Modeling	FDM	1988-1992
Selective Laser Sintering	SLS	1987-1992
3D Printing (Drop on Bed)	3DP	1985-1997

The transformation of RP systems towards RM is also influenced by customer requirements. It leads to customization and rapid production. This is the advantage of RP systems which can speed up processes and produce good quality products. However, the realization of this transformation still has its limitations. Expensive machine and materials, overall cost and production volumes are amongst the issues that need to be considered before fully utilising this technology.

The Figure 1.2 shows the transition of the physical model produced by RP technologies. The diagram clearly depicts that the optimum objective of the transformation is to have functional end use products with RM systems. There is currently much research and developments underway to achieve this aim.



**Figure 1.2 Transformation of RP to RM;** (Hopkinson, and Dickens, 2001)

Pogson et al., (2003) investigated the major processing factors that influence the production of copper parts through the SLS process. Das, et al., (1998), produced high performance metal components by SLS. Fischer, et al., (2004), successfully sintered commercially available pure titanium powders using an Nd: YAG laser source. This research has proved the use of this advanced technique for direct metal fabrication through laser sintering process.

### **1.2.2 Additive Manufacturing**

Additive manufacturing is a process of bonding materials to fabricate solid parts from digital data or CAD data, is also known as layered manufacturing, additive technology, additive fabrication, additive process and solid freeform fabrication. This system includes all applications of the technology, modeling, pattern making, tools and mould making, and the production of end use products regardless of the volume of production. Generally, all additive manufacturing systems employ the same fabrication technique; driven by digital CAD data, the data is sliced horizontally to create a 2D layered cross section. Due to the intricate interaction between the powder and the heat source, all the layers are combined to create a solid part which corresponds to the CAD data. The earliest technology use this additive method is RP (Hopkinson, and Dickens, 2001). RP has experienced exponential growth during the 1990's as the platform to produce or 'print' parts quickly and inexpensively for design verification and validation in the early stage of the product development cycle. The physical model of RP has significantly reduced the design error and increases the manufacturability of parts and assemblies. The

application of RP has expanded, not just for prototyping purposes but to overcome billions of dollars spent on tooling and mould fabrication (Simchi, 2006). This is known as ‘Rapid Tooling’ which uses the RP system to create core and cavity mould inserts for injection moulding. RP can and will evolve to successfully produce functional end parts in one step (Mognol, et al., 2006). Dimov et al., (2001), applied SLS technique to build tooling inserts in copper polyamide that can be used for fabrication of final products and used the Rapid tooling solution for fabrication of injection moulding tools. Due to its capability in creating solid parts upon layer by layer, RP is predicted to produce any part in any geometry of the highest complexity. This has led to the ‘Rapid Manufacturing’ terminology.

However, these additive technologies are still in a premature phase. Much research and developments has been undertaken in order to justify the use of this technology in terms of cost, materials and mechanical characteristics. The systems are relatively expensive and still have limitations on materials that can be processed.

### **1.2.3 Rapid Manufacturing**

Rapid Manufacturing has emerged from the advent of rapid prototyping in order to produce models and prototypes through a concept of additive manufacturing. It belongs to the RP systems, which is used for various kinds of applications during early product development in order to verify design and manufacturability, through concept evaluation, prototype models for presentation, as well as functional testing. The continuous improvement of RP in the area of powder materials and the sintering/melting technologies, pushed the limit of this system towards direct fabrication of functional parts in a small batch, which is known as Rapid Manufacturing and Rapid tooling ( for tooling and mould fabrication).

### **1.3 ORGANIZATION OF THE THESIS**

This thesis has been organized and presented in six chapters. **Chapter-1** provides an introduction to the composites, and characteristics of a composite material. MMCs and RP with advantages are also discussed briefly. The chapter ends with explanation on the transformation of RP to RM.

**Chapter-2** is devoted to the presentation of literature on composites, conventional sintering mechanism, Processing of MMCs by conventional methods, challenges faced during the processing of MMCs, Layer manufacturing methods with importance to DMLS, parameters affecting the DMLS process and fabrication of different MMCs by DMLS process. This chapter also discusses about review of literature on blending, coating on reinforcement, physical properties, mechanical properties, and corrosion behavior of MMCs, and machinability studies on laser sintered MMCs using Wire Electrical Discharge Machine.

**Chapter-3** discusses the scope of the research work with objectives set for the present research investigation.

**Chapter-4** presents details of blending, coating on reinforcement, experiment set up, specimen preparation for machinability studies, physical, mechanical, corrosion property evaluation, micro-structure characterization as per ASTM standards and also about various equipments used.

**Chapter-5** focuses on results and discussion under five sections. First section deals with characterization of procured matrix and reinforcement particles. Second section deals with characterization of coated reinforcement particles and characterization of blended particulate-mix of matrix and reinforcement. Third section deals with evaluation of physical properties of processed MMCs, Fourth section on evaluation of mechanical properties, Fifth section on evaluation of corrosion properties, and the Sixth and the final section deals with machinability studies on laser sintered MMCs using WEDM.

The major inferences drawn from the present research work along with scope for future work is presented in **Chapter-6**.

## **CHAPTER 2**

### **REVIEW OF LITERATURE**

#### **2.1 COMPOSITES**

Composite structures have shown global savings of minimum 20% over metal counterparts and a lower running and maintenance cost (Dhingra, 1986). The available data on the service life of composite structures indicates that they resist loading, maintain dimensional integrity, are durable, maintainable, and can be repaired. Composites now-a-days finds wider application in different fields of engineering but greater growth in the market for such materials will require economical methods of processing and the possibility of recycling will have to be solved.

The development of an effective metal matrix composite material depends on many factors. Since the final properties of MMC depend on the properties of the matrix and reinforcement material, careful selection of these components is very important.

##### **2.1.1 Selection of Material for Composites**

###### **Material for Matrix**

In MMCs the matrix alloy should be selected only after in-depth scrutiny regarding chemical compatibility with the reinforcement, its ability to wet the reinforcement, and to its own characteristics properties and processing behaviour (Allison, and Cole, 1993).

The natural opposition between reinforcement wettability and vigorous reaction with reinforcement plays a key role in selection of material for matrix (McKimpson, and Scott, 1989). Good load transfer from the matrix to the reinforcement strongly depends on the presence of better adherent interface (Rack, 1990 and Urquhart, 1991). In turn, a strong interface needs sufficient wetting of the reinforcement by the matrix. The aggressive reaction and sufficient wetting helps in better bonding between the matrix and reinforcement. Adjustment for chemical bonding between matrix and reinforcement involves lot of delicate compromises as many differences are involved.

As per the alloying rules the added element should not form intermetallic compounds with the matrix and stable compounds with the reinforcements. The better composite properties can be obtained when the reinforcement and matrix have good physical and chemical compatibility to the possible extent. Unique matrix alloy compositions with coatings on reinforcements are formulated to optimize the better working of many metallic composites (Chester, 1991).

The selected matrix material in MMCs should have combination of properties such as high strength, lower CTE, higher modulus of elasticity, high temperature resistance, improved wear resistance, higher electrical conductivity and better resistance to oxidation and corrosion. The above mentioned properties can be obtained only with proper selection of matrix and reinforcement (Taya, and Arsenault, 1989). Al, Mg, Cu, Ni, Ti, Si, Fe, and Ag are used as the matrix material.

### **Material for Reinforcement**

The resistance to temperature, increment in strength and stiffness with reduction in density of MMCs is possible with proper addition of reinforcement. To achieve these properties the following features such as size, shape, surface morphology, structural defects, surface chemistry, inherent properties, impurities, method of production and chemical compatibility with the matrix must be considered during selection of reinforcement.

Even after selection of a particular type of reinforcement inconsistency will continue because many of the features cited above with contamination from processing equipment and feedstock may vary to the greater extent (Adeqoyin, et al., 1991). Since most ceramics are available in the form of particles, and they can be considered as potential reinforcements for production of particulate reinforced composites (Tiwari, et al., 1990). A major concern for using particulates is to reduce the cost of the composites.

## **2.2 FABRICATION METHODS OF MMCs**

A wide recognition is given in the recent times for MMCs due to significant improvement in their performance over conventional alloys. But the manufacturing costs are still found



to be relatively high. MMCs are manufactured using different fabrication techniques and there is no distinct way in this respect. Because of choice of matrix and reinforcement and of the types of reinforcement, there is a considerable variation in the fabrication techniques of MMCs.

The different fabrication methods used to manufacture particulate reinforced MMCs can be classified as follows:

- a) Liquid phase fabrication methods
- b) Solid phase fabrication methods
- c) Two phase (solid/liquid) fabrication methods.

## **2.3 SINTERING**

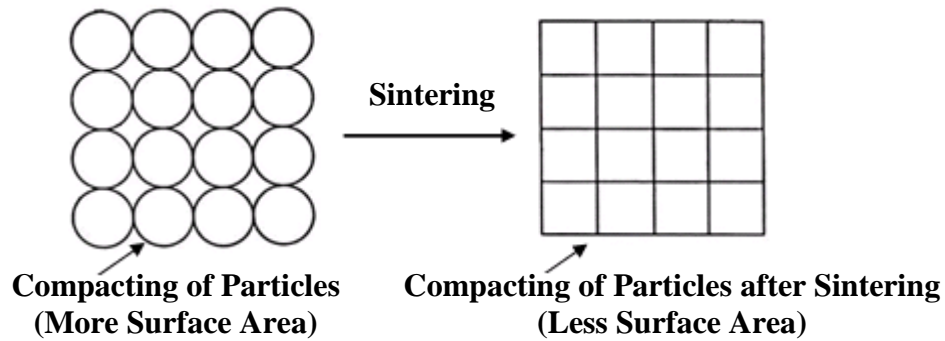
Sintering is a heat treatment process for producing solid objects by metallurgically bonding an assembly of loose or compacted particles (Exner, 1980).

In addition to particle bonding, sintering can produce the following effects:

- a) Chemical changes
- b) Dimensional changes
- c) Relief of internal stresses
- d) Phase changes

### **2.3.1 Sintering Mechanism**

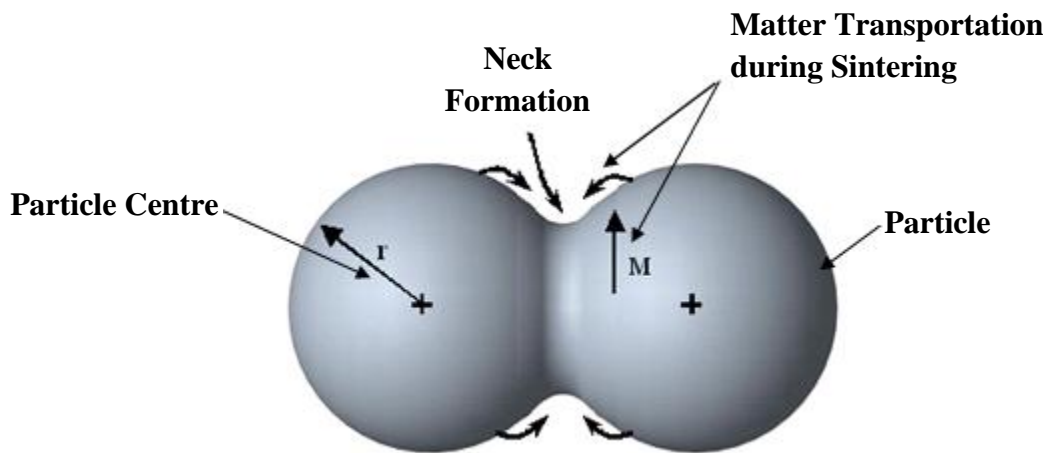
Reduction in the free surface area is the key driving force for sintering (Whittemore, and Varela, 1987). In a particle compact, the total free energy of a large number of small particles is greater than that of a smaller number of coarse particles or a solid block of equal volume. The reduction in surface energy can occur by pore shrinkage, which is associated with densification. A schematic diagram, illustrating the reduction in surface area of particles during sintering process, is shown in Figure 2.1.



**Figure 2.1 Surface Area Reduction during Sintering Process**

(Whittemore, and Varela, 1987)

The decrease in the surface area is accomplished by formation of small necks between the contacting surfaces of particles as shown in the schematic diagram, Figure 2.2.



**Figure 2.2 Formation of Neck between Spherical Particles**

(Whittemore, and Varela, 1987)

Neck formation between particles and densification of particles occurs by diffusion mechanism. Atoms or vacancies move along a surface or grain boundary or through the volume of the material in diffusion.

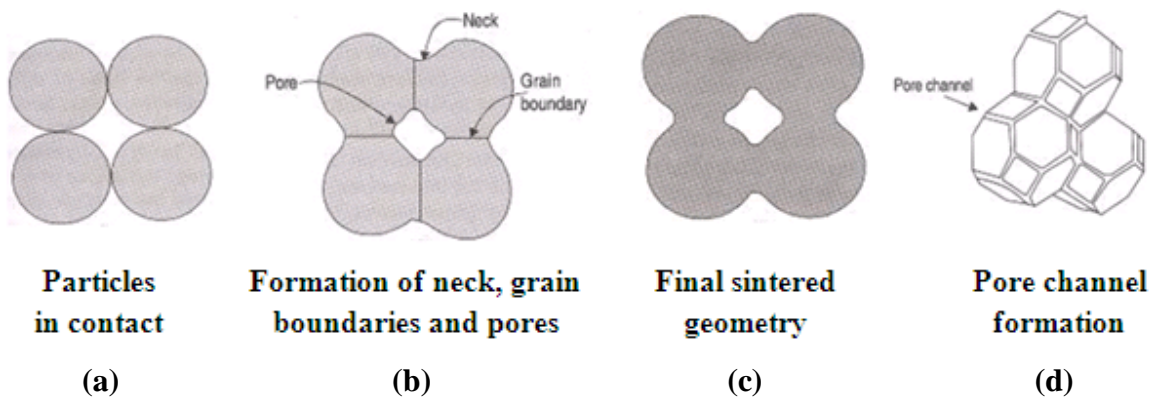
### 2.3.2 Sintering Stages

The three stages of sintering are:

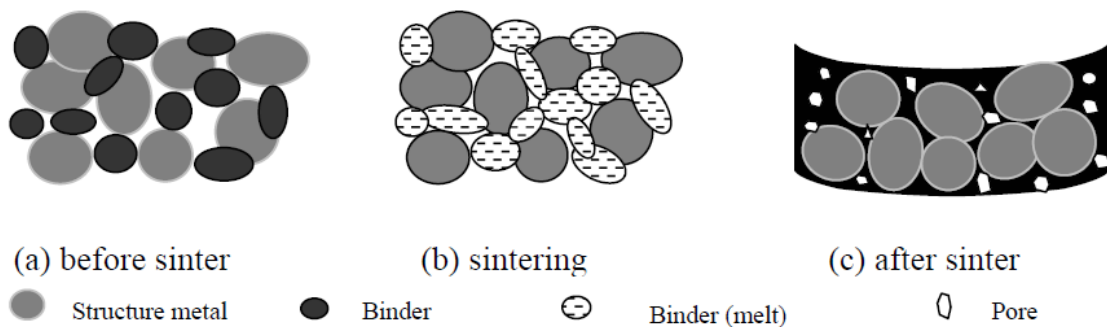
1. Primary stage.
2. Secondary stage.
3. Tertiary stage.

A stage of sintering can be defined as an interval of geometric change in which the pore shape change is totally defined. The stages during sintering are shown in Figure 2.3.

The initial stage of sintering shown in (a), and (b) would begin as soon as some atomic mobility is achieved and sharp concave necks are formed between the particles. The intermediate stage shown in (c) has solid grains with the shape of a tetrakaidecahedron, continuous channel like pores with a circular cross section. The final stage shown in (d) illustrates pinching-off of grains and their isolation at corners.



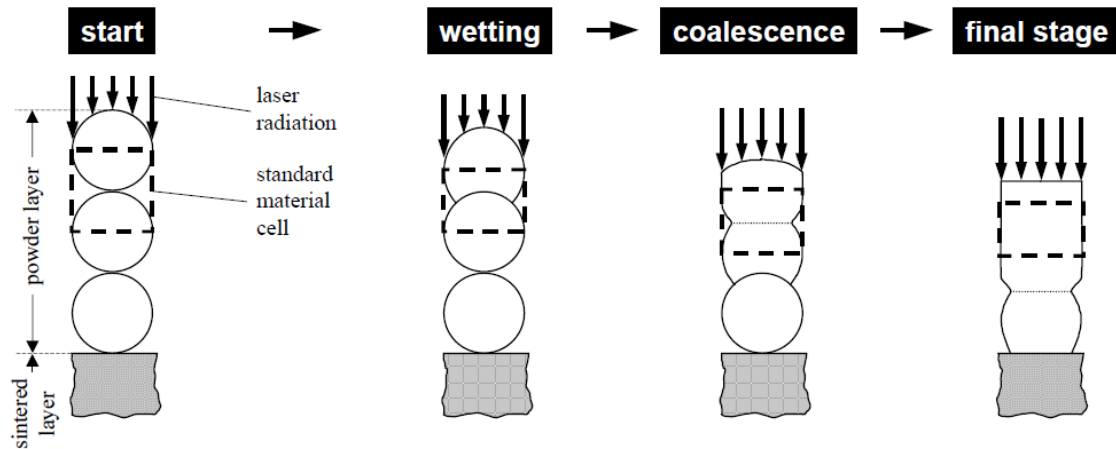
**Figure 2.3 Different Stages during Sintering Mechanism** (Stucker, 2006)



**Figure 2.4 Structural and Binder Material before and after Sintering Process**

(Gu, et al., 2012)

The structural and binder material movement before and after sintering is shown in Figure 2.4 and the movement of laser beam during sintering process is shown in Figure 2.5.



**Figure 2.5 Movement of Laser Beam during Sintering Process**

## 2.4 CHALLENGES IN PROCESSING OF MMCs

MMCs are gaining widespread popularity in several areas of applications related to automobiles, space, defense, aerospace and sports segments. The ever-increasing demands of the MMCs are mainly because of their superior mechanical, tribological and physical properties when compared with conventional alloys (Schwartz, 1984). It has been reported that the Brinell hardness is little influenced by the addition of the silicon carbide and an increment over 7% of ceramic particles content seems to be inefficient (Hartaj Singh et al., 2014). It is also reported by them that the tensile strength has an unchanged growth which is directly proportional with addition of silicon carbide and there is an increment in elastic modulus with increment in the silicon carbide content. Some of the challenges in producing MMCs are:

- MMC fabrication methods like infiltration, stir casting, squeeze casting and powder metallurgy need dies for making the final part. Fabrication of dies, generally calls for expensive machinery such as CNC lathe, milling and electrical discharge machines.

- There is a radical increment in the lead time and cost of die with the increment in complex nature of the part to be produced (Singh et al., 2014)
- Finish machining of composites is another challenge owing to the presence of hard reinforcement in the matrix (Ozben, et al., 2008).

## **2.5 RAPID PROTOTYPING**

Rapid Prototyping has transpired as a novel technology for manufacturing near-net shaped parts with complex geometry in a lesser time (Pham and Dimov, 2001 and Singh et al., 2014). Rapid prototyping refers to the production of parts layer-by-layer by additive process. The primary stage in the layer manufacturing process is the creation of three dimensional computer aided drafting model using CAD/CAM software like Unigraphics, Pro-E and Catia, followed by conversion to STL format. Further, the CAD model is electronically sliced in to thin layers using dedicated software such as ‘RP tools’. The layer information of the component is transferred to RP machine, where the part is built layer-by-layer. Rapid prototyping is a promising route to overcome some of the challenges faced in conventional processing of MMCs.

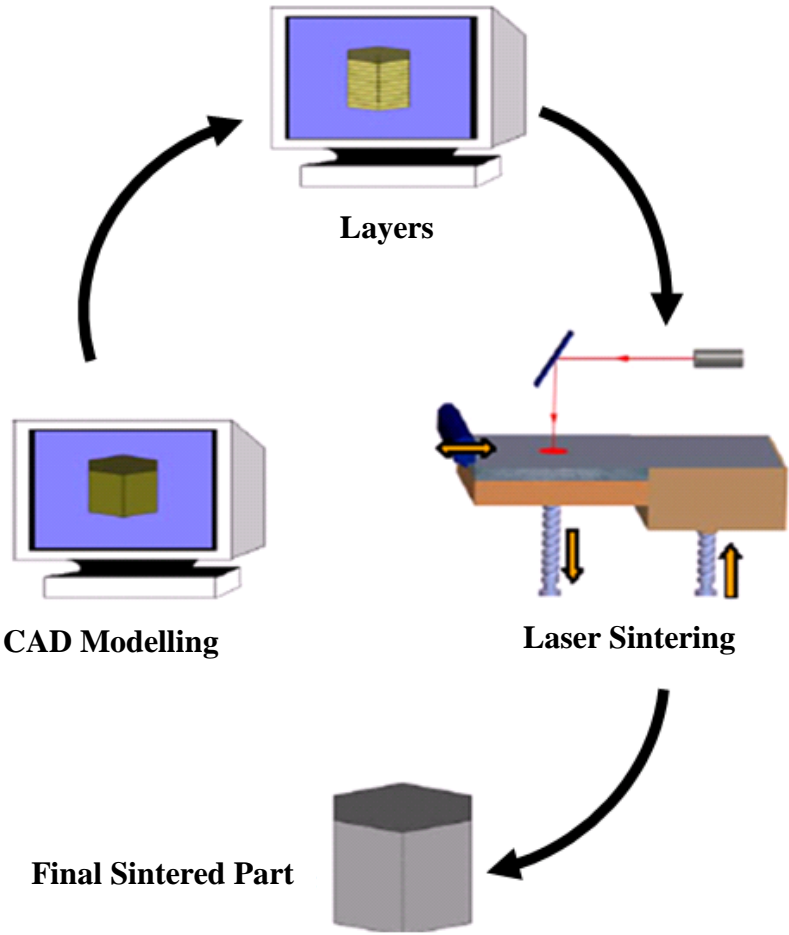
There are different metal sintering RP machines commercially available in the market. Most of these systems use laser as energy source for fusing of metal powders to produce complex parts. Most commonly used metal sintering RP machines are: LENS, DMD and DMLS. In LENS and DMD processes, metal powder is injected through a nozzle near the focus of a laser beam. Melting and solidification of the powder takes place instantaneously. DMLS is the most popular technique to produce metal prototypes and tooling.

### **2.5.1 Principle of Layer Manufacturing**

A schematic diagram, illustrating the basic principle of layer manufacturing by laser sintering process is shown in Figure 2.6.

The fundamental requirement of any RP system is a 3D CAD model of the part to be built. The model is created by using CAD/CAM software such as Unigraphics, Pro-E or Catia. Further, the CAD model is converted to Stereo lithography (STL) file format. The

STL file is electronically sliced using dedicated software such as ‘RP tools’ to produce successive cross sectional layers. The layer information is transferred to the computer of RP machine. A dedicated process software installed in the computer of RP machine, commands the different parts of the RP machine to build the physical model, layer-by-layer as per the cross sectional information.



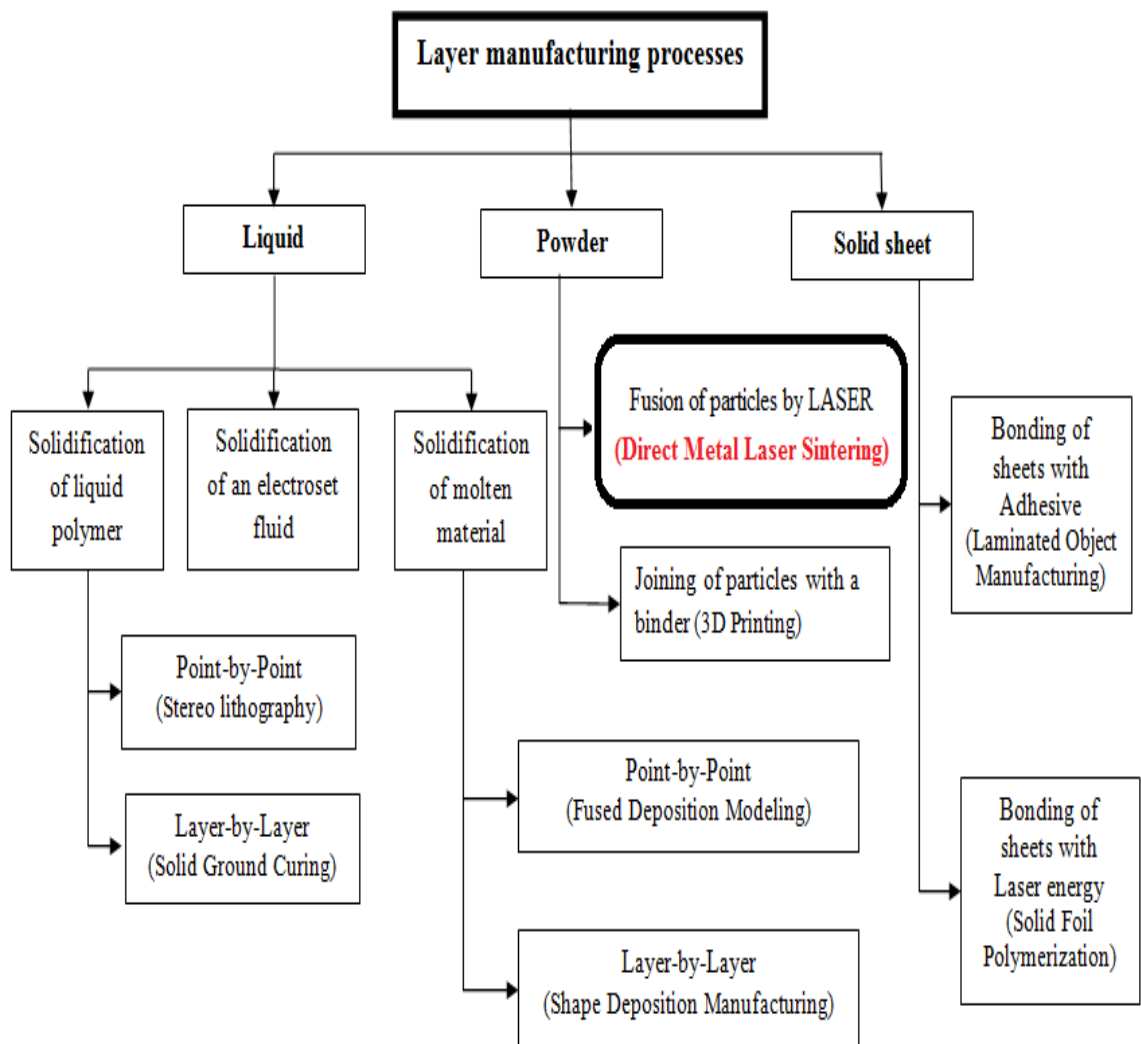
**Figure 2.6 Principle of Layer Manufacturing Process**

## 2.5.2 Classification of Layer Manufacturing

Layer manufacturing processes are classified into three types based on the state of the material before making the actual part (Kruth, 1991). They are:

- Liquid based
- Powder based
- Solid sheet based.

The classification of layer manufacturing processes is shown in Figure 2.7.



**Figure 2.7 Classification of Layer Manufacturing Processes**

(Pham, and Dimov, 2001)

## **2.6 SINTERING MECHANISM USING LASER**

Laser sintering mechanism in general is divided into four groups (Kruth, et al., 2007).

They are:

- Solid state sintering
- Liquid phase sintering
- Partial melting
- Full melting.

### **2.6.1 Solid State Sintering**

Solid state sintering is a thermal process, which occurs at temperatures below the melting point of the particles. The physical diffusion acts as a driving force for binding adjacent particles. This is a slow process, adopted normally in conventional sintering processes, where a particle compact is heated in an oven for few hours.

The slow laser scanning speeds are the result of the long interaction time between laser beam and particles. Modeling studies on solid state sintering of titanium particles by laser have revealed that the laser interaction time was of the order of magnitude 5 seconds as compared to 0.1 to 0.3 micro-seconds by other binding mechanisms (Kruth, et al., 2007). Therefore this process through laser sintering is not an economically feasible process.

### **2.6.2 Liquid Phase Sintering**

Liquid phase sintering is much faster and is applied for laser sintering of two-component particles. Of the two materials, one is the structural material having higher melting point and the other one having low-melting point is called a binder. The low-melting particles form a liquid phase and bind the structural material to form a solid mass. Sintering can occur at temperatures exceeding the melting point of the binder component but below the melting point of the main component (Agarwala, et al., 1995 and Kruth, et al., 1998).



### **2.6.3 Partial Melting**

Partial melting phenomenon is applied for single component particles. When the heat supplied by the laser beam is inadequate to completely melt the particles, only a shell or small particle will melt. Thus the molten material behaves as a binder between the adjacent particles having solid cores. Modeling studies have disclosed the full melting of particle shell, keeping the core temperature below the melting temperature (Kruth, et al., 1998).

### **2.6.4 Full Melting**

The present trend is towards processing of metal particles from partial melting to full melting. Yadroitsev et al., have performed experiments on laser melting of Inox 904L material of 20  $\mu\text{m}$  grain size and was able to produce structures of 1 mm thickness (Yadroitsev, et al., 2007). Badrossamay and Childs (2007) have studied on the laser melting of M2 tool steel and 316L steel and have reported negligible variation in mass with scan speed.

The advantages of full melting are:

- Distinct binder is not compulsory.
- Post- processes to remove polymer binder and infiltration are eliminated.
- Full dense parts can be produced.

## **2.7 DIRECT METAL LASER SINTERING**

Laser sintering is the method which manufactures solid parts by solidifying powder like materials layer-by-layer by exposing the surface of a powder bed with a laser. Direct metal laser sintering (DMLS) means laser-sintering using a metal powder so that metal parts are produced directly in the building process (Shellabear, and Nyrhila, 2007). DMLS, as a typical rapid prototyping technique, enables the quick production of complex shaped three-dimensional parts directly from metal powders. The first DMLS machine was built by EOS Gmbh, Germany, during 1994 (Shellabear, and Nyrhila, 2007). DMLS process creates parts layer-by-layer by selectively fusing thin layers of metal powder with

CO<sub>2</sub> laser beam (Bineli, et al., 2014). The powder material is fully metallic and can contain two components; a low melting and a high melting material. Bronze-nickel and steel powders are the commercially available materials developed by EOS, GmbH, for DMLS process. Direct Laser Sintering presents a technology which combines both powder metallurgy and layer manufacturing benefits. DMLS enables the manufacture of perfect tool inserts or metal components. The manufactured tool inserts find application in metal forming, injection moulding, pressure die-casting and other applications related to tooling.

### 2.7.1 Schematic Representation of DMLS Layer Manufacturing Machine

The schematic representation of DMLS layer manufacturing machine is shown in the Figure 2.8.

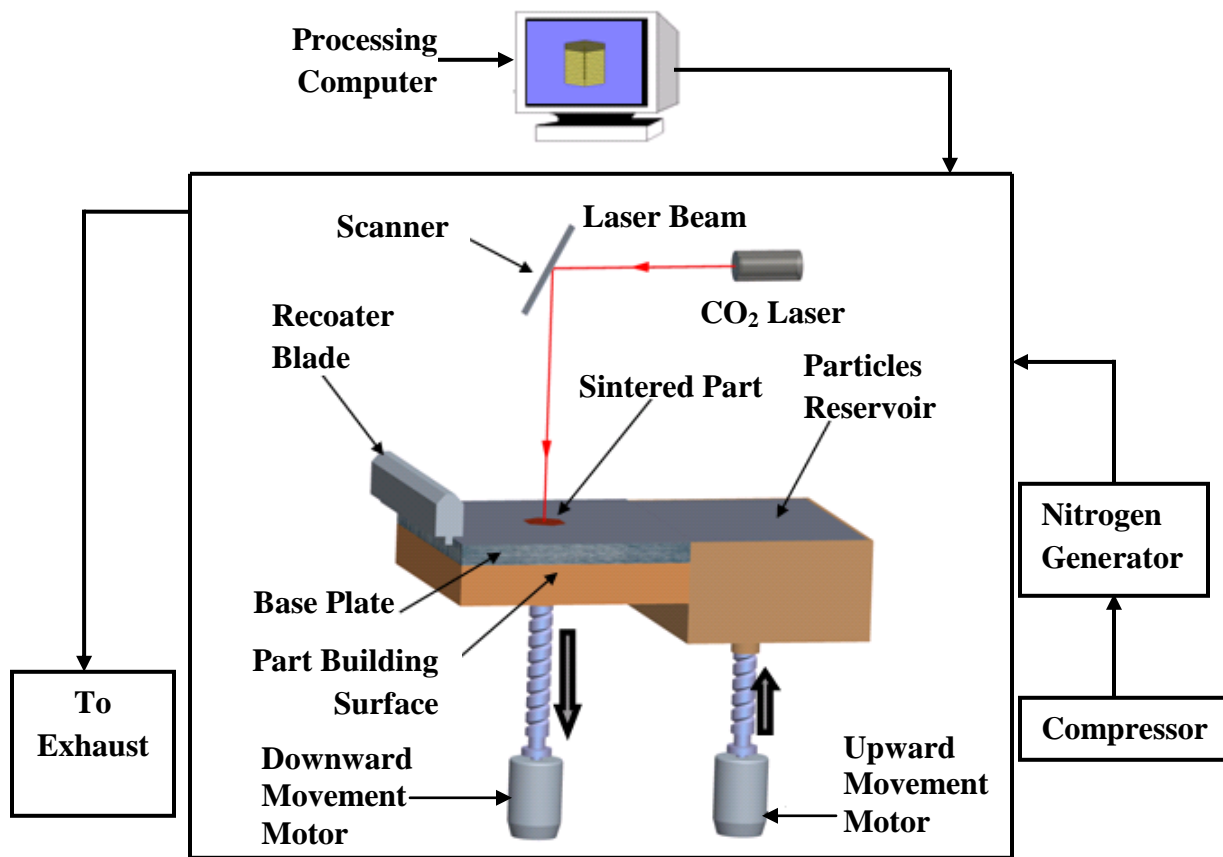


Figure 2.8 Schematic Representation of DMLS Machine

The essential parts of the machine are:

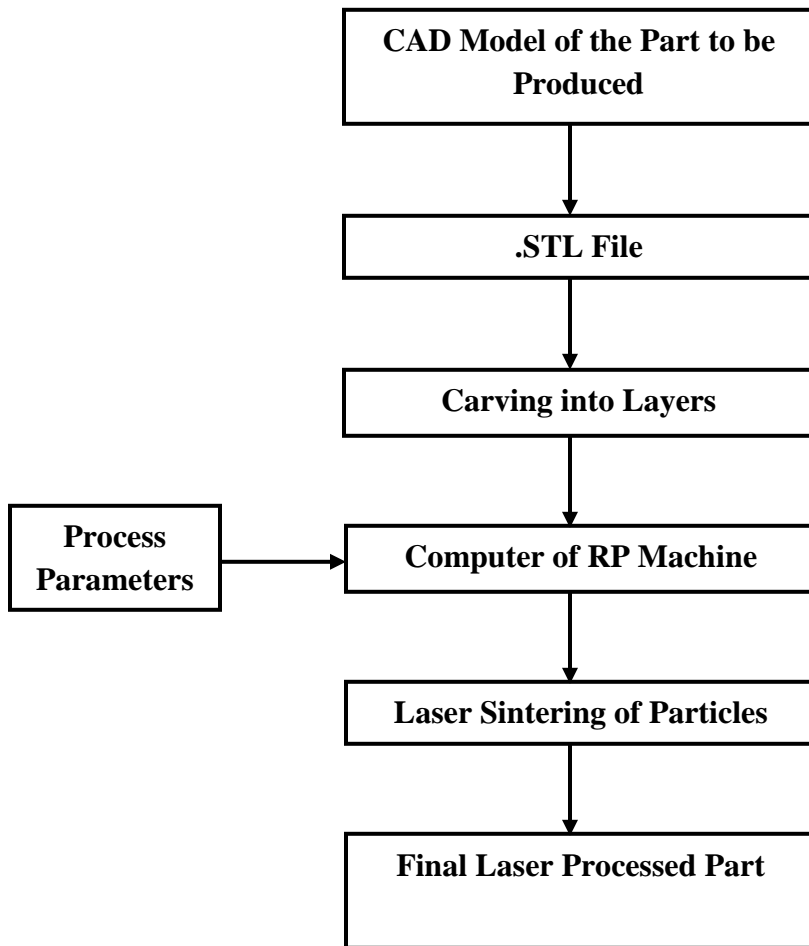
- Laser
- Mechanical elements: Re-coater Blade, Particles Reservoir, Building Surface
- Processing Computer
- Compressor
- Exhaust

A CO<sub>2</sub> laser beam of wave length 10.6 μm and laser power of 240 W was used as an energy source. The focused laser beam is of diameter 0.4 mm. The power and speed of laser can be varied for optimizing sintering process. The optics area is positioned in the upper part of the machine. The mechanical components of the system include building surface, re-coater blade and a dispenser.

The re-coater blade coats a particle layer on a base plate. Particles reservoir supplies particles for re-coating. A computer with process software (PSW) commands the working of laser optics and mechanical elements. Heat exchanger cools the laser system. Exhaust sucks out the dust particles and gases produced during sintering from the build-chamber of the machine. A nitrogen generator supplies nitrogen to the building chamber and acts as separator for removing oxygen from the compressed air.

### **2.7.2 Part Building Steps in DMLS Process**

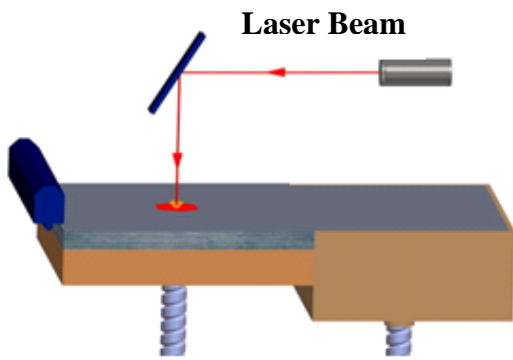
Figure 2.9 indicates the schematic diagram of the steps involved in DMLS process. A 3D model of the part to be fabricated is obtained using unigraphics or catia CAD/CAM system. It is converted to .STL file format followed by electronically slicing in to layers using 'RP tools' software. The information about the layers is send to the processing computer of DMLS machine and the part is built one layer after other by laser sintering process.



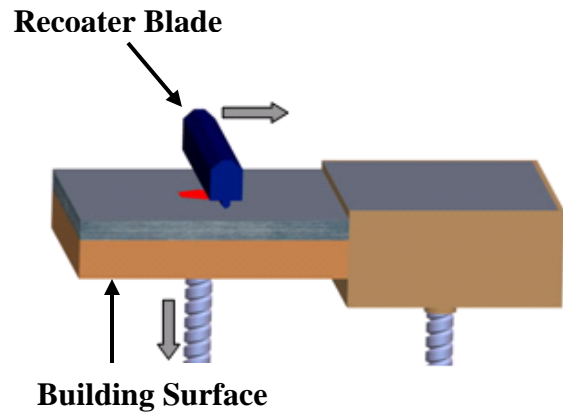
**Figure 2.9 DMLS Process Steps**

The part fabrication order in DMLS machine is shown in Figure 2.10. The order is as follows:

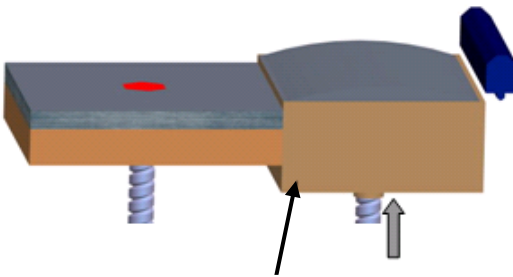
- Laser sintering of first layer as shown in Figure 2.10 (a).
- Lowering of building surface and movement of recoater blade towards particle reservoir as shown in Figure 2.10 (b).
- Upward movement of particle reservoir as shown in Figure 2.10 (c).
- Coating of particle layer on base plate as shown in Figure 2.10 (d).
- Laser sintering of particle layer as shown in Figure 2.10 (e).
- Completed part fabricated by repeating the sintering process as shown in Figure 2.10 (f).



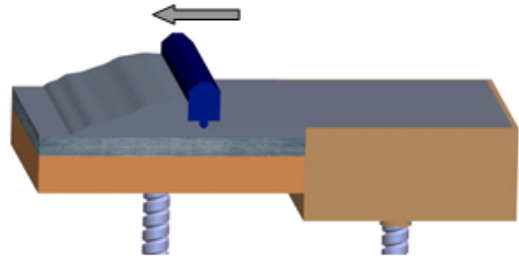
(a) Sintering Using Laser



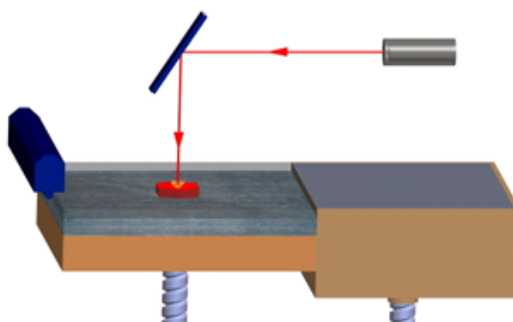
(b) Movement of Recoater Blade and Lowering of Building Surface



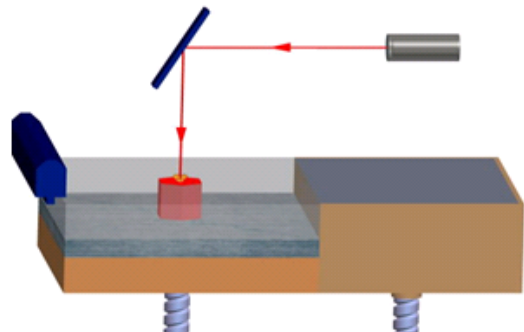
(c) Upward Movement of Particle Reservoir



(d) Particle Re-coating



(e) Repeat Sintering



(f) Completed Part

Figure 2.10 Part Fabrication Order in DMLS Process

### 2.7.3 DMLS Process Parameters

The process parameters in DMLS are:

- Power of Laser
- Scan Speed of Laser
- Hatch Width
- Hatch Spacing
- Build Atmosphere.
- Layer Thickness.

The available energy density for sintering is directly proportional to the power of laser and inversely proportional to scan speed of laser (Ramesh, et al., 2009). The power and scan speed of laser can be varied by process software. The path of laser can be programmed by process software. Hatch is the beam path of laser on the particle bed in the form of a set of parallel scan lines used to cure particles. Hatch spacing is the distance between successive laser scan lines and hatch width is the length of travel in one direction. Layer thickness can be varied from 0.02-0.06 mm. The scan path of laser is shown in Figure 2.11 and Figure 2.12.

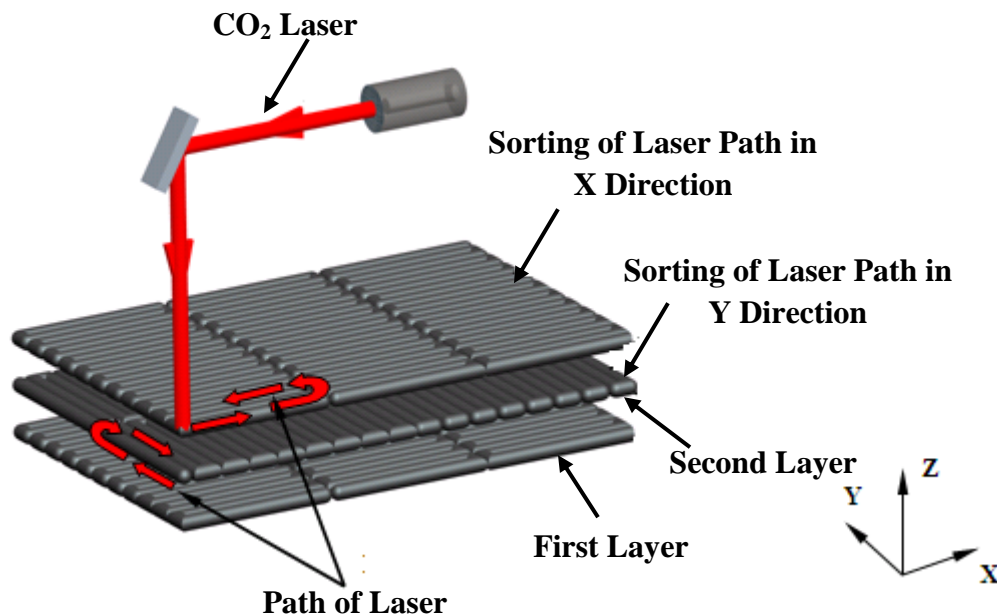
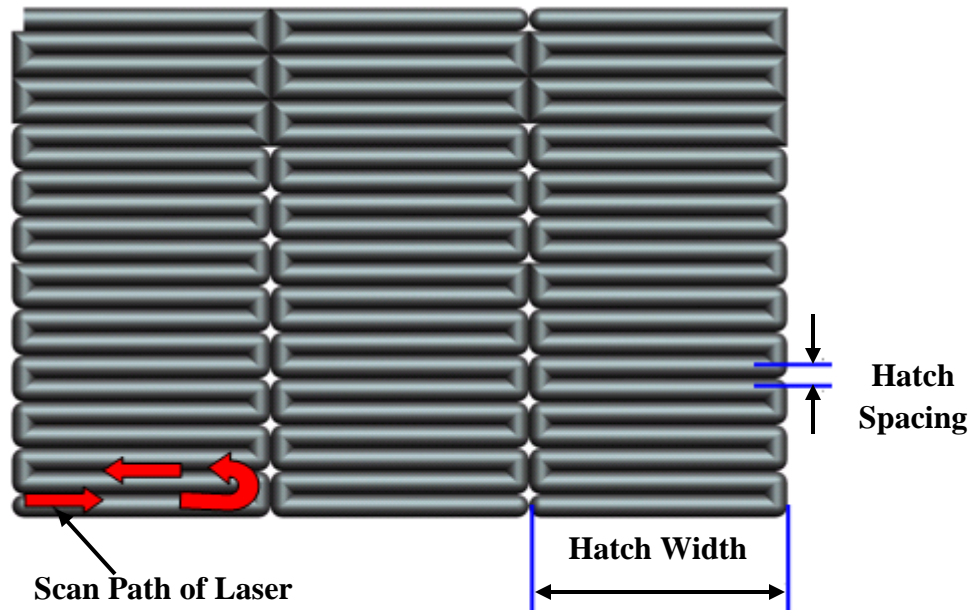


Figure 2.11 Schematic Representation of Scan Path of Laser in DMLS Process



**Figure 2.12 Schematic Representation of Scan Path of Laser in a Layer**

## **2.7.4 Effect of DMLS Process Parameters**

### **2.7.4.1 Power of Laser and Scan Speed of Laser**

The power and scan speed of laser have an intense effect on the density and surface roughness of sintered parts. The density of sintered parts increased with increased power and scan speed of laser while sintering bronze-nickel particulate mixture by DMLS process (Agarwala, et al. 1995). Higher power of laser and lower scan speed of laser results in higher energy density. The particulate bed temperature is increased by higher energy, which in turn results in large amount of liquid phase formation and hence dense parts. Less dense parts were obtained at higher scan speed of laser while sintering iron particles. This is because of balling effect, which is predominant at higher scan speed of laser (Rombouts, et al. 2006). There is a decrement in surface roughness of the laser sintered parts with decrement in scan speeds of laser (Song, 1997).

### **2.7.4.2 Powder Size and Morphology**

The density of sintered parts mainly depends on particle size. The influence of particle size on the density of parts produced by DMLS process has been studied and it has been reported that rough particles densify better than finer particles (Simchi, and Poul, 2003).

A particulate system with large particle size distribution of 45 $\mu\text{m}$  has resulted in highest sintered density when compared with particles of 10  $\mu\text{m}$  size (Simchi, et al., 2001). The reports also suggests that particles with a size distribution of 53-150  $\mu\text{m}$  have resulted in fully dense structure when compared with particles of size greater than 153  $\mu\text{m}$  (Niu, and Chang, 2000). However, finer particles with less than 38  $\mu\text{m}$  have resulted in porous structure. Gas atomized particles which are spherical in shape have resulted in better density compared to angular shaped water atomized particles (Niu, and Chang, 1999). This is because of the lower packing density and co-ordination number of non-spherical particles compared to spherical particles. Regular, equi-axed particles tend to position better compared to others. Therefore, spherical grains are more preferred (German, 1992).

#### **2.7.4.3 Build Direction**

Build time, quality of the surface and strength of the build parts mainly depends on optimum build direction in layer manufacturing process. Variation of build direction has its effect on the number of layers. Processing cost of the part increases with increase in number of layers. Support structure and the final strength of sintered part, depends on the build direction. There are reports about the samples built in x-direction having tensile strength twice that of those built in z-direction (Storch, et al. 2003).

#### **2.7.4.4 Sintering Atmosphere**

Sintering atmosphere has an intense effect on the density of laser sintered parts. Reports suggest that during DMLS process the test samples built in argon atmosphere are denser compared to those built in nitrogen atmosphere (Simchi, 2006). The presence of oxygen during sintering, leads to the formation of oxide layer which remarkably increases the absorption of laser radiation (Simchi, and Asgharzadeh, 2004). The higher laser absorption results in larger melt volume. The surface tension of the melt increases leading to “balling” while the oxide reduces the wetting and bonding. The balling effect results in reduced density of the sintered parts. Hence, sintering atmosphere has a greater effect on the density of the sintered parts.



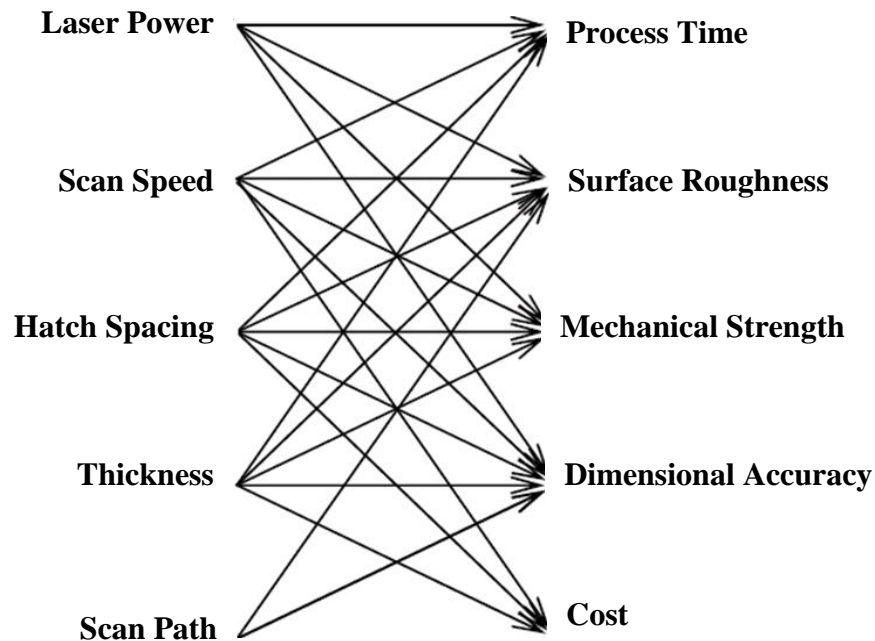
#### 2.7.4.5 Layer Thickness

Layer thickness also affects the density of laser-sintered parts. There are reports suggesting that the smaller thickness resulting in highly densified sintered parts compared to higher thickness during DMLS of steel particulates (Gu, and Shen, 2008).

#### 2.7.4.6 Hatch Width and Hatch Spacing

The density, strength and warpage of the sintered parts are affected by hatch width and hatch spacing during sintering process. During selective laser sintering of bronze particles, an increase in mechanical strength and surface quality of sintered parts was observed with reduced hatch distance. However, further reduction in hatch distance, leads to additional heating and cooling of particles resulting in increase in curling of scan lines (Song, 1997).

The relationship between process parameters and resulting properties is shown in the Figure 2.13.



**Figure 2.13 Relationship between Process Parameters and Resulting Properties**

((Niu, and Chang, 2000).

## 2.8 MMCs BY DIRECT METAL LASER SINTERING PROCESS

Processing of MMCs is the most interesting field for researchers. At present a very few companies and academic centers are able to process complex near-net shaped MMCs by rapid manufacturing techniques to fulfill the requirements of user industries. The physical and mechanical properties that can be obtained with MMCs have made them attractive materials for aerospace, automotive and numerous other applications (Ibrahim, et al., 1991). Commercially available metal particles developed by rapid manufacturing machine vendors are not able to meet the requirements of tooling industries because of low strength, poor surface finish and low wear resistance. Therefore, there is a very good opportunity for processing of MMCs for functional parts and tooling related to die-casting, metal forming and forging applications by laser sintering process. Particulate reinforced MMCs have attracted significant attention because of their low cost and typical isotropic properties. Currently, two methods are used for producing MMCs by rapid manufacturing technology. The first method is direct sintering of parts from metal-ceramic powders and the second method is fabrication of porous ceramic preforms, which are filled by subsequent liquid metal infiltration.

Some of the research work carried out in the field of development of MMCs by DMLS process is given in Table 2.1.

**Table 2.1 Research Work in Development of MMCs by DMLS Process**

<b>Research Work</b>	<b>Year</b>	<b>Research Team</b>
Development of an in-situ multi-component reinforced Al-based metal matrix composite by direct metal laser sintering technique-Optimization of process parameters.	2014	Ghosh, et al.
From powders to dense metal parts: Characterization of a commercial AlSiMg alloy processed through direct metal laser sintering.	2013	Manfredi, et al.

Laser additive manufacturing of metallic components: materials, processes and mechanisms.	2012	Gu, et al.
Crack and wear behavior of SiC particulate reinforced aluminium based metal matrix composite fabricated by direct metal laser sintering process.	2011	Ghosh, and Saha.
Blending of iron and silicon carbide powders for producing metal matrix composites by laser sintering process.	2010	Srinivasa, et al.
Friction and wear behavior of iron-silicon carbide composites.	2009	Srinivasa, et al.
Influence of processing parameters on particulate dispersion in direct laser sintered WC-Co <sub>p</sub> / Cu MMCs.	2008	Gu, et al.
Effect of processing parameters on consolidation and microstructure of W-Cu components by DMLS.	2008	Gu, et al.
Direct laser cladding of SiC dispersed AISI 316L stainless steel	2008	Majumdar, et al
Effect of SiC particles on the laser sintering Al-7Si-0.3Mg alloy.	2008	Simchi, and Godlinski
Influence of reinforcement weight fraction on microstructure and properties of submicron WC-Co <sub>p</sub> / Cu bulk MMCs prepared by direct laser sintering.	2007	Gu, and shen
Micro structural characterization and wear behavior of Fe-Ni - TiC MMC prepared by DMLS.	2006	Gaard, et al.
Microstructure and property of sub-micro WC-10% Co particulate reinforced Cu matrix composites prepared by selective laser sintering.	2006	Gu, and Shen
Direct laser sintering of iron-graphite powder mixture.	2004	Murali, et al.
Selective laser sintering of Al-SiC Metal Matrix Composites.	2002	Vaucher et al.
Mechanical and thermal expansion behavior of laser deposited metal matrix composites of Invar and TiC.	2000	Li, et al.

### 2.8.1 Nickel based MMCs

Most of the work on MMCs is centered on light metal alloys to improve their strength and stiffness. However, there is not much work has been reported on the nickel based MMCs using laser because of the cost factors. But now-a-days with lot of money has been spent in the field of research and cost is not the criteria, researchers are now looking towards the different types of superalloys which play vital role in the field of high temperature applications. Since India as a developing country facing lot of problems in the field of power sector, it is interested in investing in this field of research.

Superalloys find wider application in the present metallurgical world. The jet flight is made possible because of these alloys, and they show what can be done by exploring all the resources of present physical and process metallurgy in chasing a very challenging target. IN625 is one such superalloy which finds application in different fields of engineering. IN625 is a non-magnetic, corrosion and oxidation-resistant, nickel-base alloy. Its outstanding strength and toughness in the temperature range cryogenic to 1093<sup>0</sup>C are derived primarily from the strengthening effects of the refractory metals, niobium and molybdenum, in a nickel–chromium matrix. Nickel and chromium provide resistance to oxidizing environment, while nickel and molybdenum to non-oxidizing environment. Pitting and crevice corrosion are prevented by molybdenum. Niobium stabilizes the alloy against sensitization during welding. Its resistance to chloride stress-corrosion cracking is excellent. It also resists scaling and oxidation at high temperatures. Some typical applications for IN625 are heat shields, furnace hardware, gas turbine engine ducting, chemical plant hardware and nuclear reactor control rods (Paul, et al., 2007). The material possesses a high degree of formability and shows better weldability than many highly alloyed nickel-base alloys. It is also used in functional prototypes and high temperature turbine parts.

The reinforcing material silicon carbide is a covalent material of great technological interest due to its excellent properties including good mechanical resistance, high thermal conductivity, good thermal shock behavior, and erosion resistances (Liu, et al., 2010). Its applications are involved in both structural and functional materials. Indeed, it is

currently used in the reinforcement of metal–matrix composites, in nuclear plants, for heat exchangers, for optical devices and as the ceramic component of metal/ ceramic couples. The selection of SiC as the ceramic reinforcement phase was based on wide availability and high thermal conductivity and its use in electronics packaging industry and it is available in powder form and it is stable under laser. The increase in SiC content results in decrease of CTE and also the additive nature of laser sintering avoids the problems associated with machining of the ceramic phase.

Thermal management is important in a wide range of applications from computers to power semiconductor devices and packaging for microwave devices used in telecommunications. A high thermal conductivity ( $\lambda$ ) is required and the specific thermal conductivity ( $\lambda/\rho$ ) is a useful property for components that are part of a moving system, such as components in aerospace systems. CTE is the second primary property for thermal management. Thermal management materials that perform best are those that possess a CTE from 4 to  $7 \times 10^{-6}/\text{K}$  (Miracle, 2005). Therefore the IN625 with marginally high CTE can be mixed with silicon carbide with low CTE.

Good wetting and low reactivity of metal/ceramic couples are key factors in many technological processes, in particular in metal/ceramic joining, to avoid degradation of ceramics and to achieve the desired properties during service (Liu, et al., 2010). Nickel when added to silicon carbide gives silicides. These reactions yield "pest effect" that induces brittleness, to avoid this the nickel surface is coated using silver foils of 200 micro-meter which will avoid pest effect and also improves the mechanical shear resistance (Hattali, et al., 2009). The surface alloying of Incoloy 800H with SiC results in the formation of the carbides  $M_7C_3$  which are precipitated in the melted zone. The precipitation is because of decomposition of the silicon carbide during the laser melting. Silicon carbide absorbs large fraction of the incident laser energy and the metal surface reflects large fraction of the incident laser beam. The hardness of the surface is also found to be increased because of the extensive precipitation of the carbides and also due to laser treatment (Zhu, et al., 1995).

## 2.9 COATING ON REINFORCEMENTS

Coating on reinforcements plays an important role during the composite formation to obtain better mechanical properties in MMCs. Properties of the MMCs strongly depend on the interfacial phenomena between the metal matrix and the ceramic reinforcement (Lloyd, 2008). The DMLS process used here for fabrication of MMCs is based on liquid phase sintering (LPS) mechanism involving a partial melting of the particles (Kruth, et al., 2007, Simchi, et al., 2001 and Gu, et al., 2015). The multi-component particulate mixture is composed of high melting point metallic/ceramic component acting as reinforcement and low melting point metallic component acting as a binder (Khaing, et al., 2001, and Kruth, et al., 2003).

Densification of solid/liquid system and the wetting characteristics of the metal/ceramic inter-phase decide the final success of the laser sintered part. The wettability of reinforcement by liquid metal is the key factor to achieve high interface bonding strength (Burak, et al., 2011). Hence the coating on metal/ceramic plays an important role in both wetting and densification. SiC used here possesses good thermal conductivity, electrical conductivity, chemical stability, and high mechanical strength, and has been used to prepare MMCs to enhance their mechanical properties and to resist high-temperature (Planson, et al., 1999). It has been reported that the coating on these ceramic particles not only improves the green density and sintering activity, but also enhances phase uniformity and mechanical properties of the sintered body (Tuan, et al., 1995 and Yao, et al., 2011).

Even though, different coating methods such as co-precipitation, sol-gel and electroless plating are used for coating powders, the electroless plating is considered as an important coating technique to coat the surface of different ceramic powders (Dai, et al., 2006). This method of coating is also used to coat material surfaces such as plastic, alloy and powders (Ozols, et al., 2006). Thin metallic films on plastics, metals and ceramics is obtained by dipping the substrate in electrolyte solution by electroless plating method. In this method conducting and non-conducting materials are deposited with metals and alloys by controlled autocatalytic electro-chemical reactions. This auto-catalytic metal

plating represents an easy and effective method, since variety of metals can be used and a thick coating can be formed (Leon, et al., 2000). Brenner and Ridell invented electroless nickel coating in 1940s (Agarwala, and Agarwala, 2003). It is called as electroless plating due to the absence of external electrodes. Here substrate acts as cathode and metal is supplied by metallic salt and electrons are supplied by the reducing agent. This plating process offers more number of advantages compared to the conventional electroplating. The important features of the electroless plating are its excellent coating power, ability to coat uniformly reaching down deep bores, corners and edges in a short period of time for whatever the complexities involved in geometry of the surface to be plated. High corrosion, High hardness especially when deposited as a nickel-phosphorous and heat treated and wear resistance of nickel coatings have already been reported (Chung, et al., 1996) and as a result of which it finds wide range of applications in aerospace, automotive, electronics and computer related industries.

Recent literature reports about metallic coating use to overcome the challenges posed during the development of metal matrix composites. MMCs normally have two distinct phases, the matrix and reinforcement with different physical and mechanical properties. The thermal mismatch exists because of the large difference in the coefficient of thermal expansion (Burak, et al., 2011 and Singh, 2012) of the matrix and reinforcement, which are commonly ceramic in nature, leading to thermal stresses. De-cohesion effect occurs because of the residual stresses. Applications of MMCs are limited due to decrease in strength and wear resistance of developed MMCs because of de-bonding of the ceramic reinforcements in MMCs. Poor wettability of the ceramic reinforcement is the main reason for the de-bonding phenomenon (Simchi, et al., 2001). Literature reports about nickel coated ceramic powders performing better with respect to wettability when compared with uncoated ceramic reinforcements (Zhan, and Zhang, 2003). While making review on “particulate reinforced MMCs”, researchers have reported that application of metallic coatings such as nickel and copper on to ceramic particulates decreases the overall surface energy of the particulates resulting in good wettability at the interface (Ibrahim, et al., 1991).

Literature also reports about a uniform and continuous nickel-phosphide coating on both  $\text{Al}_2\text{O}_3$  and SiC powders (Leon, and Drew, 2000), where experiments have been performed on infiltration of nickel coated SiC powders with molten aluminum resulting in improved adhesion and wettability of reinforcements in MMCs. Some researchers concentrated on coating of nickel on nano SiC powders and have reported that pre-treatment of powders have greater impact on the rate of nickel plating (Chen, et al., 2003). Experiments are performed with respect to coating on nano particles of SiC and reports about greater impact of coating on the dielectric nature of the coated SiC (Zou, et al., 2006). The pH range and holding time are very important for better coating of Nickel-Phosphide on ceramic powders.

## **2.10 BLENDING OF MATRIX AND REINFORCEMENT PARTICLES**

Blending is the process of preparing a more valuable mixture from less valuable raw materials. Blending plays a key part in deciding the quality of laser sintered MMCs. Blending of solids is most commonly employed in the manufacture of plastics, glass, ceramics, fertilizers, detergents, pharmacy field, processed food and also in powder metallurgy. The science of particles mixing is a new technique compared to an ancient tradition of particles mixing. The process of obtaining particles of same nominal composition is called as blending of particles (Dotter, 1984). As the degree of blending increases, the energy consumption cost, and maintenance cost increases. The annual cost of inefficient industrial mixing in USA, amounts to as high as US\$10 billion (Moakher, et al. 2000). Therefore, the degree of blending should be related to the intended use of the product.

The quality of a particulate mixture has to be described in three quantities: the scale of scrutiny, the allowable variation from the mean composition and the frequency with which this variation may be exceeded. The composition and the quality of the particulate mixture can be assessed by sampling process. Many researchers have used different statistical tools to analyze the quality of powder-mixture.



## **2.11 PHYSICAL PROPERTIES OF MMCs**

### **2.11.1 Density and Surface Roughness**

The properties of the MMCs depend on the size, shape, percentage and distribution of the reinforcement material, matrix material and communion of the matrix with reinforcement.

Simchi, et al., (2003), reported about the importance of the powder characteristics such as size, shape, and distribution of the particles while reinforcing nickel with Iron. The experimental studies resulted in development of the laser processed parts with agreeable density with lesser porosity. It was also reported that the density of the laser processed parts can be further increased by post-sintering treatment. Murali, et al., (2004), conducted direct metal sintering of Iron and graphite particles, it was found that the density of the composite parts were lesser compared to the base Iron due to the formation of some voids during the sintering process because of balling effect. Simchi, (2006), studied about mechanics and kinetics of the DMLS process and concluded that the density of the parts produced depends upon parameters such as laser power, scan rate, and line spacing.

Kumar, (2009), conducted experiments on direct metal sintering of WC-Co and concluded that the density of the composite depends on high power of the laser beam. Ramesh, et al., (2009), conducted direct sintering of Iron-SiC particles and concluded that the density of the composite reduces with increment in weight percentage of SiC reinforcement, and perfect bonding has occurred between matrix and reinforcement because of NiP coating on the reinforcement particles. Gu, et al., (2009), conducted direct sintering of copper alloy and nickel particles and only a small amount of small-sized pores were occasionally observed and a densification of 95.3 % was obtained for the laser processed parts. Ozgur, (2013), conducted experiments on sintering of nickel based 625 superalloy and concluded that higher density was obtained by sintering at 1300<sup>0</sup> C for 3 hours. Manfredi, (2013), conducted direct metal laser sintering of the commercial AlSiMg Alloy and concluded that the processed parts have a porosity of 0.8 % and the porosities are of the order 20 to 30  $\mu\text{m}$ . Simchi, (2010), conducted experiments on co-

sintering of Ni-base superalloy powders and concluded that an enhanced densification was possible at temperatures higher than 1260<sup>0</sup> C, when solid sintering was employed.

Gu, et al., (2007), conducted direct laser sintering of Cu–CuSn–CuP mixed particles and concluded that highly densified parts were obtained due to improvement in liquid-solid wetting characteristics by addition of phosphorus element. Wilson, and Shin, (2012), conducted experiments on reinforcing TiC with Inconel 690 MMCs and concluded that there was a decrement in density of the composites by 20 % compared to the base metal. Ghosh, et al., (2014), conducted direct laser sintering of SiC reinforced Al MMCs and concluded that the powder composition has profound effect on density of the processed parts compared to layer thickness and hatching distance.

Manfredi, et al., (2013), conducted direct laser sintering of Aluminium alloy particles and concluded that there was a decrement in surface roughness after secondary operation like shot peening on the laser processed parts. Calignano et al., (2014), conducted direct laser sintering and selective laser melting of aluminium matrix composites and concluded that surface roughness of selective laser melted parts are higher compared to direct laser sintered parts and further secondary operations like abrasive jet machining can be done on the laser processed parts to improve the surface finish.

## **2.12 MECHANICAL PROPERTIES OF MMCs**

### **2.12.1 Hardness and Strength**

The hardness and strength of the particulate reinforced MMCs are influenced by many factors. Out of those many factors one of the important factors which influence the mechanical characteristics is the matrix material. Matrix which exhibits higher tensile and yield strength, results in increment in strength with poor deformation characters. Increment in volume fraction of the reinforcement results in increment in strength of MMCs. The mechanical properties are also influenced by the residual stress, which is the result of disputed coefficient of thermal expansion between the matrix and reinforcement (Zhan, and Zhang, 2003).

Zhu, et al., (1995), conducted laser surface alloying of Incoloy 800H with SiC; it was found that the addition of SiC to the surface of Inconel has resulted in higher hardness due to fine dendritic structure, extensive precipitation of carbides and high dislocations against carbides. Murali, et al., (2003), conducted direct metal sintering of graphite reinforced Iron composites; it was found that the micro-hardness is high at the locations which are free from internal voids and cavities and macro-hardness which is influenced by internal voids is lower. It is also reported that the presence of graphite and porosity resulted in lesser macro-hardness compared to micro-hardness. An experimental design approach on direct laser sintering of low carbon steel was conducted and it was reported that hardness depends on layer thickness and hatch space has no role to play on hardness of the material (Chatterjee, et al., 2003).

Kumar, (2009), conducted experiments on direct metal sintering of WC-Co composites and concluded that the 9 wt. % Co reinforced WC processed at lower laser power results in higher hardness due to lower laser energy and infiltration. Ramesh, et al., (2009), conducted direct sintering of SiC reinforced Iron composites and concluded that the hardness of the composites increases with the increase in weight percentage of SiC and maximum of 400 VHN is obtained for 3 weight percent SiC reinforcement compared to the base Iron with an hardness of 240 VHN. The increment in the hardness is imputed to the higher hardness of SiC and high density of dislocation due to thermal mismatch between matrix and reinforcement. Gu, et al., (2009), conducted direct sintering of nickel reinforced copper composites and it was reported that the dynamic nanohardness of Ni reinforcing phase reached 1.82 GPa, indicating increment compared to copper based matrix alloys with nanohardness of 0.99–1.35 GPa. The tensile studies reveal that a strong ductile type of fracture is the feature of the fracture surface of laser-sintered parts.

Li, et al., (2009), conducted direct sintering of TiC reinforced Ni composites and concluded that micro-hardness of MMCs with 60 volume percentage TiC is higher compared to 20 volume percentage of TiC. There is gradual increment in the micro-hardness with increment in TiC reinforcement due to higher hardness of the TiC. Ahmad, et al., (2011) conducted studies on novel micro-structural growth in the surface

of Inconel 625 by addition of SiC under electron beam melting and concluded that the introduction of C and Si atoms in the matrix of Inconel 625 has resulted in increased hardness by two times compared to as-received alloy. Wilson, and Shin, (2012), conducted experiments on reinforcing TiC with Inconel 690 MMCs and concluded that the addition of TiC particles into the matrix of Inconel 690 results in refining the matrix micro-structure resulting in increased hardness. The higher density of dislocation is also the factor for increment in hardness.

Cooper, et al., (2013), conducted experiments on reinforcing  $Al_2O_3$ , SiC and TiC with Inconel 625 and concluded that the addition of SiC particles into the matrix of Inconel 625 has resulted in higher increment in hardness compared to  $Al_2O_3$  and TiC reinforcements. An increment in hardness by 150 HV compared to base Inconel 625 was observed with SiC reinforcement. Bi, et al., (2013), conducted experiments on reinforcing nano-TiC with Inconel 625 MMCs and concluded that the addition of nano-TiC particles into the matrix of Inconel 625 has resulted in 12 % improvement in micro-hardness compared to base Inconel 625. The tensile studies has resulted in improvement in UTS and YS by 18.5 % and 30 %, respectively compared to base Inconel 625 with addition of 1 wt. % of nano-TiC into the matrix of Inconel 625. The studies conducted on sintering of nickel based 625 superalloy has resulted in hardness up to 303 HV and tensile strength of 674 MPa was obtained (Ozgun, et al., 2013).

Ghosh, et al., (2014), conducted direct laser sintering of SiC reinforced Al MMCs and concluded that the increment in the reinforcing materials are responsible for increment in the micro-hardness.

### **2.13 CORROSION BEHAVIOUR OF MMCs**

Corrosion is the decay or deterioration of the material which starts at the surface of metals due to chemical and electrochemical attacks. The accelerated corrosion test uses polarisation and salt spray test methods. In case of salt spray accelerated corrosion test the metal specimens are exposed alternatively or continuously to a fine mist of salt water solution. The exposed surface of the samples are subjected to a spray of corrosive

medium and the samples are kept in a closed unit for different interval of time at particular temperature and humidity conditions.

Cooper, et al., (1996), conduction corrosion tests on TiC and WC reinforced IN625 alloy composites. TiC reinforced IN625 had better corrosion resistance compared to WC reinforced IN625. TiC found to be partially dissociated during the laser treatment with IN625. The corrosion resistance of both composites was found to be better compared to IN625. Valente, and Galliano, (2000), conducted corrosion tests on plasma-sprayed titanium composite coatings on AISI304 substrate. It has been reported that the corrosion resistance of the coated test specimen was found to be depend on the porosity in the coating. Further, it has been reported that bulk titanium had better corrosion resistance property compared to titanium based coating.

Yilbas, et al., (2001), conducted corrosion tests on IN617 which finds application in thermal systems. The presence of Mo and Cr in the matrix of IN617 make the alloy resistant to corrosion. The tests were conducted in a solution of 0.1 N sulphuric acid and 0.05 N sodium chloride at room temperature. The surface of the IN617 after laser treatment found to showing more resistance to corrosion compared to the original base metal. Rossia, et al., (2004), conducted corrosion tests on prototypes fabricated by DMLS process. Three different coatings were done on prototypes before conducting corrosion tests. The specimens coated with PTFE and PVD coatings showed poor resistance to corrosion when they are placed in the salt spray chamber. The specimens coated with nickel showed higher corrosion resistance when they are exposed to salt spray.

Tan, et al., (2008), conducted corrosion tests on nickel base alloys used in high temperature water-cooled nuclear plants. Three alloys, IN617, 625 and 718 were used for the study. Serious pitting was observed on 718 samples compared to 625 samples. The performance of the IN625 was better when it was compared with IN617 samples. Borowski, et al., (2009), conducted corrosion tests on IN625 modified by glow discharge assisted nitriding. It was found that the chromium nitride layer produced on the surface of IN625 showed better corrosion resistance compared as-procured IN625. It was concluded that the nitriding process can be used for increasing the service life of the IN625.

Ahmed, et al., (2010), conducted corrosion tests on bulk IN625 and high-velocity oxy-fuel (HVOF) sprayed IN625. It was reported that the HVOF sprayed IN625 showed little bit lower resistance to corrosion compared to bulk IN625. The occurrence of porosity and oxidation immediately because of the nature of thermal spray has resulted in lower corrosion resistance. Cho, et al., (2010), conducted corrosion tests on ceramic coated IN617. TiAlN and Al<sub>2</sub>O<sub>3</sub> thin films were coated on IN617 by physical vapour deposition methods. The coated samples were subjected to corrosion tests. The results clearly reveal that the Al<sub>2</sub>O<sub>3</sub> showed better performance compared to TiAlN as protective layer for IN617.

Zahrani, and Alfantazi, (2012), conducted molten salt induced corrosion on IN625. The solution of PbSO<sub>4</sub>-Pb<sub>3</sub>O<sub>4</sub>-PbCl<sub>2</sub>-Fe<sub>2</sub>O<sub>3</sub>-Z was used for this purpose. The degradation of IN625 was found to be because of transfer of the sulphur from the molten salt. Changa, et al., (2012), conducted corrosion tests on IN625 in supercritical water environments. The samples of IN625 were exposed to supercritical environments with mixed O<sub>2</sub> at 400 and 600<sup>0</sup> C and 24.8 MPa for various periods of time up to 1000 hours. Pits found on the surface of the samples could be imputed to carbide inclusions in the as-received IN625.

## **2.14 MACHINABILITY STUDIES ON PROCESSED MMCs**

Machinability is one of the unique tests for identifying material suitable for a particular application. Greater than 75-80 % of the produced parts are machined before they are fit to be used. Machinability of a material determines its cost in different applications. Tool life, rate of metal removal, machining time, surface finish and chip are the various benchmark used to estimate the machinability of a material using different machine tools (Dwivedi, 2000). The traditional machining methods find it very difficult to machine the MMCs. To machine the MMCs normally hard cutting tools are used. During machining many researchers have faced difficulties such as work hardening of matrix and crack with matrix or reinforcement, faster wear of the tool and lot of harm to the sub-surface. The answer to such difficulties is the use of advanced machining techniques like wire electrical discharge machining (WEDM). WEDM is the flexible and the most potential technique to machine the hard ceramics and metal matrix composites (Ho, et al., 2004).

The machinability studies were conducted using WEDM and sinking EDM using copper-silicon carbide electrode and it was concluded that sinking EDM performed better compared to WEDM with respect to MRR, SR and wear of the electrode while machining IN718 superalloy which is considered to be the tough material to machine by traditional machine tools because of the higher strength it possess at elevated temperatures (Li, et al., 2015). The WEDM studies conducted on high strength IN706 alloy reveal that the pulse on time and pulse off time have greater impact on the SR and MRR. The higher toughness of IN706 has resulted in zero percent micro cracks on the machined surface and there is a reduction in micro voids at low pulse on time with thick white layer formation at high pulse on time. There is a change in micro-hardness because of remarkable thermal degradation (Priyaranjan Sharma, et al., 2015). The WEDM of IN625 was conducted using regression analysis to establish the relation between control factors such as pulse on time, pulse off time, wire tension and responses like wear of electrode, and hardness. It was concluded that the experimental and the predicted values are in good terms with each other (Rodge, et al., 2013).

The tool wear rate and MRR were found to be increased with increase in discharge current during EDM of 10 weight percent SiC particle reinforced with cast Al alloy (Dhar, et al., 2007). The experimental studies on WEDM of ZrO<sub>2</sub> reinforced Al MMC reveal that there is an increment in cutting velocity with increment in pulse width and remain constant with increment in wire tension ( Parveen kumar saini, et al., 2014). Increment in MRR with increment in pulse current and pulse-on-time up was noticed during machining of SiC particulate reinforced Al MMCs (Dwivedi et al., 2008).The WEDM studies were conducted on SiC reinforced Al2024 MMC and the experimental results clearly revealed that there is an increment in SR with an increment in pulse on time and percentage reinforcement of SiC. Also there is an increment in MRR with an increment in pulse on time and decrement with the increment in percentage reinforcement (Ashish Srivastava, et al., 2014). The WEDM studies conducted on 10 weight percent B<sub>4</sub>C reinforced Al 7075 MMC revealed that there is an increment in MRR and SR with

increment in pulse on time and there is a reduction in electrode wear rate with higher pulse off time (Gopalkannan, et al., 2012).

Surface roughness and MRR were found to be increased with increment in discharge current and decreased with increment in weight percentage of reinforcement during EDM of 1, 3 and 5 weight percentage SiC reinforced Al composites fabricated by pressure die casting and vortex method (Kathiresan, and Sornakumar, 2010). The study on Al<sub>2</sub>O<sub>3</sub> reinforced 6061 Al alloy reports about increment in cutting rate with increment in machining current (Guo, et al., 2002). High rate of MRR was observed in copper electrode compared to silver-tungsten and copper-tungsten electrodes during micro electro discharge machining of silicon nitride using copper, copper-tungsten and silver-tungsten electrodes of diameter ranging from 40 to 50 microns (Muthamara, et al., 2010). The studies on machining of SiC reinforced Al composites was done with abrasive jet using water, laser and EDM and it was concluded that during EDM, there was an increment in MRR with increment in discharge current and decrement with increment in SiC percentage. (Muller, and Monaghan, 2000).

The experimental study on Al<sub>2</sub>O<sub>3</sub> reinforced 6061 Al composites reports about decrement in the cutting speed for composites compared to base 6061 Al alloy and higher surface roughness for 20 volume percent Al<sub>2</sub>O<sub>3</sub> (Yan, et al., 2005). The machinability study on SiC and Al<sub>2</sub>O<sub>3</sub> reinforced Aluminium based MMCs using WEDM reports about increment in the surface roughness and cutting speed with increment in discharge current (Rozenek, et al., 2001). The experimental studies conducted on the laser processed SiC reinforced Iron composites reveal that there is a decrement in machining time with increment in discharge current and decrement in machining time was observed with increment in the weight percentage of the reinforcement because of better absorptivity of the laser by the reinforcement (Srinivasa, et al., 2012). The experimental studies on 30 volume percentage alumina reinforced Aluminium 6061 composite reveal that there is an increment in machining time with increment in peak current and on-time and more tool wear was observed for composites compared to base Al alloy with increment in off-time (Nanimina, et al., 2011). The studies on electro discharge machining of 10 percent SiC



particulate reinforced as cast Al composites reports that an increment in MRR and surface roughness with increment in discharge current (Singh, et al., 2004).

The mathematical model was proposed using response surface methodology for the study of effect of machining parameters on performance characteristics during EDM of TiC reinforced  $Al_2O_3$  and it was concluded that the discharge current and pulse on time have highest impact on SR, MRR and wear of electrode (Ko Ta Chiang, 2008). The Taguchi method was used for process parameters optimisation during machining of carbon-carbon composites by EDM and it was reported that pulse current and gap voltage are directly responsible for electrode wear rate and MRR (George, et al., 2004). The Taguchi method of optimization technique was applied for formulation of experimental trails for cutting micro-size hole in IN718 super alloy material using micro-EDM with brass electrode. It was concluded that the discharge current, pulse on time and pulse off time have greater impact on MRR (Manikandan, and Venkatesan, R., 2012).

## CHAPTER 3

### SCOPE OF THE WORK

Metal Matrix Composites (MMCs) have been explored for wider applications in the field of engineering for the past three decades. The unique properties such as higher stiffness and lower density which are not possible by conventional materials can be achieved through MMCs. This type of combined yields can be achieved through the use of ceramic reinforcements in MMCs. Most of the work on MMCs till date is focused on development of aluminium, copper, magnesium, and titanium based MMCs. Lot of interest is shown now-a-days on aerospace and high temperature materials such as IN625 nickel based superalloy which finds application in important sectors like power generation turbines, engine air craft components and electronic parts like cathode ray tube spiders, and springs. Also, the excellent resistance to corrosion by high purity water led to its use in construction of control rods of nuclear reactors.

SiC a ceramic compound of silicon and carbon was chosen as reinforcement for preparing IN625 MMCs. The high hardness and wear resistance, low density, high mechanical strength, ability to retain strength at high temperature, resistance to thermal crack, low thermal expansion and excellent chemical resistance has made SiC as a choice of reinforcement in nickel based IN625 matrix. In addition to its low cost and better mechanical properties, the selection of SiC as the ceramic reinforcement was based on its wide availability in particulate form and stability under laser.

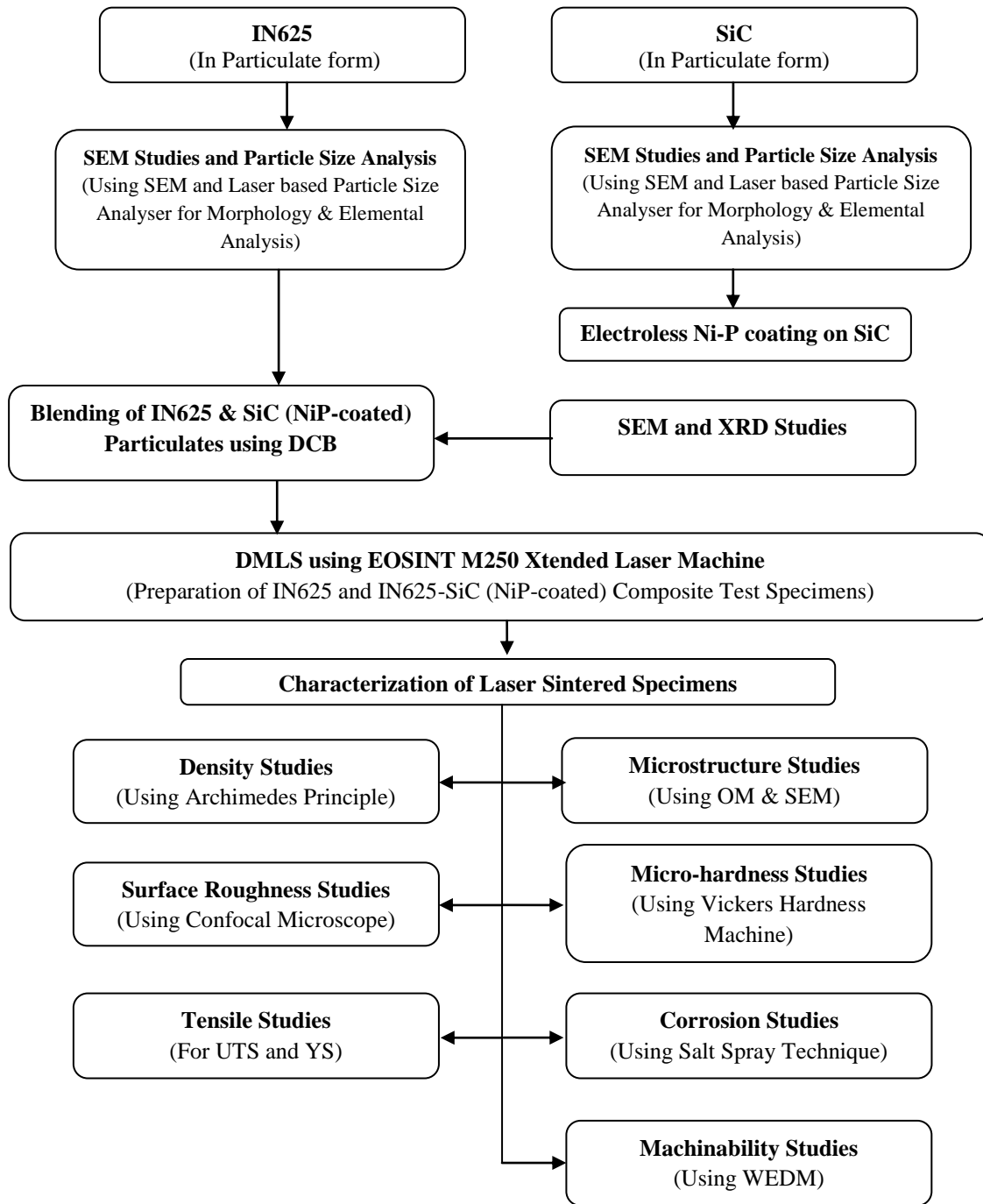
Literature review reveals that most of the MMCs are developed by conventional manufacturing methods such as powder metallurgy, melting, and casting and very few researchers have reported about processing of MMCs by different laser based additive manufacturing process. The present work involves processing of NiP coated SiC reinforcement with IN625 matrix by DMLS technique for producing Ni based MMCs. The problem statement is given as: “Processing and Characterisation of Inconel 625–SiC Metal Matrix Composites by Direct Metal Laser Sintering”.

The aims / objectives of the present investigation have been set as follows:

1. Examining of IN625 (matrix) and SiC (reinforcement) particles for their morphology and chemical composition.
2. Coating of nickel-phosphide (Ni-P) on SiC particles, and their characterization.
3. Optimization of process parameters for the preparation of IN625-SiC (NiP-coated) MMCs.
4. Processing of IN625 MMCs for 1, 3, and 5 wt. % of SiC (NiP-coated) reinforcement using DMLS.
5. Characterization of processed MMCs for physical, mechanical and corrosion properties.
6. Machinability studies of processed MMCs using WEDM.

IN625 and SiC are used in the particulate form as a matrix and a reinforcement material respectively. The reinforcement SiC is coated with NiP by electroless coating process for proper bonding between matrix and reinforcement. IN625 matrix composites are processed with 1, 3, and 5 wt. % of SiC (NiP-coated) reinforcement for optimized process parameters under inert atmosphere. Blending of matrix and reinforcement is done for homogeneity of particulate mix using double cone blender. Metallographic, physical properties (density and surface roughness), mechanical properties, corrosion properties and machinability studies will be carried out on the laser processed test specimens.

The schematic representation of the experimental procedure and studies conducted under this investigation is shown in the Figure 3.1 below.



**Figure 3.1 Schematic Representation of the Experimental Procedure and Studies Conducted under this Investigation**

## **CHAPTER 4**

### **EXPERIMENTATION**

#### **4.1 INTRODUCTION**

The objectives pursued in this investigation were presented in the previous chapter. The scheme of the work to be undertaken in the present investigation, with different stages, has also been described. This chapter presents the details of experimentation and measurement procedures adopted to evaluate different properties of the IN625 and IN625-SiC (NiP-coated) composites.

#### **4.2 MATERIAL SELECTION**

In the present work, IN625 and SiC in particulate form were used for developing IN625 and IN625-SiC composite parts by laser sintering process. The properties of IN625 and SiC are discussed in the following section.

##### **4.2.1 Matrix Material and its Properties**

IN625 was selected as matrix material for preparing the composites owing to its excellent mechanical and physical properties and its wide industrial applications. The important properties of IN625 are as follows:

- Inconel-625 is non-magnetic.
- It is corrosion and oxidation-resistant, nickel-base alloy.
- Its outstanding strength and toughness in the temperature range cryogenic to 1093<sup>0</sup>C.
- Its resistance to chloride stress- corrosion cracking is excellent.
- It also resists scaling and oxidation at high temperatures (Paul, et al., 2007).

Some of the other thermal and mechanical properties of IN625 are given in the Appendix A. IN625 particles procured from Powder Alloy Corporation, Ohio, USA, will be used as a matrix material. The chemical composition of IN625 is also given in the Appendix A.

#### **4.2.2 Reinforcement Material and its Properties**

SiC was chosen as reinforcement for preparing composites. SiC is a ceramic compound of silicon and carbon. The choice of SiC as reinforcement in IN625 matrix is due to its following properties:

- High hardness and wear resistance
- Low density
- High mechanical strength
- Ability to retain strength at high temperature
- High thermal conductivity
- Resistance to thermal crack
- Low thermal expansion
- Excellent chemical resistance

Some of the other thermal and mechanical properties and the chemical composition of SiC are given in the Appendix A. SiC light black in color, procured from Grindwell Norton, Bangalore was chosen as reinforcement to prepare the composites. The density of SiC used in the present work was 3.2 g / cc.

#### **4.3 CHARACTERIZATION OF MATRIX AND REINFORCEMENT MATERIAL**

IN625 and SiC particles were characterized for size, morphology and composition. The experimental procedure adopted for characterization of powders is described in this section.

##### **4.3.1 Particle Size Analysis**

Particle sizes of the matrix and reinforcement particles were evaluated using laser-based particle size counter. The photograph of particle size counter and its salient features are given in the Appendix B. Particle size counter works on the principle of light blockage. The particle sizes of IN625 particles were evaluated as follows:

A known quantity (20 mg) of IN625 particles was mixed with two liters of clean hydraulic oil of grade MIL-H-5606 having NAS class 0, in a bottle-shaker for 15

minutes. 200 ml sample of oil-powder mixture was taken from the bottle-shaker and further subjected to ultrasonic vibration for 10 minutes to obtain a homogeneous mixture. Further, the bubbles in the oil-powder sample were degassed by vacuum pump. The bottle containing the oil-powder sample was placed in the particle size counter equipment. 10 ml of sample was made to pass through nozzle located between the laser beam and laser diode. The flow rate was maintained at 10 ml/min. 8 electronic channels were calibrated to measure the particle size in steps of 10  $\mu\text{m}$ . Particle size was automatically recorded in the computer connected to the electronic channel. The same procedure is adopted for particle size analysis of SiC particles.

#### **4.3.2 Morphology**

Scanning Electron Micrograph (SEM), Energy Dispersive Spectroscopy (EDS) and X-ray Diffraction (XRD) studies were carried out on IN625 and SiC particles using Scanning Electron Microscope of make: Carl Zeiss, Germany and model: Neon 40 Crossbeam and X-ray Diffractometer of make: Brucker and model: XRDD8ADVANCE. The photograph of scanning electron microscope, X-ray Diffractometer and their salient features are given in the Appendix B.

#### **4.4 NiP COATING ON SiC PARTICLES**

NiP coating was carried out on SiC particles by electroless coating process as per procedure described by Kang, et al., (2002). The SEM, EDAX and XRD studies were carried out on the coated SiC particles for evaluation of NiP coating on SiC particles.

##### **4.4.1 Experimental Procedure**

The experimental procedure adopted for electroless coating of Nickel Phosphide (NiP) on SiC particles is as follows.

A measured quantity of 5 gram of SiC taken in a beaker was soak cleaned by immersing in toluene and propane followed by acetone wash. The dust, oil and other unwanted materials from the surface of SiC were removed by rinsing in distilled water. The cleaned particles after sinking in nitric acid were subjected to ultrasonic vibrations to roughen the surface, for further sensitization and activation. This was followed by a rinse in distilled

water. Further, the particles were sensitized in a solution containing stannous chloride and hydrochloric acid (0.63 gram stannous chloride in 0.2 ml hydrochloric acid and 25ml of water) followed by rinsing in distilled water (Ramesh, 2009).

The roughened and sensitized SiC particles were treated with palladium chloride solution (0.005 g Palladium Chloride in 0.2 ml of hydrochloric acid and 50 ml of water) for energizing its surfaces prior to nickel coating. Duration of five minutes was taken for the energizing. Palladium-activated SiC particles were then cleaned in distilled water and were dried in air for 2 hours. The palladium-coated SiC particles were sinked in the freshly prepared electroless nickel bath. The composition of the nickel bath is given in the Appendix C.

The temperature of the bath was maintained at 85<sup>0</sup> C. The pH of the bath was kept at 4.5. The period for coating was varied from 15 to 90 minutes with intervals of 15 minutes. In general, pH level of the solution changes as a result of the formation of hydrogen ions (H<sup>sup+</sup>) during the plating process. The rate of deposition also tends to increase with the pH level of the solution. The operating pH level range for nickel electroless plating is 4 to 8. Basically, the minimum pH level for any deposition is about 3.0; however, as the pH level increases to above 7.0, the hypophosphite spontaneously oxidizes, thus making plating impossible beyond this range. In practice, the preferred pH range is between 4.3 and 4.9. The coated SiC particles were then perfectly cleaned in distilled water and dried by heating in an oven at a temperature of 100<sup>0</sup> C for 30 minutes.

Scanning Electron Micrograph, Energy Dispersive Spectroscopy analysis and X-ray diffraction studies on coated SiC particles were carried out at NITK, Surathkal. The make and model of the equipments are given in the Appendix C. Further, the coating deposit was evaluated as described in the following section.



#### 4.4.2 Evaluation of Coating Deposit

The following procedure was used to evaluate the coating deposit.

- A weighed sample of 1g of SiC particles coated with NiP was taken in a beaker into which 10 ml. of concentrated hydrochloric acid was added followed by heating for 5 minutes at 50° C.
- As soon as bubbles were noticed, 5 ml. of concentrated nitric acid was added into the beaker and the heating was continued for another 3 minutes to ensure the complete dissolution of NiP coating from the surface of SiC particles.
- The above solution was filtered. The filter paper was dried in an oven at 100° C for 30 minutes.
- The dried filter paper containing NiP particles was weighed in an electronic balance and the coating deposit was calculated as follows.

##### 4.4.2.1 Coating Deposit Calculations:

Weight of coated SiC particles	=	w <sub>1</sub>
Weight of fresh filter paper	=	w <sub>2</sub>
Weight of de-coated SiC particles with filter paper	=	w <sub>3</sub>
Weight of decoated SiC particles	=	w <sub>3</sub> -w <sub>2</sub>
Weight of coating	=	w <sub>1</sub> - (w <sub>3</sub> -w <sub>2</sub> )
Weight percentage of coating	=	[w <sub>1</sub> -(w <sub>3</sub> -w <sub>2</sub> )] x 100 / (w <sub>3</sub> -w <sub>2</sub> )

#### 4.5 FABRICATION OF IN625 TEST SPECIMENS BY DMLS PROCESS

##### 4.5.1 Modeling of Test Specimens

The CAD models of test specimens for density, microstructure, microhardness, tensile, corrosion and machinability studies were modeled using Pro-E CAD/CAM software. 2D and 3D drawings of the test specimens are given in the Appendix D. The models were sliced into layers using PSW RP software, with each layer having thickness of 50 µm. An allowance of 1 mm was given on diameter and height in all 3D models for finish

machining. The tensile specimens were prepared as per drawing mentioned in the table, a small fillet all round the bottom side of specimen was allowed for the purpose of thermal gradient and to avoid warpage of build parts. The test specimens were prepared as per the ASTM standards.

#### **4.5.2 DMLS Machine and Machine Setup**

EOSINT M250 Xtended RP machine was used for producing IN625 and IN625-SiC (NiP-coated) composites by laser sintering process. The EOSINT M250 Xtended DMLS machine is given in the Appendix E. The salient features of DMLS machine are given in the Appendix E. The machine setup includes filling of the dispenser with the required powder. This was followed by mounting a base plate of 250 x 250 x 25 mm on building platform of machine with four screws as shown in Appendix E. The surface of the base plate was made horizontal with the help of leveling screws and dial indicator as shown in Appendix E. A thin layer of particle bed of 50  $\mu\text{m}$  was spread on the base plate.

#### **4.5.3 Optimization of Laser Sintering (Processing) Parameters**

Studies on the optimization of sintering parameters were carried out on IN625. Sintering was carried out in inert nitrogen atmosphere to find the effect of hatch spacing on density, and tensile strength of sintered IN625 parts. The laser scan speed was varied from 2.5 to 10 mm/s in steps of 2.5, hatch spacing from 0.2 to 0.4 mm in steps of 0.1, while laser power, hatch width and layer thickness were maintained constant at 240 W, 5 mm, 50  $\mu\text{m}$  respectively with laser beam diameter of 0.4 mm.

#### **4.5.4 Preparation of Test Specimens**

IN625 test specimens for density and tensile strength were produced with the sintering parameters shown in Table 4.1.

**Table 4.1 Process Parameters used for Laser Sintering of IN625**

<b>Laser Power (P) (Watts)</b>	<b>Laser Scan Speed (v) (mm/s)</b>	<b>Beam Dia. (mm)</b>	<b>Hatch Width (mm)</b>	<b>Layer Thickness (mm)</b>	<b>Hatch Spacing (<math>\delta</math>) (mm)</b>	<b>Energy Density (<math>J/mm^2</math>)</b>
240	2.5	0.4	5	0.05	0.2	191.52
	5					95.76
	7.5					63.84
	10					47.88
	2.5	0.4			0.3	127.68
	5					63.84
	7.5					42.56
	10					31.92
	2.5	0.4			0.4	95.76
	5					47.88
	7.5					31.92
	10					23.94

The preparation of the test specimens using the parameters mentioned in Table 4.1 is shown in the Appendix F.

#### **4.5.4.1 Separation of the Test Specimens from Base Plate**

The specimens sintered on the stainless steel substrate were firmly fixed. The specimens were separated from the base plate using wire-cut electro discharge machine of make: Charmilles Technologies, Switzerland and model: ROBOFIL 290, the wire-cut EDM is as shown in the Appendix F. The separated test specimens from the WEDM were deburred for measuring density and micro-structure, and machined using tool room lathe as per ASTM standards to measure tensile strength.

## **4.6 CHARACTERIZATION OF IN625 TEST SPECIMENS FOR DENSITY, TENSILE STRENGTH AND MICRO-STRUCTURE**

### **4.6.1 Density Studies**

The density of the sintered specimens was measured by Archimedes's principle using electronic balance of make: Sartorius, Germany and model: MC-2105 with an accuracy of 0.01 mg. The test specimens were first weighed in air and then weighed in water as shown in the Appendix G. The density evaluation was done as follows:

Weight of the test specimen in air =  $w_1$

Weight of the test specimen in water =  $w_2$

Volume of the specimen =  $w_1 - w_2$ ,

Then density =  $w_1 / [w_1 - w_2]$

### **4.6.2 Tensile Studies**

The tensile tests were conducted on IN625 test specimens using tensile testing equipment INSTRON-5569 at Shriram Institute for Industrial Research, Bangalore. The tensile test equipment is shown in the Appendix H. The salient features of the equipment are given in the Appendix H. Ultimate, yield strength and percentage elongations were evaluated. Scanning Electron Microscope and Energy Dispersive Spectroscopy studies of the fractured surfaces were carried out using SEM of make: Carl Zeiss and model: Neon 40 Crossbeam at NITK, Surathkal.

### **4.6.3 Micro-structure Studies**

Optical micrograph studies of IN625 test specimens were done using optical microscope of make: Nikon, Japan and model: Optiphot-100S. A mixture of 10 ml  $\text{HNO}_3$ , 15 ml HCl and 10 ml  $\text{CH}_3\text{-COOH}$  etchant (Dinda, et al., 2009) was used for optical microscopic studies.

## 4.7 FABRICATION OF IN625-SiC (NiP-Coated) COMPOSITES BY DMLS PROCESS

### 4.7.1 Studies on Blending of IN625 and SiC (NiP-coated) Particulates and Their Characterization

The homogeneity of powder-mixture decides the quality of MMCs. The blending of powders plays an important role in processing of MMCs. Blending was carried out in a double cone blender of make: Hindustan Engineering company, Calcutta and model: DCB-LAB. It is shown in the Appendix I. The electronic digital balance as mentioned earlier in section 4.3 and one more balance of make: Sartorius and model: MC210S were used for weighing the powders before mixing them using the double cone blender. The blending time of 5 minutes and blending speed of 48 rpm (Srinivasa, et al., 2010) was used to prepare 250 gram of IN625 and 1, 3, 5, 7 wt. % SiC (NiP-coated) powder mixture. The time used for different weight percentage of SiC (NiP-coated), is shown in the Table 4.2. Further the blended powders were characterized using Scanning Electron Microscope for Scanning Electron Micrograph (SEM), and Energy Dispersive Spectroscopy (EDS) studies.

**Table 4.2 Blending Time for Different Weight Percentage of SiC (NiP-coated) Particles**

<b>SiC (NiP-coated) (Wt. %)</b>	<b>Total Weight of IN-625 and SiC (NiP-coated) (grams)</b>	<b>Blending Time (minutes)</b>	<b>Blending Speed (rpm)</b>
1	250	5	48
3	250		
5	250		
7	250		

#### 4.7.2 Preparation of Test Specimens

IN625 and IN625-SiC(NiP-coated) composites test specimen for density, surface roughness, micro-hardness, tensile, corrosion and machinability studies were produced with the sintering parameters shown in Table 4.3 using the blended IN625 and SiC (NiP-coated) particles for 1, 3, 5 and 7 wt. %.

**Table 4.3 Process Parameters used for Laser Sintering of IN625-SiC (NiP-coated) Composites**

Laser Power (P) (Watts)	Laser Scan Speed (V) (mm/s)	Beam Dia. (mm)	Hatch Width (mm)	Layer Thickness (mm)	Hatch Spacing ( $\delta$ ) (mm)	Energy Density (J/mm <sup>2</sup> )
240	2.5	0.4	5	0.05	0.3	127.68
	5					63.84
	7.5					42.56
	10					31.92

#### 4.8 CHARACTERIZATION OF IN625 AND IN625-SiC (NiP-Coated) COMPOSITES TEST SPECIMEN FOR MICRO-STRUCTURE, PHYSICAL PROPERTIES, MECHANICAL PROPERTIES, CORROSION BEHAVIOUR AND MACHINABILITY STUDIES OF PROCESSED MMCs USING WEDM

The test specimens from the base plate were separated using wire cut electro discharge machine and further studies on micro-structure, physical properties (density and surface roughness), mechanical properties (micro-hardness and tensile properties), corrosion properties and machinability studies of the processed MMCs using WEDM will be discussed in this section.

### **4.8.1 Micro-structure Studies**

The micro-structure of the IN625 and IN625-SiC (NiP-coated) test specimens was taken after making the surface of the specimens suitable for observation under optical and scanning electron microscope. The sintered test specimens in the inert nitrogen atmosphere were machined to a diameter of 10 mm and 5 mm as per the ASTM standards using precision tool room lathe of make: Schaublin, Switzerland and model: 125 given in the Appendix J. The test specimens were placed in denture based polymer as shown in the Appendix J and then the test specimens were polished using emery paper and diamond paste. The equipments used and the steps followed for surface preparation is given in the Appendix J.

#### **4.8.1.1 Optical Micrograph and Scanning Electron Micrograph Studies**

Optical micrograph studies of IN625 and IN625-SiC (NiP-coated) composites test specimens were done using optical microscope of make: Nikon, Japan and model: Optiphot-100S. The salient features of the optical microscope used are given in Appendix B. A mixture of 10 ml HNO<sub>3</sub>, 15 ml HCl and 10 ml CH<sub>3</sub>-COOH etchant (Dinda, et al., 2009) was used for optical and scanning electron microscopic studies. Scanning Electron Microscope and Energy Dispersive Spectroscopy studies of the polished test specimens for micro-structure were carried out using SEM of make: Carl Zeiss, Germany and model: Neon 40 Crossbeam at NITK, Surathkal.

### **4.8.2 Studies on Physical Properties**

#### **4.8.2.1 Density Studies**

The density of the IN625 and IN625-SiC (NiP-coated) test specimens was measured by Archimedes's principle using electronic balance of make: Sartorius, Germany and model: MC-2105 with an accuracy of 0.01 mg. The test specimens were first weighed in air and then weighed in water. The density evaluation of the IN625-SiC (NiP-coated) test specimens were done as follows:

Weight of the test specimen in air =  $w_1$

Weight of the test specimen in water =  $w_2$

Volume of the specimen =  $w_1 - w_2$ ,

Then density =  $w_1 / [w_1 - w_2]$

#### **4.8.2.2 Surface Roughness Studies**

The surface roughness of the IN625 and IN625-SiC (NiP-coated) composites was measured using confocal microscope of make: Olympus, Japan and model: OLS4000. The surface roughness along the sintered surface of the specimens was measured. The dimensions of the test specimens were 30 x 40 x 3 mm. An area of 2.5 mm x 2.5 mm (5X) was covered during measurement. The confocal microscope is shown in the Appendix K. Surface roughness was measured at three different places on the specimen surfaces and the average value is taken for final reporting.

#### **4.8.3 Studies on Mechanical Properties**

##### **4.8.3.1 Micro-hardness Studies**

The micro-hardness test of the IN625 and IN625-SiC (NiP-coated) specimens was conducted using micro-hardness tester of make: Clemex, Canada and model: ST-2000 and the indentation was measured using Clemex image analyser software. Hardness was measured at five different locations on the sintered specimens, using a 300 g load for a dwell time of 13 seconds. An average of all the five readings was taken as micro-hardness of each specimen. The micro-hardness tester and its salient features are given in Appendix K.

##### **4.8.3.2 Tensile Studies**

###### **4.8.3.2.1 Preparation of Tensile Test Specimen**

The tensile tests were conducted on IN625 and IN625-SiC (NiP-coated) composites using tensile testing equipment INSTRON-5569 at Shriram Institute for Industrial Research, Bangalore. Before conducting the tensile test the composites specimens fabricated using laser sintering machine as per the drawings shown in the Appendix D were machined to the ASTM E8 standards. The tensile specimens were machined to the above standards using CNC lathe shown in the Appendix L of make: Schaublin, Switzerland and model:



125 CCN at GT & TC, Bangalore. The salient features of the CNC lathe is given in the Appendix L.

#### **4.8.3.2.2 Tensile Testing**

The tensile tests were conducted on IN625 and IN625-SiC (NiP-coated) composites using tensile testing equipment INSTRON-5569 at Shriram Institute for Industrial Research, Bangalore. The tensile test equipment used and its salient features are given in Appendix H. Ultimate, yield strength and percentage elongations were evaluated. Scanning Electron Microscope and Energy Dispersive Spectroscopy studies of the fractured surfaces of the composites were carried out using SEM of make: Carl Zeiss and model: Neon 40 Crossbeam at NITK, Surathkal.

#### **4.8.4 Studies on Corrosion Behaviour of MMCs**

Corrosion tests on IN625 and IN625-SiC (NiP-coated) composites were conducted using the salt spray apparatus at Ragavendra Spectro metallurgical laboratory, Bangalore as per the ASTM B117 standards. The specimens were prepared by laser sintering for conducting corrosion test.

The salt spray apparatus shown was used to perform corrosion studies. The salient features of the apparatus and the closed view of the specimens during the corrosion test are shown in Appendix M.

##### **4.8.4.1 Preparation of Corrosion Test Specimen**

The IN625 and IN625-SiC (NiP-coated) composites test specimens were machined to a size of 30 x 40 x 3 mm for conducting corrosion test. Preparation of the specimens was done as per the ASTM G1 standards. The specimens were properly marked for the accurate identification. The test specimens were degreased by cleaning with acetone, rinsed perfectly using water and then dried in hot air. The specimens were then weighed in an electronic digital balance of least count 0.01 mg.

#### 4.8.4.2 Corrosion Testing

The specimens after cleaning and weighing were mounted on the support structure as shown in the Appendix M. The support structure with the test specimens was placed inside the salt spray chamber. The sodium chloride salt solution was prepared mixing 5 parts by mass of sodium chloride in 95 parts of distilled water. The pH salt spray solution was measured at about 25<sup>0</sup>C using a pH meter. The pH of the prepared solution was 6.72. The salt spray test was done using the following process parameters: Temperature within the testing chamber 35±1<sup>0</sup>C, pressure of air of 1.4 bars and condensation rate of 1.15 ml/hr/100 cm<sup>2</sup>. The tests were done for duration of 96, 120 and 144 hours.

The specimens were collected from the salt spray apparatus and cleaned as per ASTM G1 standards. The salt deposition from the surface of the specimens was removed by washing them using running tap water and distilled water. The specimens were submerged in the solution of 20 g of SnO<sub>2</sub> and 50 g of SnCl<sub>2</sub> in 1000 ml of HCl with specific gravity of 1.19 at a temperature of 25<sup>0</sup>C for 10 minutes and the products of corrosion were taken off using soft brush. Finally the specimens were cleaned with tap running water and dried using hot air.

#### 4.8.4.3 Corrosion Rate Calculation

Weight loss because of corrosion was measured with the help of digital electronic balance by drying the specimens using hot air. Repeated weight measurement was done to obtain constant weight after cleaning each specimen. The weight loss was recorded for the specimens for test duration of 96, 120 and 144 hours. As per the ASTM G1 standards the rate of corrosion was calculated as follows:

Rate of corrosion (g/m<sup>2</sup>.hr) = [K x ΔW] / [A x T x D], where,

ΔW= Mass loss in grams

A= Area in cm<sup>2</sup>

T= Exposure time in hours

D= Density in g/cm<sup>3</sup> and

K= Constant=D x 10.

#### **4.8.5 Machinability Studies of Processed MMCs Using WEDM**

The IN625 and IN625-SiC (NiP-coated) composites test specimens with 10 mm diameter and 5 mm length made by laser sintering process were used for the machinability studies. The composite test specimens processed at scan speeds of 2.5 mm/s to 10 mm/s were used for machinability studies. The macrographs of the composite test specimens were obtained using optical microscope of make: Nikon, Japan and model: Optiphot-100S. The density studies done as per the discussion and the values were noted for the composite test specimens. The porosity was calculated by the equation: Porosity = {[Theoretical density – Measured density] / Theoretical density} x 100.

Machinability investigations on the IN625 and IN625-SiC (NiP-coated) composites were conducted on WEDM machine of make: Charmilles technologies, Switzerland and model: Robofil 290 shown in the Appendix N. WEDM of IN625 and IN625-SiC (NiP-coated) composites was done with discharge currents of 10, 15 and 20 A by maintaining the wire speed at 90 mm/min. Brass wire of 0.25 mm diameter was used as electrode material. De-ionised water was employed as di-electric medium. The stop watch was used to record the machining time. Confocal microscope of make: Olympus, Japan and model: OLS 4000 was used to compute the surface roughness of the machined surfaces. The micrographs of the composite test specimens were obtained using optical microscope of make: Nikon, Japan and model: Optiphot-100S and the scanning electron micrographs of the machined surfaces were done by SEM of make: Carl Zeiss, Germany, and model: Neon 40 Crossbeam.

## CHAPTER 5

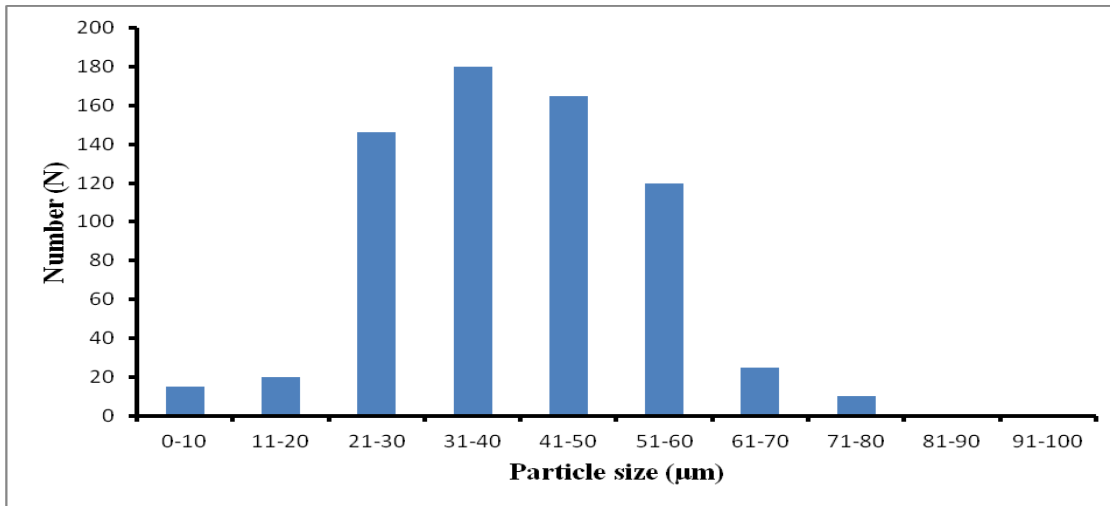
### RESULTS AND DISCUSSION

#### 5.1 PARTICLE SIZE AND MORPHOLOGY

##### 5.1.1 IN625 and SiC Particles

###### 5.1.1.1 Particle Size Analysis and Scanning Electron Micrographs Studies

The particle size analysis of IN625 is shown in the Figure 5.1. It clearly indicates that most of the particles of the procured particles are in the range of 20 to 60  $\mu\text{m}$  in size and very less percentage of them are in the range of 10 to 20  $\mu\text{m}$  and beyond 60  $\mu\text{m}$  size. The SEM of IN625 shown in the Figure 5.2 confirms the size of procured particles matching with the results obtained in particle size analysis.



**Figure 5.1 Particle Size Distribution of IN625 Particles**

The SEM shown in Figure 5.2 reveal that the particles are spherical in shape. EDS analysis shown in the Figure 5.3 of the procured IN625 particles confirms the presence of all the elements as per the certificate provided by the supplier. The elemental analysis also confirms the minimum presence of aluminium and titanium content. The minimum presence of these two elements are very important for developing MMC by laser sintering.

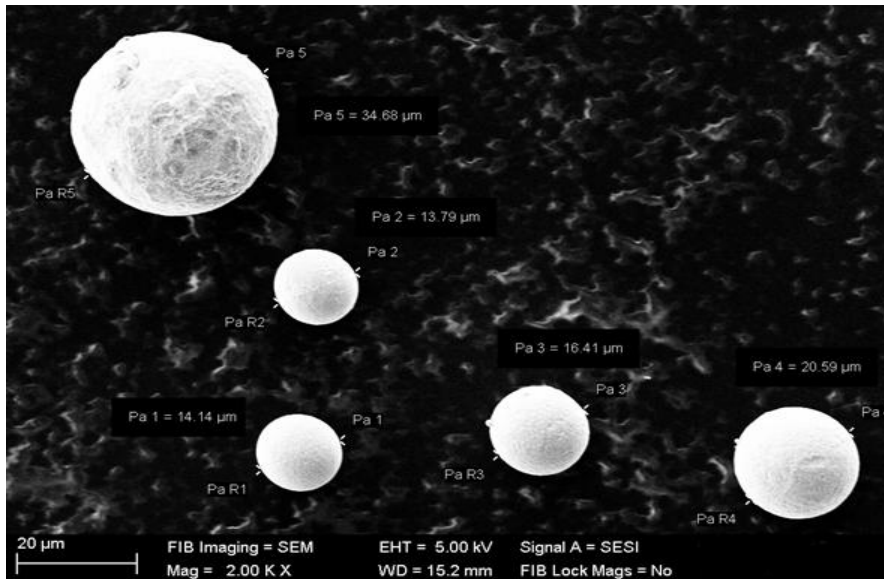


Figure 5.2 SEM Showing Shape and Size of IN625 Particles

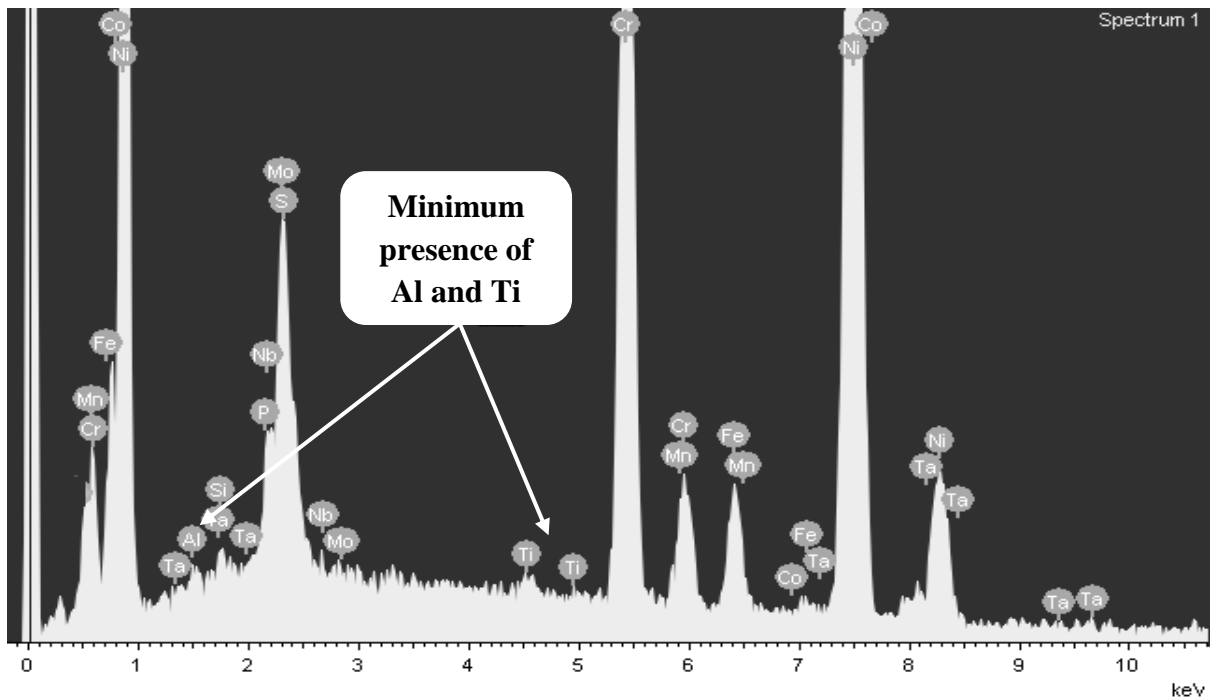
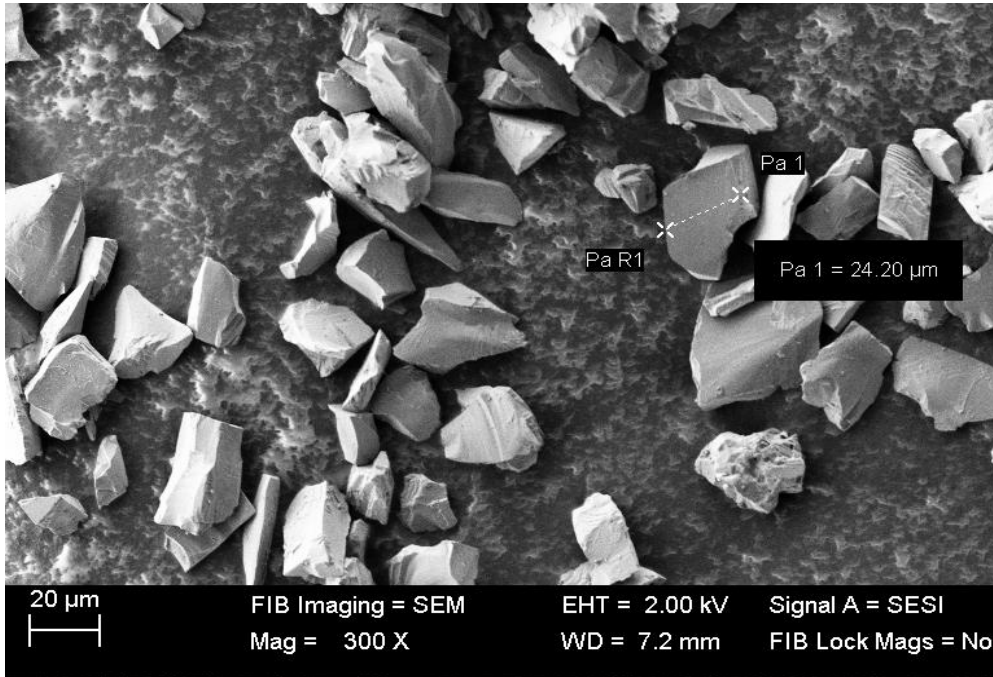
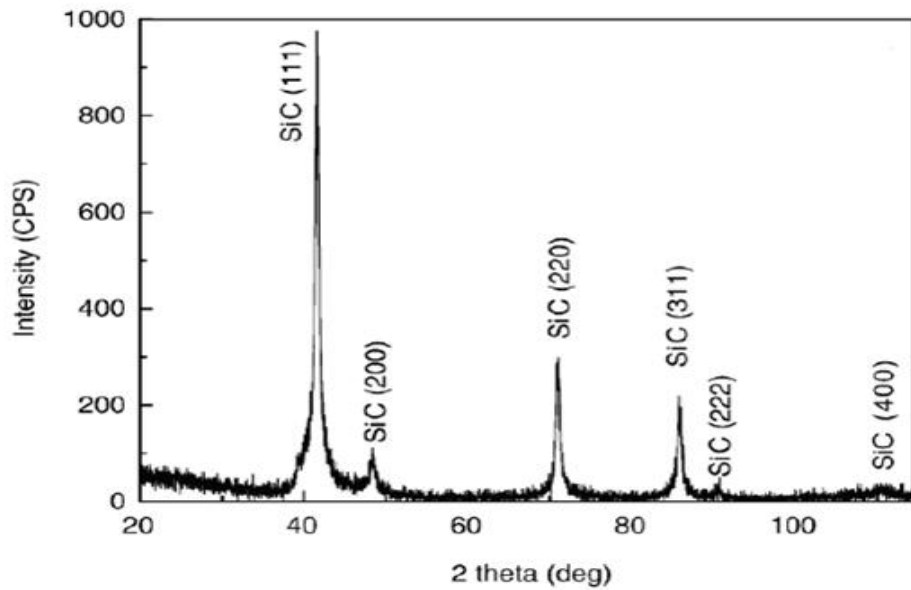


Figure 5.3 Energy Dispersive Spectroscopy (EDS) of IN625 Particles



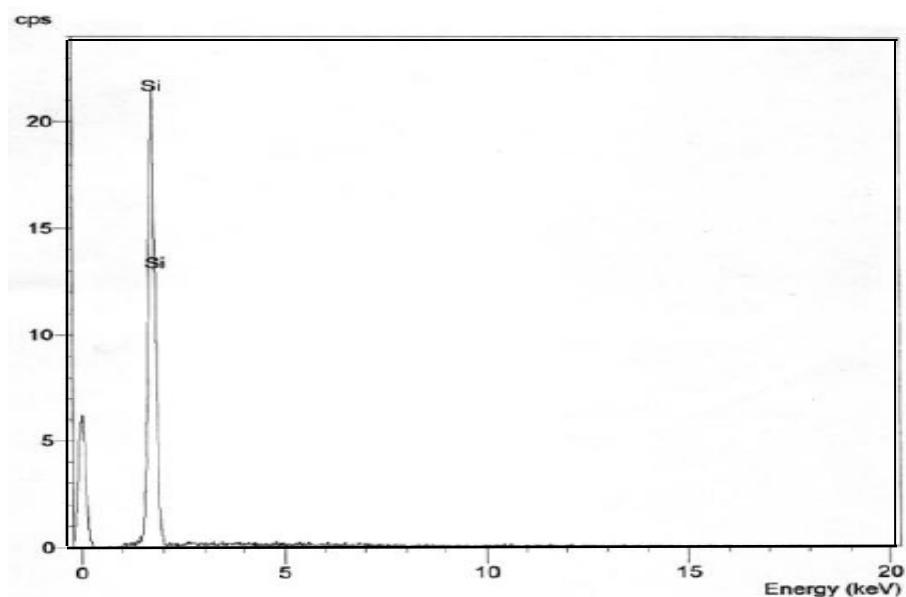
**Figure 5.4 SEM Showing the Shape and Size of SiC Particles**

The SEM of uncoated silicon carbide is shown in Figure 5.4. It clearly shows that the particles are bright and smooth with irregular shape. The average particle size of silicon carbide is around 28μm.



**Figure 5.5 X-ray Diffraction (XRD) Pattern of SiC Particles**

The XRD patterns of the procured SiC particles are shown in Figure 5.5. The X-ray diffraction patterns of the particles clearly shows only the diffraction peaks of SiC. The EDS analysis of the procured SiC particles are shown in Figure 5.6. It clearly indicate the presence of silicon and carbon peaks.



**Figure 5.6 EDS of SiC Particles**

## **5.2 STUDIES ON ELECTROLESS COATING**

### **5.2.1 Nickel-Phosphide Coating on Silicon carbide (SiC)**

#### **5.2.1.1 SEM, EDS and XRD Studies**

The surface of the SiC powders are at first coated with palladium. The SEM of the palladium coated SiC is shown in Figure 5.7. The rough surfaces are observed indicating the presence of palladium coating on SiC particles.

It is once again confirmed by carrying out EDS analysis on palladium coated SiC powder which is shown in the Figure 5.8. EDS analysis of palladium treated SiC powder shows the presence of palladium chloride. This study also confirms that the pre-treatment procedure followed in the experimental work to activate the surfaces of ceramic particles is in accordance with the standard procedure available in different literatures.

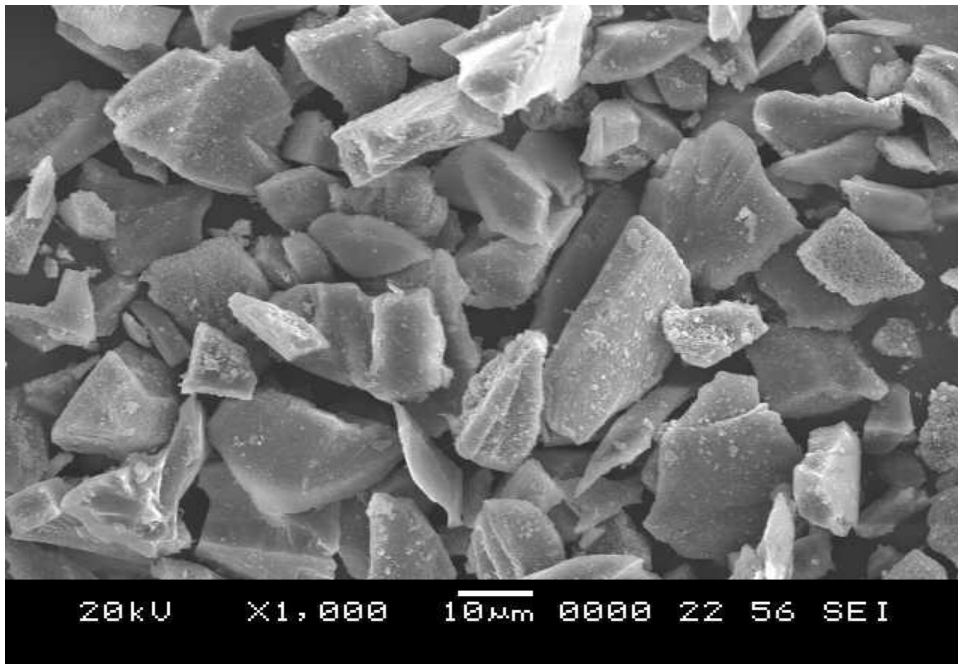


Figure 5.7 SEM of Palladium Coated SiC Particles

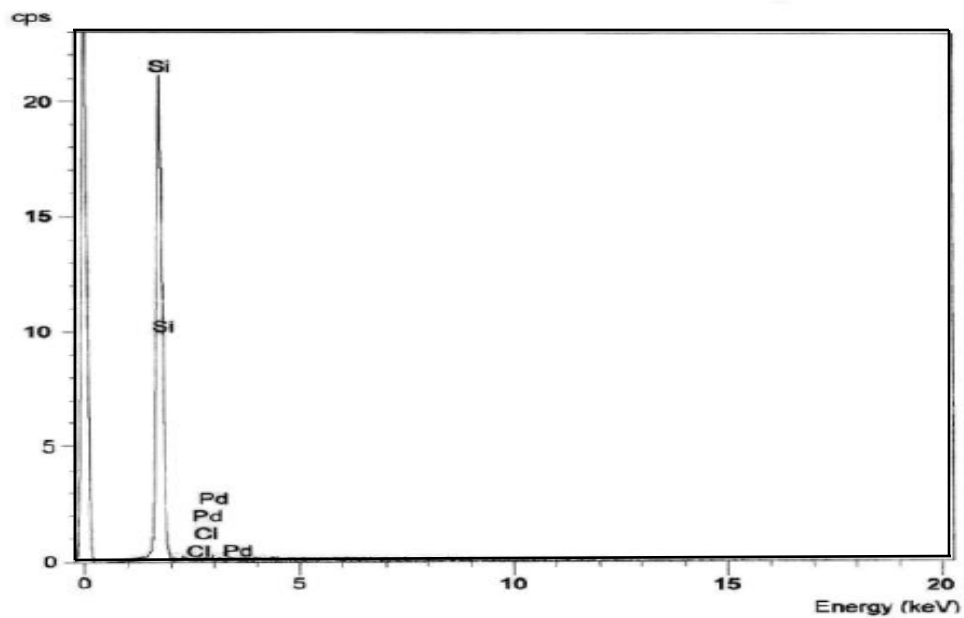
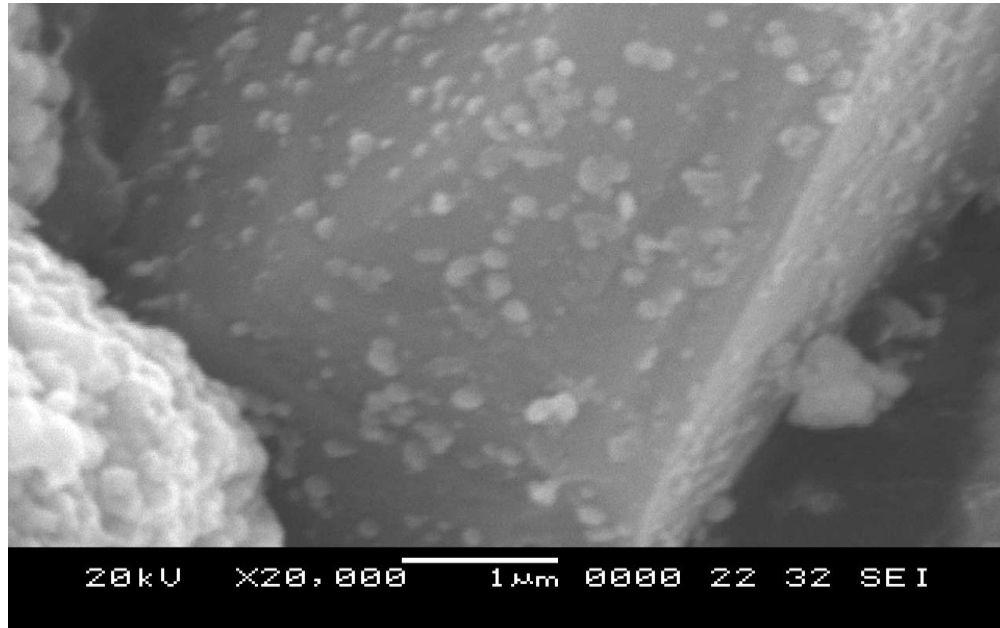


Figure 5.8 EDS of Palladium Coated SiC Particles

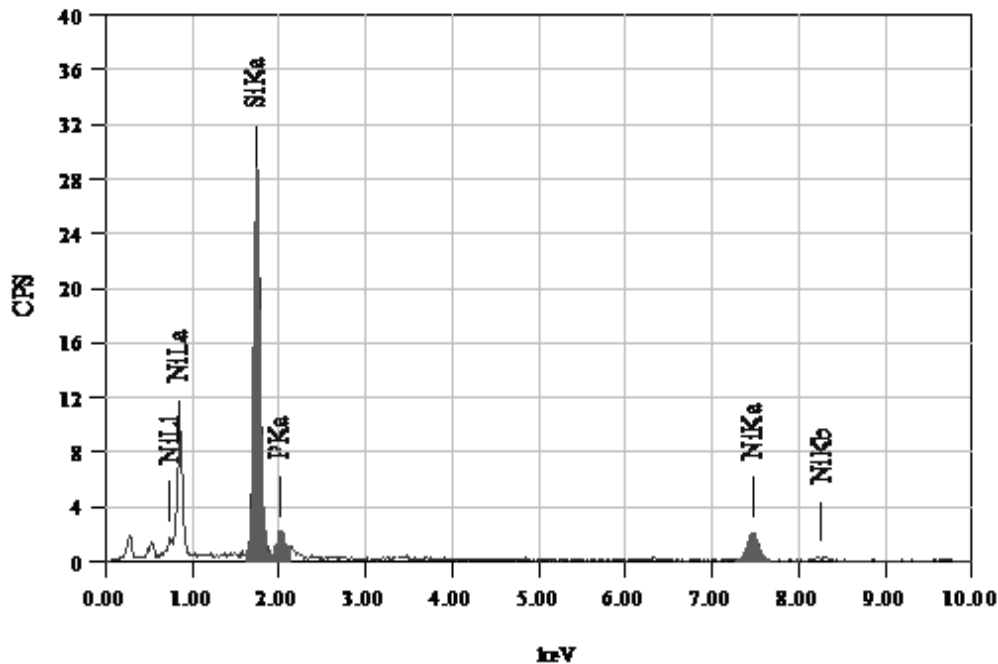


The palladium coated SiC particles is now coated with NiP. The SEM of the NiP coated SiC particles is shown in Figure 5.9.



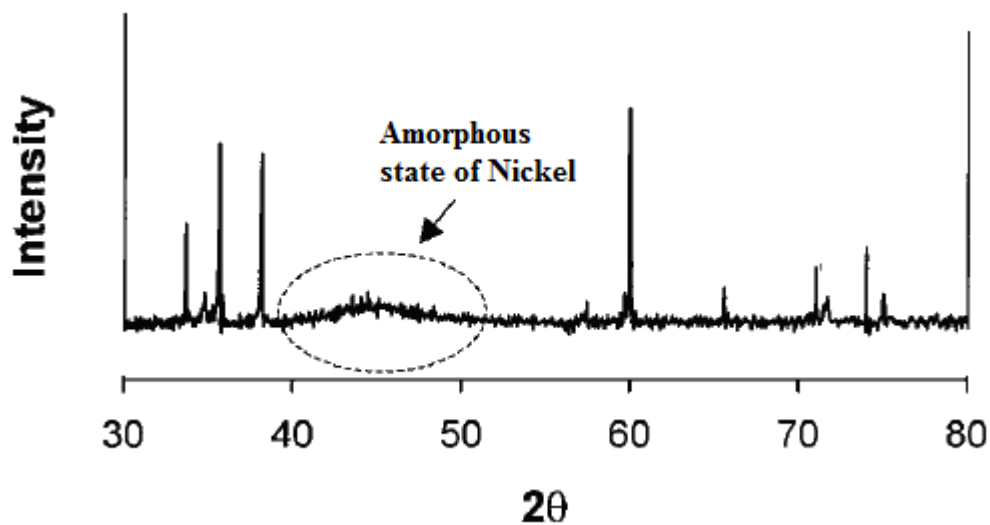
**Figure 5.9 SEM of NiP Coated SiC Particles**

The coated particles shows a uniformly distributed nickel coating on the surface, and at high magnification (X 20,000), a continuous nickel coating is observed over the entire surface; the coating is present on all the regions of the particles regardless of size and shape. The EDS analysis of nickel coated SiC shown in Figure 5.10 indicates the presence of both the nickel and phosphorus. Since, Nickel is low melting eutectic, its presence on the surfaces of the ceramics to be used as reinforcements to develop metal matrix composites (MMCs) will lead to considerable improvement in wettability of the ceramics with the molten matrix. This factor leads to better interfacial bond strength and also minimizes the formation of interfacial complex products such as carbides and silicides.

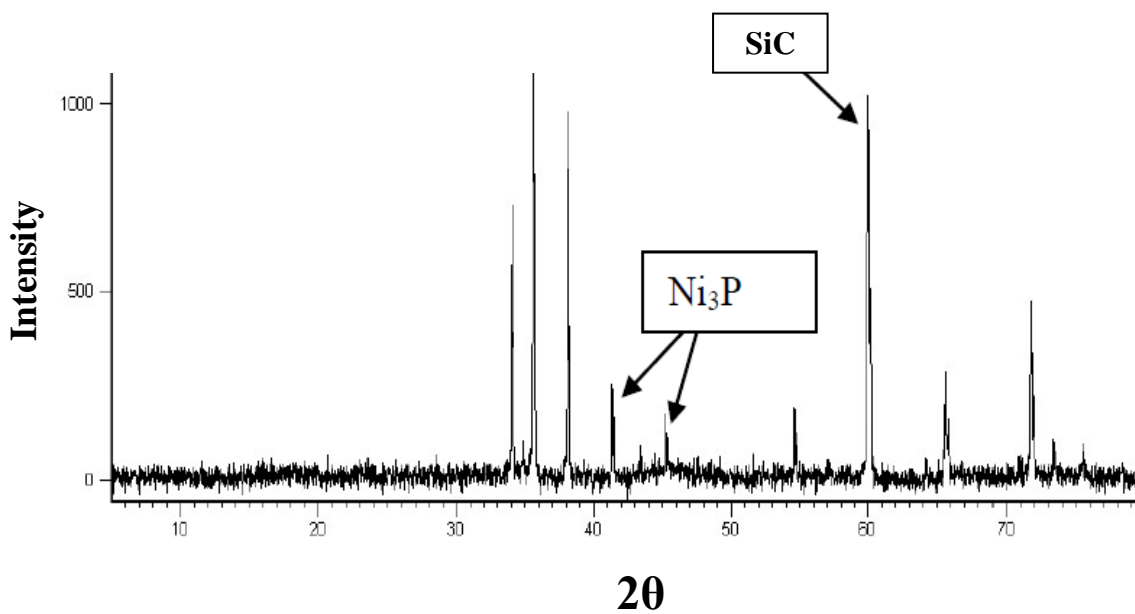


**Figure 5.10 EDS of NiP Coated SiC Particles**

Literature suggests that coating also results in increase in the specific surface area after nickel coating. This is because of the fine nickel particles of about 1  $\mu\text{m}$  found on the outer layer of the deposit and the presence of micro voids between the fine trapped particles. The literature also suggests that electroless nickel deposits, which have not been heat-treated, can have structures ranging from extremely small crystallites to those that are fully amorphous. So the XRD studies have been made to check this suggestion given in the literature. The XRD studies in the Figure 5.11 indicate a pronounced broad band in the region corresponding to the Ni (111), signifying that this particular deposits contain the metal in amorphous state. Now this coated particles upon heat treatment at 400<sup>0</sup>C, transformed into a mixture of crystalline Ni and Ni<sub>3</sub>P. XRD result is shown in Figure 5.12 on the heat treated particles indicates sharp peaks corresponding to a fully crystallized structure. Therefore it is clear that amorphous character of coated nickel particles becomes crystalline after heat treatment, showing deposits containing the stable Ni and Ni<sub>3</sub>P phases.



**Figure 5.11 XRD Pattern of Coated SiC before Heat-treatment**



**Figure 5.12 XRD Pattern of Ni<sub>3</sub>P Coated SiC after Heat-treatment**

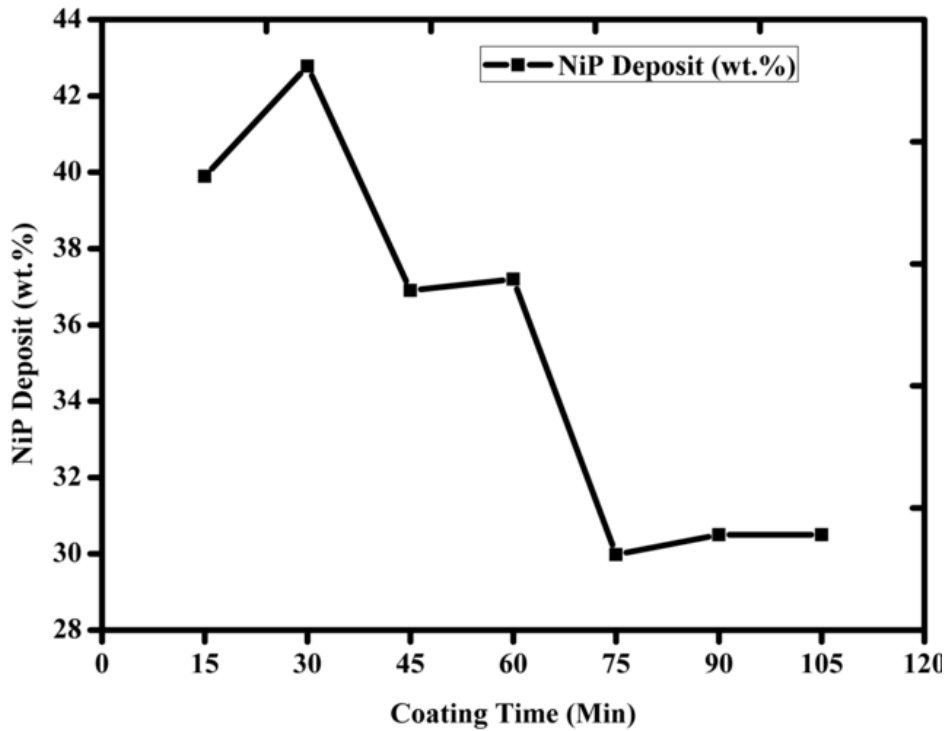
### 5.2.1.2 Effect of Coating Time on the NiP Deposition on SiC Particles

The effect of coating time on the deposition of nickel on silicon carbide particles is shown in Figure 5.13. It is observed that initially upto a time period of 30 minutes, an

increase in holding time of the ceramic particles in the electroless bath leads to an increase in deposition of nickel. With further increase in holding time, a gradual decrease in the deposition of nickel on the ceramic particles is being observed. This can be imputed to following:

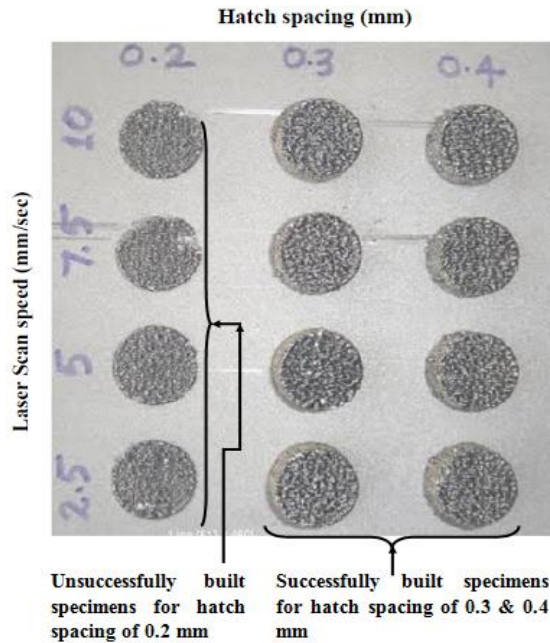
- a) Lowering of coating efficiency due to changes in pH values of the electroless bath and also due to rise in temperature of the bath because of stirring.
- b) Electroless nickel bath solution will be exhausted because of availability of lesser amount of nickel plating solution, when it is compared with larger surface area of SiC particles.
- c) The longer stirring time resulted in debonding of coating from SiC particles.

Similar results were observed by the other researchers during coating of NiP on SiC particles by the electroless nickel coating process (Leon, et al., 2000).



**Figure 5.13 Coating Time Effect on NiP Deposition**

### 5.3 OPTIMIZATION OF LASER SINTERING (PROCESSING) PARAMETERS



**Figure 5.14 Laser Sintered IN625 Test Specimens**

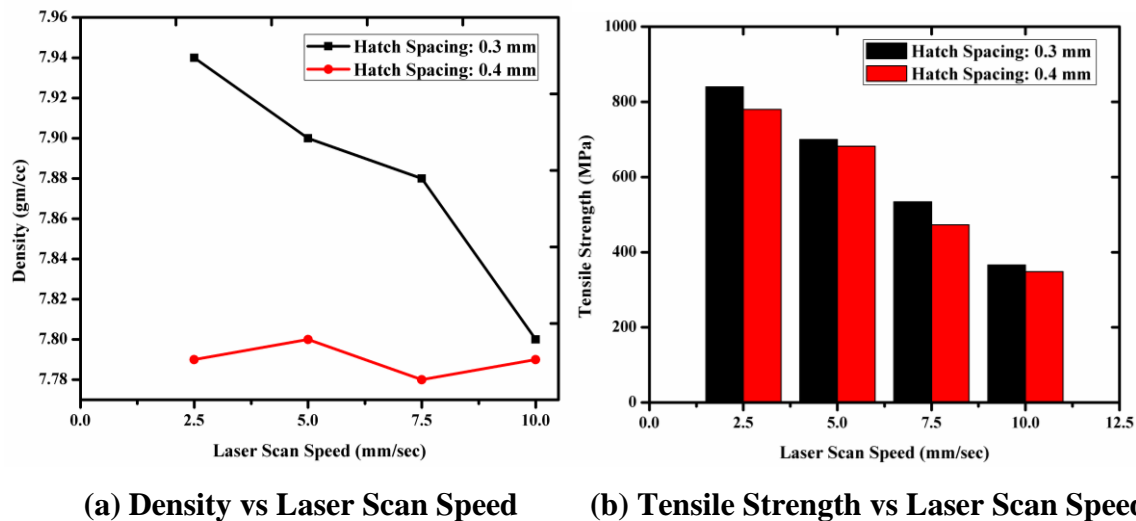
Figure 5.14 shows the photograph of IN625 specimens sintered using the parameters mentioned in the Table 4.9. It can be observed from the figure that specimens with hatch spacing of 0.2 mm were not built to full height for all laser scan speeds. Sintering was done to some height for laser scan speed of 2.5 and 5 mm/s and was not possible for laser scan speed of 7.5 and 10 mm/s. The sintering process cannot be continued further because of jamming of the re-coater blade. The jamming of the re-coater blade can be attributed to laser energy density, since laser energy density is proportional to laser power and inversely proportional to laser scan speed. Increased laser scan speed results in large deposits of un-melted particles and also at higher laser scan speed, the total amount of heat energy may not be quite sufficient to completely melt the particles. One more reason for jamming of the re-coater blade at lower hatch spacing may be attributed to balling effect. The balls formed hinder the movement of re-coater blade. Then the sintering was carried out with hatch spacing of 0.3 mm, there was no jamming of the re-coater blade and specimens were built almost to the required height of 7 mm and diameter 12 mm, for

all laser scan speeds. Then the specimens were successfully sintered for hatch spacing of 0.4 mm, but with lesser efficiency in dimensions compared to hatch spacing of 0.3 mm. So, from the Figure 5.14 it is also evident that hatch spacing of 0.3 mm yields specimens with better dimensions compared to hatch spacing of 0.4 mm.

The laser processed specimens from the substrate were removed using Wire Electrical Discharge Machine and characterized further for density, and tensile strength and microstructure to optimize the process parameters.

### 5.3.1 Density, Tensile strength and Microstructure Studies

The effect of laser scan speed on density and tensile strength of IN625 specimen's laser processed at hatch spacing of 0.3 mm and 0.4 mm are shown in Figure 5.15 (a) and Figure 5.15 (b). It can be imputed from the graphs that density and tensile strength of the specimen's laser processed at hatch spacing of 0.3 mm are better than at hatch spacing of 0.4 mm.

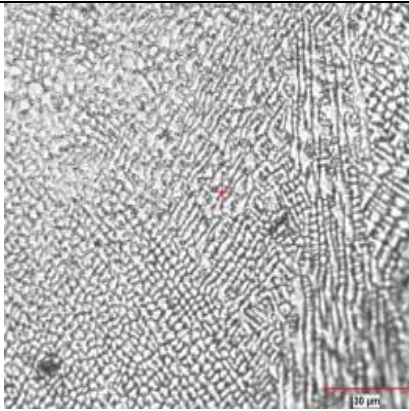
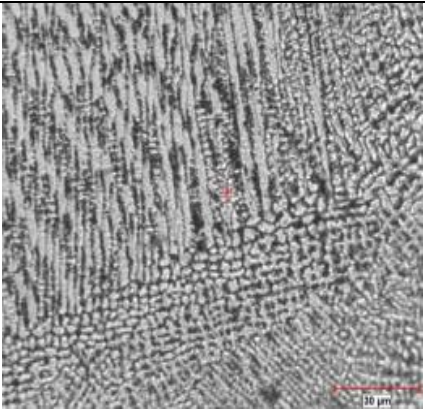
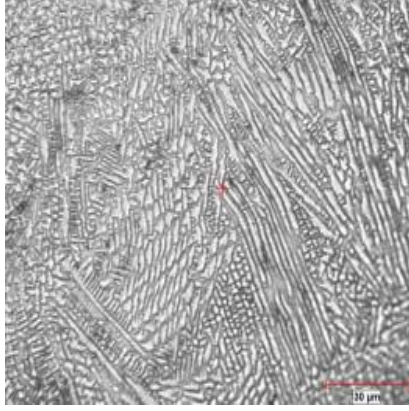
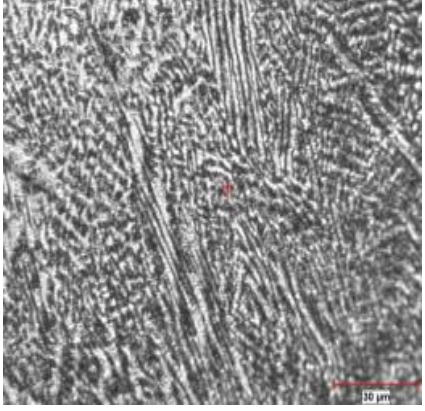


**Figure 5.15 Effect of Laser Scan Speed on Density and Tensile Strength of IN625 Processed at Hatch Spacing of 0.3 mm and 0.4 mm.**

The decrement in density of laser processed IN625 with increment in scan speed of laser is in agreement with several other researchers (Badrossamay, and Childs, 2007; Simchi, and Pohl, 2003) and it can be explained in terms of laser energy. Laser energy density is

proportional to the laser power and inversely proportional to the laser scan speed (Niu, and Chang, 2000).

At lower scan speeds, higher heat energy is induced into the powder bed, leading to an increase in melt temperature. Higher melt temperature leads to less viscosity, lower contact angle and higher Marangoni flow and capillary force, resulting in higher densification (Zhu, 2005). Higher the densification results in better strength and hence higher tensile strength can be noticed in laser processed specimens at lower scan speed.

Hatch Spacing (in mm)	Laser Scan Speed (mm/s)	
	2.5	10
0.3		
0.4		

**Figure 5.16 Optical Micrographs of Laser Processed IN625 at 0.3 and 0.4 mm Hatch Spacing**

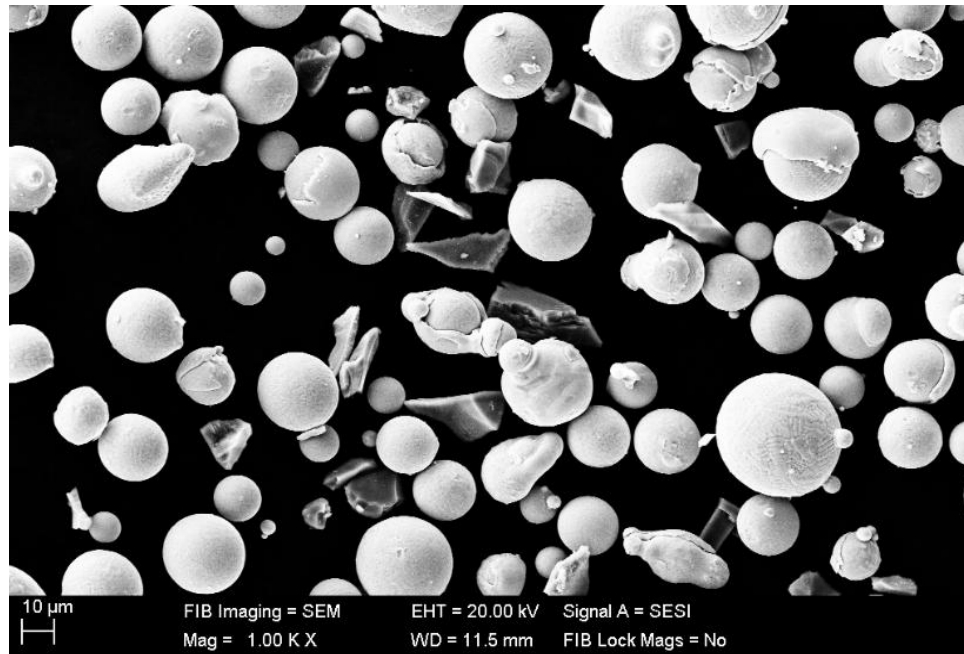
At higher scan speed, lower energy density is not sufficient to melt all the particles and therefore un-melt particles are left in the laser processed specimens, which results in higher porosity. The porosity of the specimens results in decrement in the strength and hence a reduction in the tensile strength with increment in the laser scan speed can be observed. These observations are confirmed by the micro-structure studies of IN625 also. Figure 5.16 shows the optical micrographs of laser sintered IN625. The microstructure examination clearly indicates the presence of less dendritic and more cellular microstructure for hatch spacing of 0.3 mm and more dendritic microstructure is observed for hatch spacing of 0.4 mm. The cellular microstructure is attributed to reduced cooling rate and the dendritic microstructure is attributed to rapid cooling rate (Paul, et al., 2007).

Thus from the above discussions it is considered that the specimens at hatch spacing of 0.3 mm as the potential candidature compared to specimens at hatch spacing of 0.4 mm for laser processing of MMCs by DMLS process.

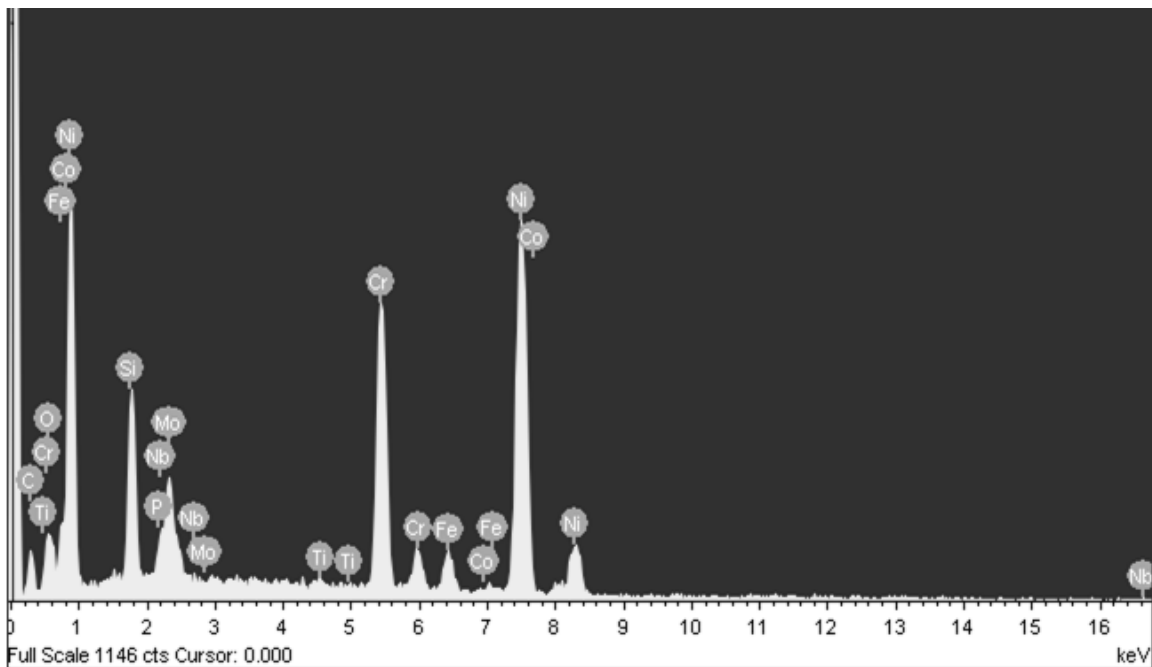
#### **5.4 STUDIES ON BLENDING OF IN625 AND SiC (NiP-COATED) PARTICLES**

Blending of IN625 and SiC (NiP-coated) particles by double cone blender is discussed in this section. Best mixing of the particles is achieved with blending speed of 48 rpm and blending time of 5 minutes (Srinivasa, et al., 2010). The best mixing achieved in this experimentation can attributed to the fact that the IN625 and SiC (NiP-coated) particles are less than 50  $\mu\text{m}$  size. It is reported that particulate mixture with particles less than 75  $\mu\text{m}$  will assist in mixing rather than in segregation. The homogeneity of the particulate mixture for different wt. % of SiC (NiP-coated) is evaluated by Scanning Electron Micrograph and Energy Dispersive Spectroscopy studies. The micrograph shown in Figure 5.17 and the spectroscopy studies shown in Figure 5.18 clearly reveal the presence of silicon carbide and IN625 in the composite particulate mixture.





**Figure 5.17 SEM of IN625-1 Weight Percentage SiC (NiP-coated) Particulate Mix**




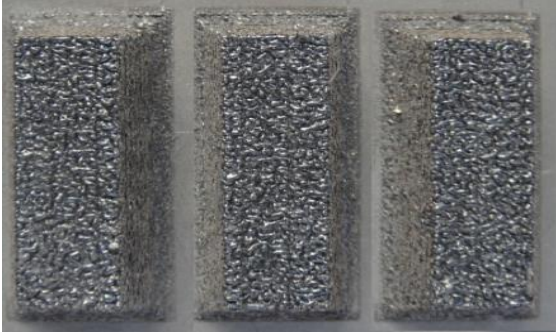
**Figure 5.18 EDS of IN625-1 Weight Percentage SiC (NiP-coated) Particulate Mix**

IN625-SiC (NiP-coated) composites up to 5 wt. % of reinforcement was successfully built in nitrogen atmosphere. However, composites with 7 wt. % of SiC (NiP-coated) reinforcement could not be produced successfully because of jamming of re-coater blade

with the sintered surface. The jamming occurs because of the uneven sintered surface caused by thermal cracks. Thermal cracks can be attributed to the difference in the thermal properties such as thermal conductivity, co-efficient of thermal expansion and laser absorptance of IN625 and silicon carbide particles. The intensity of thermal cracks increases with increase in reinforcement, as the laser absorptivity of SiC is more than that of IN625.

### 5.5 TEST SPECIMENS BY DMLS PROCESS

IN625 and IN625- 1, 3, 5 wt. % SiC (NiP-coated) composites were successfully produced in inert nitrogen atmosphere, at laser scan speed of 2.5, 5.0, 7.5 and 10 mm/s for density, micro-structure, micro-hardness, machinability, tensile strength, surface roughness and corrosion studies as shown in the Figure 5.19.

<b>Test Specimens Produced by Laser Sintering Process</b>	
<b>Density / Micro-structure / Micro-hardness /Machinability</b>	
<b>Tensile</b>	



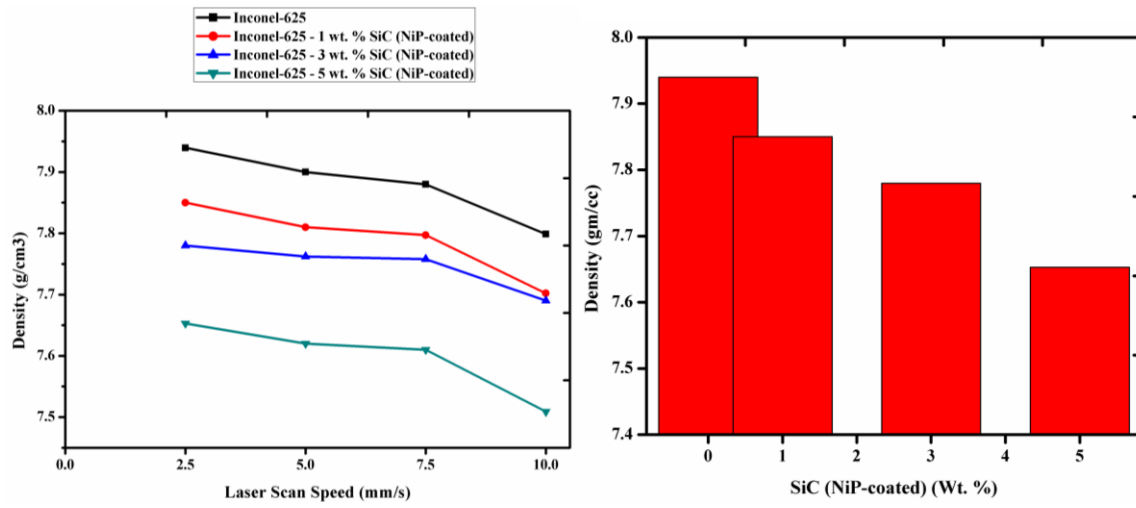
**Figure 5.19 Test Specimens Produced by DMLS Process**

The sintered specimens on the substrate were removed using wire electrical discharge machine and characterized for physical, mechanical, micro-structure, corrosion resistance and machinability.

## **5.6 CHARACTERIZATION OF IN625-SiC (NiP-coated) COMPOSITE SPECIMENS FOR PHYSICAL PROPERTIES**

### **5.6.1 Density**

The decrease in density of laser processed IN625 and IN625-SiC composites can be explained in terms of the laser energy. The energy density of the laser is proportional to the power of laser and inversely proportional to the scan speed of laser (Calignano, et al., 2013).



(a) Density vs Laser Scan Speed      (b) Density vs SiC(NiP-coated) (in wt %)

**Figure 5.20 Effect of Laser Scan Speed and Weight Percentage of Reinforcement on Density**

The variation in density with increase in speed is shown in Figure 5.20 (a). At lower scan speeds, higher heat energy is induced into the particle-bed, leading to an increase in melt temperature. High temperature of the melt leads to less viscosity, higher capillary force and lower contact angle, resulting in higher density (Wilson, and Shin, 2012). At higher laser scan speed, the lower energy density is not good enough to melt all the particles and therefore un-melt particles are left in the laser processed part, which reduces the density. Also the lower energy density induced into the particle-bed, is insufficient for the full melting and therefore the high viscous melt spheroidises to form spheres whose diameter is approximately equal to the laser beam diameter. The formation of such spheres (balling) will lead to poor bonding and high porosity in the laser processed part. The resultant effect of balling is poor surface quality, and decrease in density as a consequence of pores (Gu, and Shen, 2008). Balling effect in the composites is suppressed by the reinforcements due to higher laser absorption, leading to increase in the melt temperature and thus decreasing its viscosity (Simchi, and Godlinski, 2008).

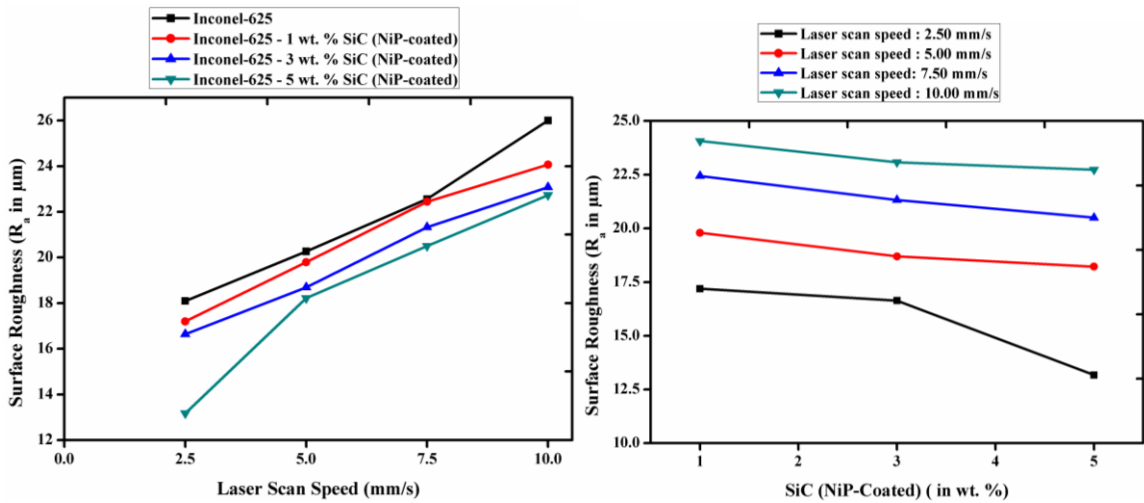
The decrease in the density of the composites as shown in Figure 5.20 (b) can be imputed to the lower density of NiP-coated SiC reinforcement when compared with IN625 matrix. The density of SiC and IN625 are 3.2 and 8.44 g/cc respectively. The population of

reinforcement per unit volume increases with addition of more weight percentage of SiC. Therefore, the density of the composites decreases with increase in percentage of the reinforcement (Li, et al., 2000). Reduction in density with addition of SiC weight percentage is significant in case of 5 wt. % of SiC reinforcement, where a considerable 3.8 % reduction in density with IN625 is observed for a laser scan speed of 2.5 mm/s.

### 5.6.2 Surface Roughness

The surface roughness measured along the laser processed surface of IN625 and IN625-SiC (NiP-coated) composites, processed in inert nitrogen atmosphere is discussed in this section.

The laser scan speed effect on the surface roughness of the laser processed Inconel-625 and IN625-SiC (NiP-coated) composites are shown in Figure 5.21 (a). It is evident that the surface roughness increases with increase in laser scan speed. Further, it is observed that the surface roughness value of IN625 is highest in comparison with its composites. The surface roughness ( $R_a$ ) for IN625 and IN625-SiC (NiP-coated) composites are 26  $\mu\text{m}$  and 22.73  $\mu\text{m}$  respectively, processed at 10 mm/s. Confocal microscope or Macrographs of the IN625 processed at laser scan speed of 2.5 mm/s and 10 mm/s is shown in Figure 5.22.



(a) SR vs Laser Scan Speed

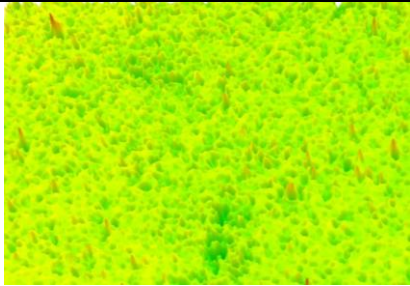
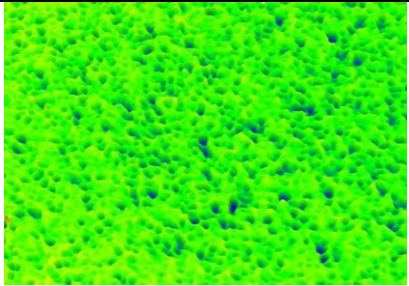
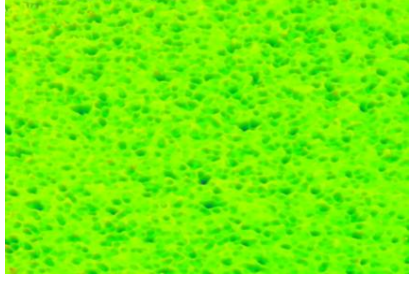
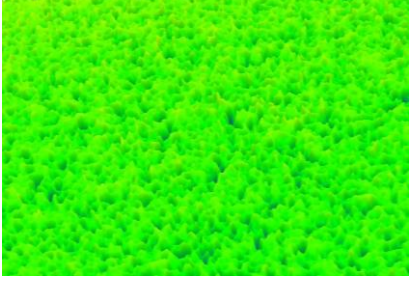
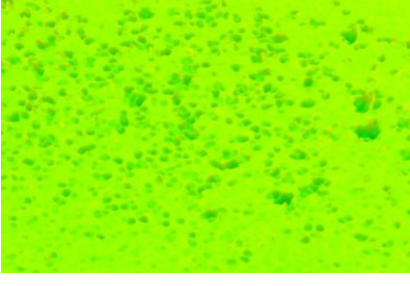
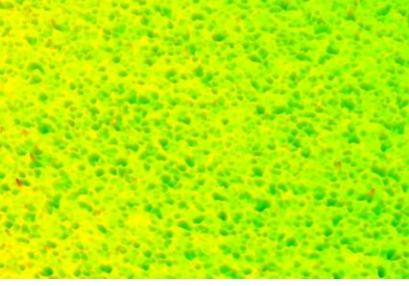
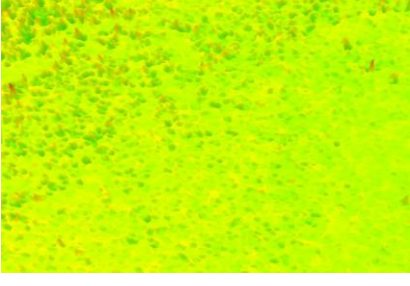
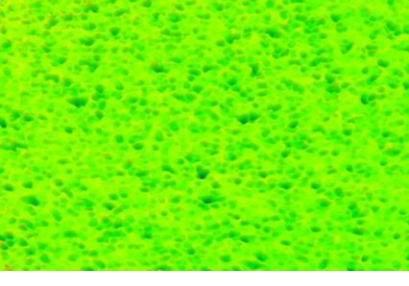
(b) SR vs SiC(NiP-coated) (in wt %)

Figure 5.21 Effect of Laser Scan Speed and Weight Percentage of Reinforcement on SR

It is observed from these figures that IN625 processed at laser scan speed of 2.5 mm/s are smooth compared with those laser processed at 10 mm/s. The variation in the surface roughness with laser scan speed can be explained in terms of laser energy density as per discussions in density.

The laser scan speed is having the greatest influence on the surface roughness during the DMLS process (Calignano, et al., 2013). Lower laser scan speed leads to higher laser energy density as laser energy density is inversely proportional to the laser scan speed (Das, et al., 1998). Surface roughness depends on laser power density and line spacing (Song, 1997). At lower laser scan speed, full melting of powders takes place, resulting in reduced melt viscosity, balling effect and increased melt-cylinder diameter, leading to better connectivity and reduced inter-pore size. Higher laser scan speed leads to lower energy density resulting in partial melting and higher viscosity leading to balling effect. The balling effect results in poor surface finish.

The variations of surface roughness of IN625-SiC (NiP-coated) composites with wt. % SiC (NiP-coated) reinforcement is shown in Figure 5.21 (b). It can be observed that surface roughness decreases with increase in wt. % of reinforcement. Further, it is observed that the surface roughness values are highest for IN625 and least for IN625-5 wt. % SiC (NiP-coated) composite. The surface roughness values (Ra) of IN625 and 1 wt. %, 5 wt. % SiC (NiP-coated) reinforced composites processed at 2.5 mm/s are 18.10, 17.19 and 13.17 respectively. The macrographs of the IN625-SiC (NiP-coated) composites processed at a laser scan speed of 2.5 and 10 mm/s are shown in Figure 5.22.

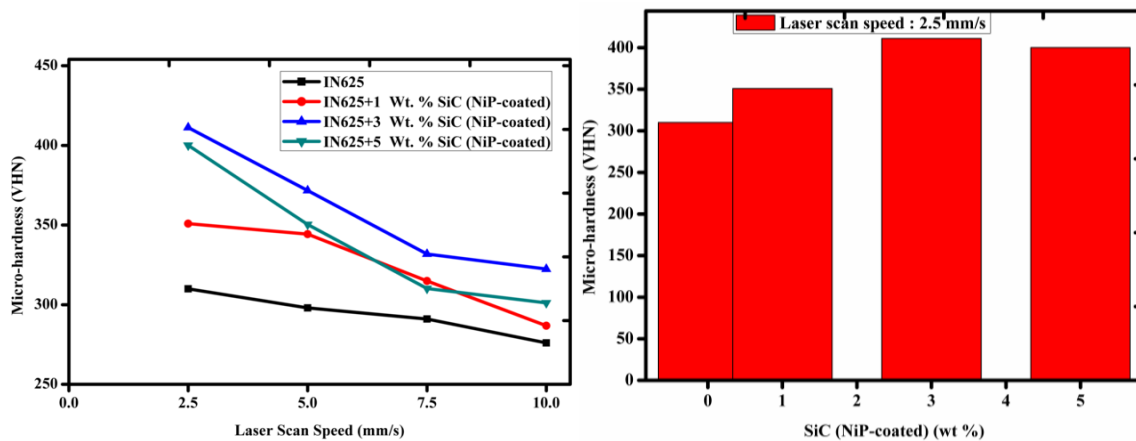
Laser Processed Parts	Laser Scan Speed	
	2.5 mm/s	10 mm/s
IN625		
IN625 - 1 wt. % SiC (NiP-Coated)		
IN625 - 3 wt. % SiC (NiP-Coated)		
IN625 - 5 wt. % SiC (NiP-Coated)		

**Figure 5.22 Confocal Macrographs of IN625 & IN625-SiC (NiP-Coated) Composites**

## 5.7 CHARACTERIZATION OF IN625-SiC (NiP-coated) COMPOSITE SPECIMENS FOR MECHANICAL PROPERTIES

### 5.7.1 Micro-hardness

The improvement in the micro-hardness of the IN625 and Ni-P-coated IN625 composites as shown in Figure 5.23 (a) at lower scan speed can be attributed to the increase in density of laser processed parts. Density of the laser processed parts increases with decrease in laser scan speed. As the hardness is because of resistance to plastic deformation, there is an increased resistance to plastic deformation because of increased density, and hence increase in hardness. The higher hardness of SiC and addition of hard phase into IN625 matrix results in improvement in composite hardness with weight percentage increase of the SiC reinforcement (Wilson, M.J., and Shin, Y.C., 2012) as shown in Figure 5.23 (b).



(a) Micro-hardness vs Laser Scan Speed (b) Micro-hardness vs SiC(NiP-coated)(in wt %)

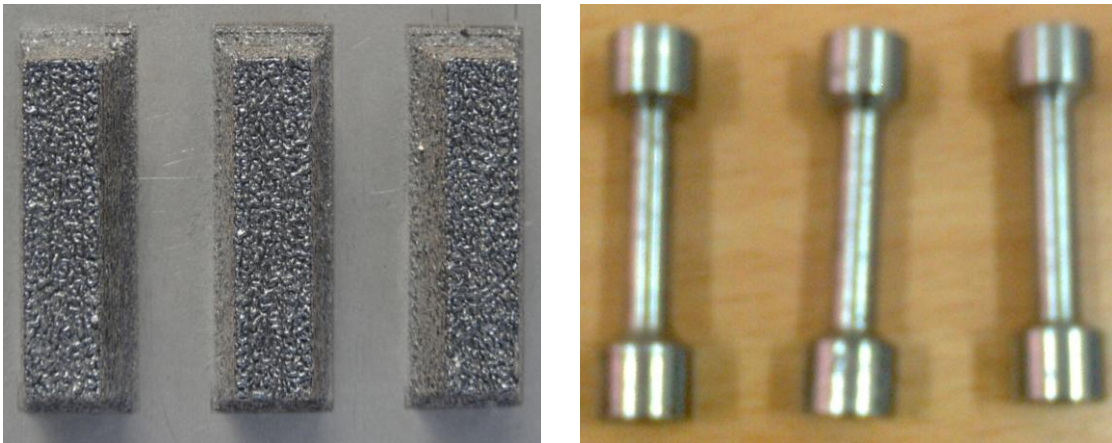
**Figure 5.23 Effect of Laser Scan Speed and Weight Percentage of Reinforcement on Micro-hardness**

Figure shows that there is about 13 to 33 % improvement in micro-hardness with the addition of 1 to 3 wt. % reinforcement into the matrix of IN625 for a laser scan speed of 2.5 mm/s. So, there is a significant improvement in the micro-hardness of the composites by adding different wt. % of SiC compared to addition of other carbides such as TiC into the matrix of IN625 (Bi, et al., 2013). One more reason for micro-hardness improvement



can be attributed to increased density of dislocation at the matrix-reinforcement interface, which will lead to lowering of mobility of dislocation, which in turn retards the plastic deformation. Higher resistance to plastic deformation results in higher micro-hardness. The increase in the dislocation density can be mainly attributed to the difference in the co-efficient of thermal expansion (CTE) of IN625 and SiC (Zheng, et al., 2010). The CTE of IN625 and SiC are 12.8 and 4.8 respectively. Further, the significant improvement in the micro-hardness of the laser processed composites can be attributed to excellent bonding between the reinforcing particle and the matrix as evident from the optical and scanning electron micrographs shown in Figure 5.27 and 5.28. Thus laser deposition helps in simultaneous building of a material with low density and higher micro-hardness.

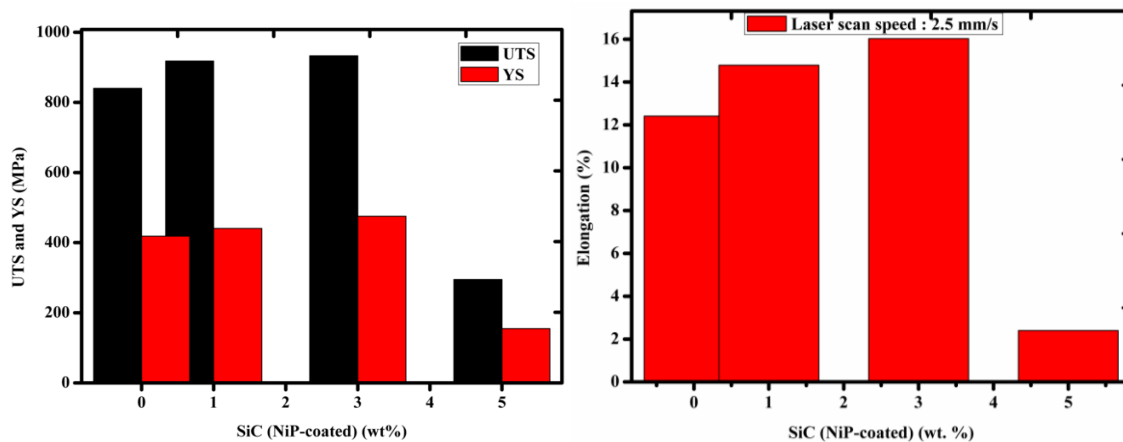
### 5.7.2 Tensile Properties



**(a) & (b) Tensile Specimens before and after machining as per ASTM E8 Standard  
Figure 5.24 Laser Processed IN625 Composite Specimens at 0.3 mm Hatch Spacing**

Figure 5.24 (a) and Figure 5.24 (b) shows the photograph of tensile specimens before and after machining for evaluating ultimate tensile strength (UTS), yield strength (YS) and elongation. The tensile specimens were deposited as shown in the figure by making fillet all round the bottom side of the specimen for the purpose of thermal gradient and to avoid warpage of build parts during laser deposition. The out puts of the tensile test of the laser

deposited IN625, IN625-1 wt. % SiC, IN625-3 wt. % SiC, IN625-5 wt. % SiC MMCs are summarised in the Figure 5.25 (a) and Figure 5.25 (b). The laser deposited IN625 MMCs shows a significant improvement in the UTS, YS and reduction in elongation compared to laser deposited IN625 for a laser scan speed of 2.5 mm/s. With the addition of 3 wt. % of SiC, the UTS and YS increases by 11.92 % and 9.93 % respectively, compared to laser deposition of IN625. The increasing trend is observed for UTS, and YS with increase in addition of SiC into IN625 matrix upto 3 wt. % and further addition of SiC has resulted in drastic reduction in UTS, and YS. The addition of SiC results in absorption of larger part of the incident laser beam; this in turn improves the solidification with creation of more grain boundaries. More grain boundaries mean more opposition to dislocation which finally results in strengthening of the material. The refractory effect of SiC particles also results increased dislocation density. Better flowability and improvement of interfacial behaviour between reinforcement and the matrix because of NiP coating on SiC also results in increased strength and reduction of porosity.

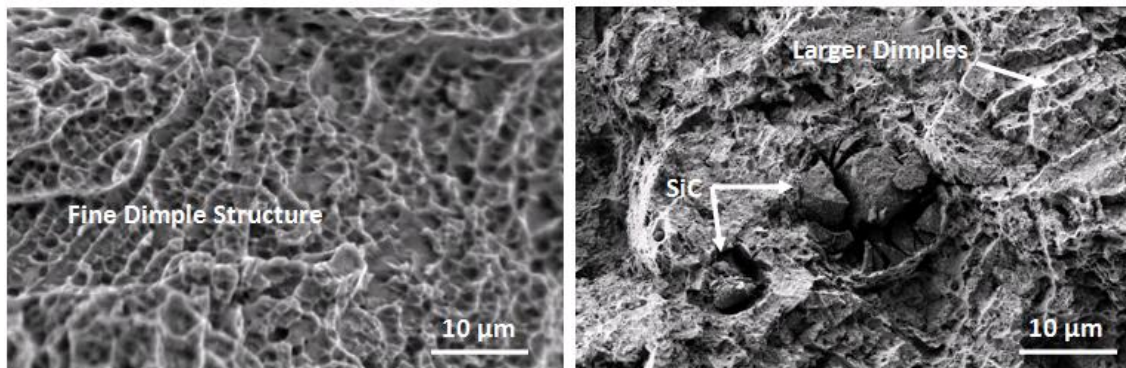


**(a) UTS & YS vs wt. % of SiC (NiP-coated) and (b) % Elongation vs wt. % of SiC (NiP-coated)**

**Figure 5.25 Effect of Weight Percentage of Reinforcement on UTS, YS and % Elongation**

The fracture surface of the pure IN625 shown in Figure 5.26 exhibits a fine dimpled surface, which is the characteristic of dimpled ductile mode of failure with good tensile properties, whereas IN625 with 5 wt. % SiC shows dimples of larger size, which is the characteristic of brittle mode of failure with poor tensile properties because of increased

weight percentage of SiC particles. The drastic reduction in UTS, YS and elongation with the increase in SiC wt. % beyond 3 can be attributed to increase in thermal cracking and due to large stress concentration near the reinforcement leading to premature failure during straining because of thermal mismatch between the IN625 matrix and SiC reinforcement. This inference is in agreement with other researchers also (Zheng, et al., 2010).



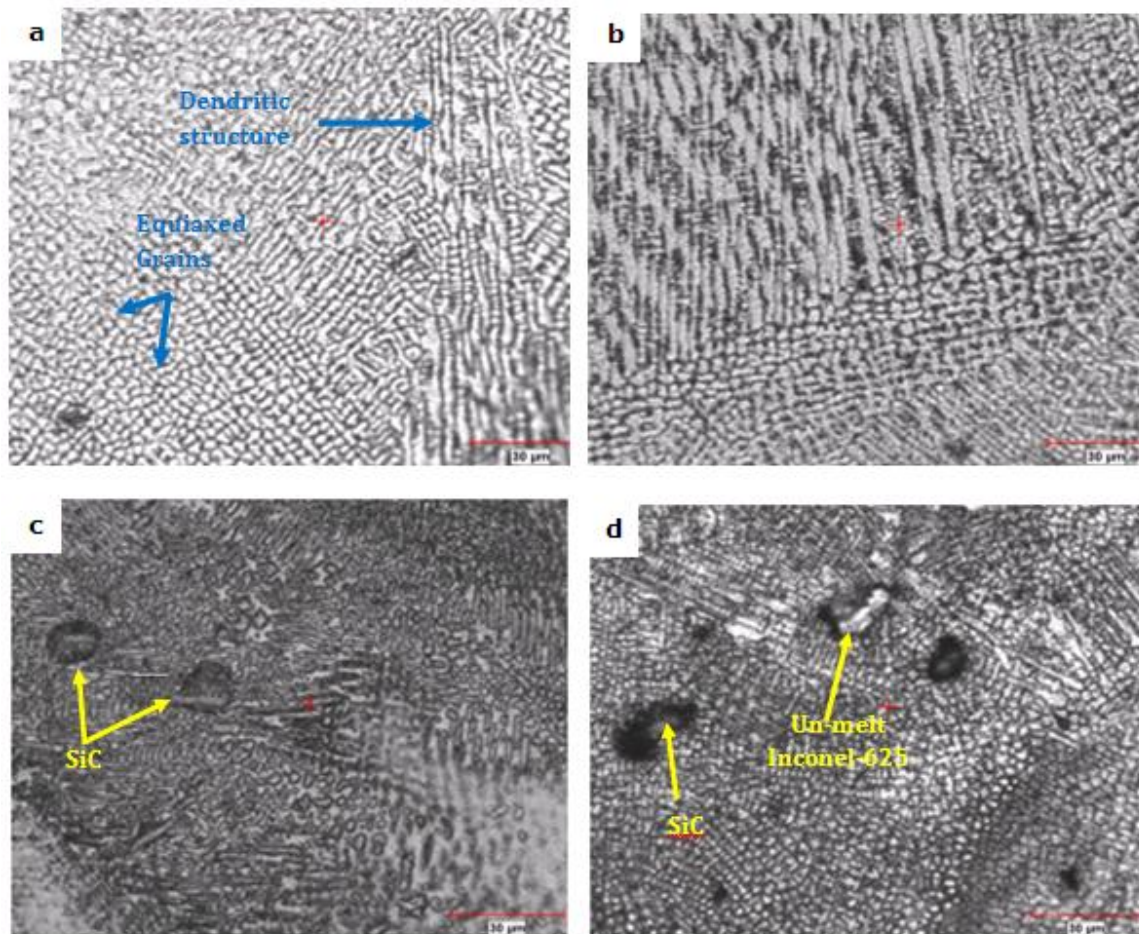
**Figure 5.26 Fractured Surfaces for IN625 and IN625 - 5 Weight Percentage SiC (NiP-coated)**

## **5.8 MICRO-STRUCTURE ANALYSIS**

Figure 5.27 and Figure 5.28 shows the optical and scanning electron micrographs of laser processed pure IN625 and IN625 composites for different laser scan speeds of 2.5 mm/s and 10 mm/s. The microstructure examination clearly reveals the presence of both cellular and dendritic form of microstructure. The ductility is kept intact because of the presence of cellular microstructure (Paul, et al., 2007). The cellular and dendritic microstructures are attributed to reduced cooling rate and rapid cooling rates respectively. The high hardness is because of the presence of fine microstructures with high dislocation density. The rapid cooling rate and an increased dislocation density during laser processing results in grain refinement of IN625 matrix. The large amount of dislocations is the result of residual stress between the matrix and reinforcement, generated due to rapid cooling and heating because of difference in CTE between the SiC reinforcement and the IN625 matrix. The additive nature results in lot of changes in the thermal behaviour of the process. The thermal stress developed during the process

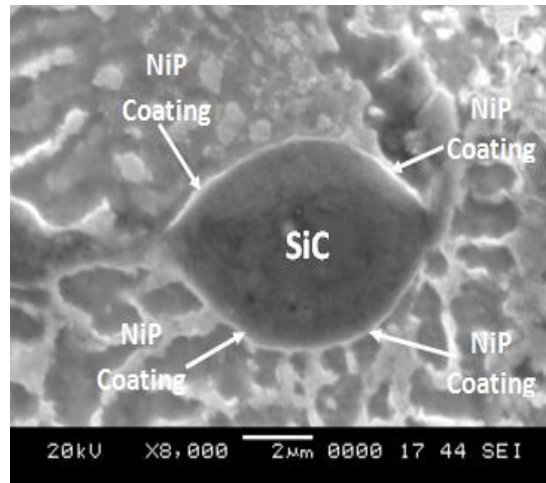
because of multiple reheating cycles also results in generation of high dislocations in IN625 matrix. The perfect interface between the SiC and the matrix without any voids, cracks shows the dispersion of SiC particles in the IN625 matrix.

Lower scan speed results in higher laser power, which increases the temperature of melt and higher melt temperature increases the cooling rate, increase in cooling rate leads to fine microstructure with dendrites. The movement of dislocations is hindered due to the presence of dendritic phase. The hardness is increased due to dendritic phase and the secondary SiC, which acts as dispersoid and hinders the movement of dislocations (Ahmad, et al., 2005). The dendrites grow along the direction of deposition.

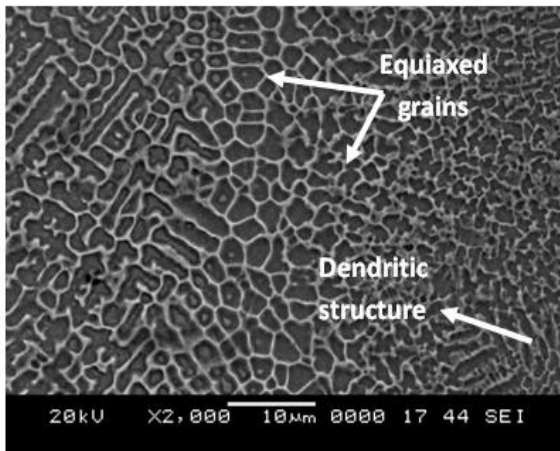


**Figure 5.27 Optical Micrographs of IN625 (a) & (b) and IN625-5 wt. % SiC (NiP-coated) (c) & (d) at a Laser Scan Speeds of 2.5 mm/s and 10 mm/s Respectively**

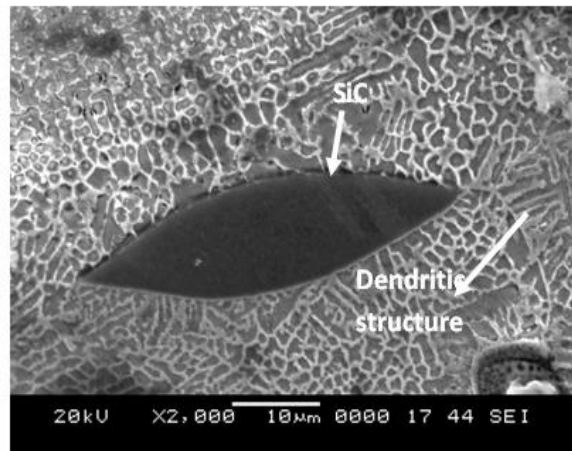
The scanning electron micrograph shown in Figure 5.28 (a) indicates the complete encapsulation of the irregular SiC particles by NiP coating with a thickness of 1 to 2  $\mu\text{m}$ . The morphology of coated SiC particles is smooth and more spherical when compared to the uncoated SiC particles. The evidence shown by the scanning electron micrograph for the presence of SiC particles supports the suggestion of a perfect bonding between SiC particles and NiP coating.



(a) SiC Particle Encapsulated with NiP Coating



(b) IN625



(c) IN625-5 wt. % SiC (NiP-Coated)

**Figure 5.28 Scanning Electron Micrographs of IN625 and IN625-SiC (NiP-coated) Composites**

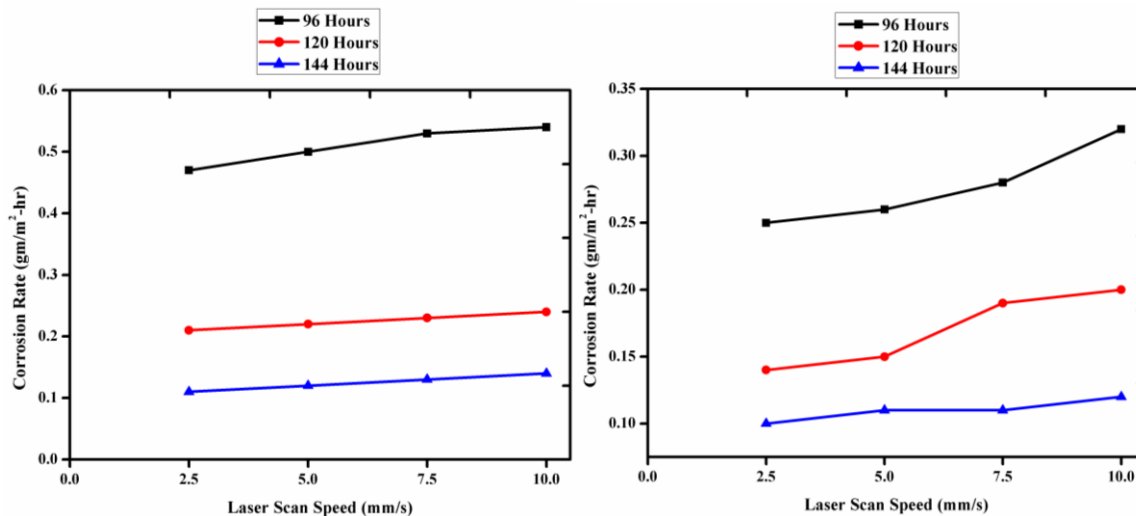
Thus the micrographs clearly indicate that the laser scan speed and the SiC reinforcement have significant effect on microstructure of the laser processed parts.

## 5.9 CORROSION STUDIES

The corrosion of IN625 and IN625-SiC (NiP-coated) composites processed in nitrogen atmosphere is discussed in this section. Salt Spray test was conducted in 5.0 % NaCl solution.

### 5.9.1 Effect of Laser Scan Speed

The effect of laser scan speed on rate of corrosion is shown in Figure 5.29 (a) and Figure 5.29 (b) for IN625 and IN625- 3 wt. % SiC (NiP-coated) composites.

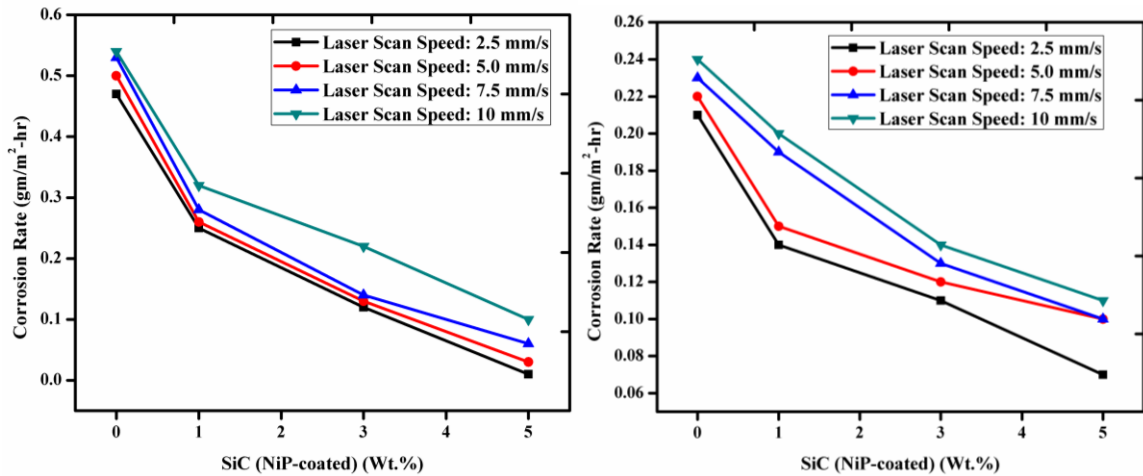


**Figure 5.29 Effect of Laser Scan Speed on Corrosion Rate for (a) IN625 and (b) IN625-3 Weight Percentage SiC (NiP-coated) Composites**

It is observed that the corrosion rate increases with increase in laser scan speed for both IN625 and its composites. This can be attributed to increase in porosity of composites with increase in laser scan speed. With increase in porosity, the surface area available for corrosion increases and hence the corrosion rate increases. Further it is observed that the corrosion rate of IN625 is more when compared with its composites, at all laser scan speeds studied.

### 5.9.2 Effect of Reinforcement

The effect of SiC (NiP-coated) reinforcement on rate of corrosion is shown in Figure 5.30 (a) and Figure 5.30 (b) for IN625 and IN625-SiC (NiP-coated) composites.



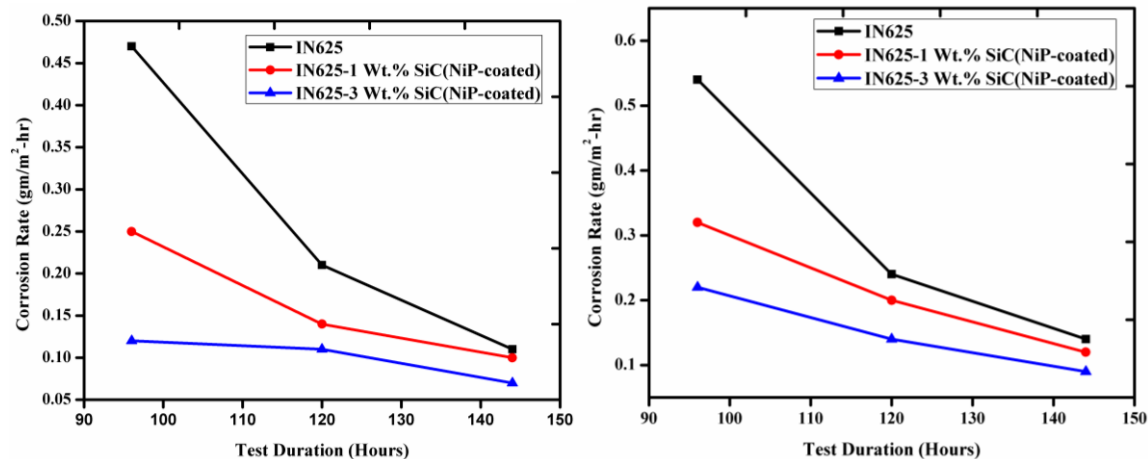
**Figure 5.30 Effect of SiC (NiP-coated) on Corrosion Rate for (a) 96 Hours and (b) 120 Hours Duration**

It is observed that with increase in wt. % of SiC (NiP-coated), there is a decrease in corrosion rate of composites, indicating high corrosion resistance of composites when compared with IN625 matrix. This is because Nickel-phosphide coating on SiC, has reduced the interfacial reaction as evidenced from the studies of IN625-SiC (NiP-coated) composites as discussed in effect of nickel-phosphide coating. It has been reported that nickel develops a passive film in alkaline environments, thereby increasing the corrosion resistance of the substrate. Further, phosphorus presence in electroless nickel coating provides higher resistance to corrosion. Lesser extent of porosity in the material leads to lesser extent of pitting in marine environment, thereby minimizing the material removal. Decrease in porosity of IN625-SiC (NiP-coated) composites with increase in weight percentage of SiC (NiP-coated) reinforcement as per density and porosity discussion. Lesser the extent of pitting, lower the material removal rate due to lower galvanic action between IN625 and SiC (NiP-coated) reinforcement in the developed composites. The extent of pitting is reduced in IN625-SiC (NiP-coated) composites when compared with

IN625. With increase in surface roughness, more surface area is available for corrosion. The surface roughness of IN625 composites decreases with increase in reinforcement content as discussed in surface roughness studies for reinforcement. Hence, composites with higher reinforcement content with lower surface roughness are less attacked by corrosion.

### 5.9.3 Effect of Test Duration

Figure 5.31 shows the variation of corrosion rate of IN625-3 wt. % SiC composite tested for a duration of 96, 120, and 144 hours. It is observed that the corrosion rate decreases with increase in test duration. However, for all the test durations studied, the developed composites do exhibit a higher corrosion resistance when compared with laser processed IN625.



(a) For a Laser Scan Speed of 2.5 mm/s (b) For a Laser Scan Speed of 10 mm/s

**Figure 5.31 Effect of Test Duration on Corrosion Rate for IN625 and IN625-SiC (NiP-coated) Composites**

### 5.10 MACHINABILITY STUDIES

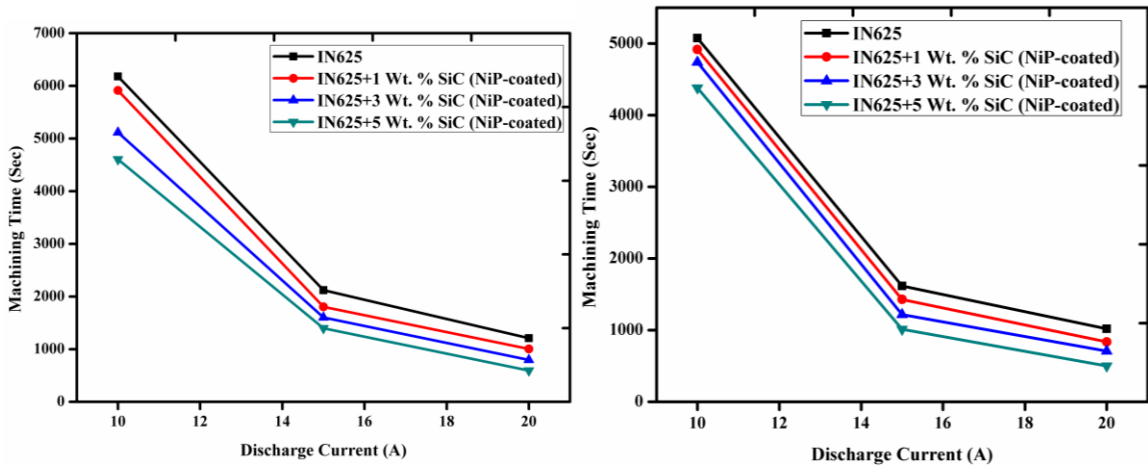
The machinability studies were conducted on IN625 and IN625-SiC (NiP-coated) composites using WEDM. Machining time and surface roughness are evaluated to find the machinability of IN625 and IN625-SiC (NiP-coated) composites.



## 5.10.1 Machining Time

### 5.10.1.1 Effect of Discharge Current

The variation of machining time with the discharge current is shown in Figure 5.32 (a) and Figure 5.32 (b) for IN625 and IN625-SiC (NiP-coated) composites. The plots clearly reveal about the variation of machining time with the variation of discharge current. With the increment in discharge current we observe the decrement in machining time. The above observation is due to the higher energy availability at higher discharge currents. Higher energy availability results in high rate of metal removal. This statement is in agreement with other research results also.



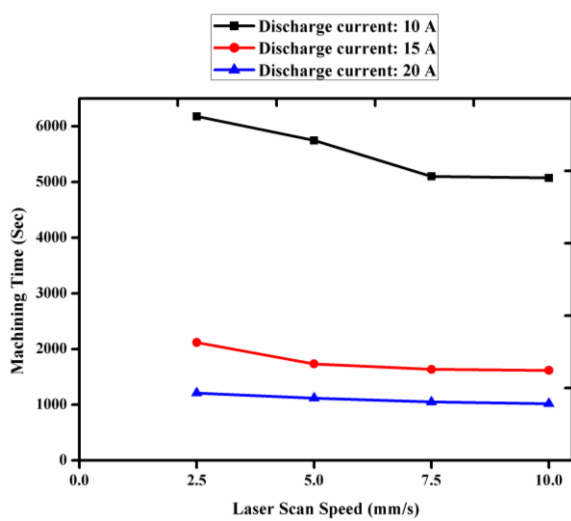
(a) For a Laser Scan Speed of 2.5 mm/s (b) For a Laser Scan Speed of 10 mm/s

**Figure 5.32 Effect of Discharge Current on Machining Time for IN625 and IN625-SiC (NiP-coated) Composites**

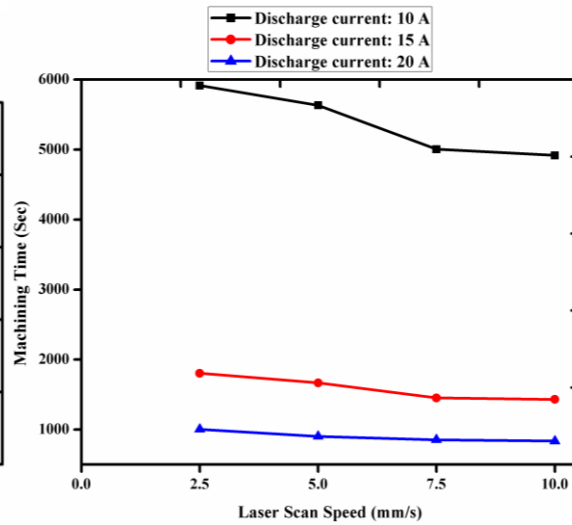
### 5.10.1.2 Effect of Scan Speed of Laser

The variation of machining time with the scan speed of laser is shown in Figure 5.33 (a) to Figure 5.33 (d) for IN625 and IN625-SiC (NiP-coated) composites. The plots clearly show that the specimens processed at a scan speed of 10 mm/s have taken lesser machining time when compared to a scan speed of 2.5 mm/s. This is due to the porosity of laser processed parts. The change in porosity is because of balling effect and laser energy density. The density of IN625 and IN625-SiC (NiP-coated) composites is less at a scan

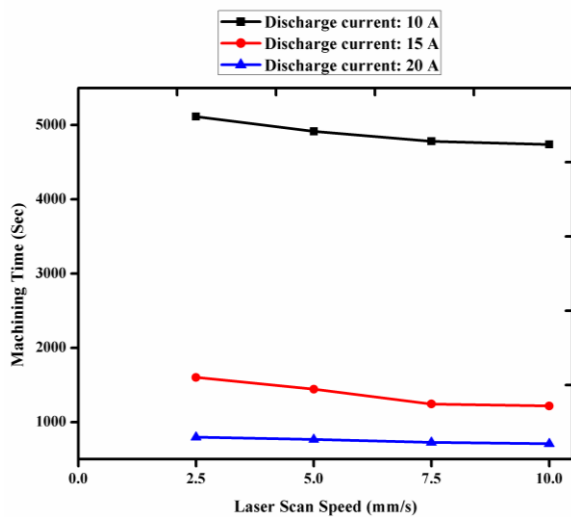
speed of 10 mm/s because of balling effect and lesser energy density compared to those composites laser processed at scan speed of 2.5 mm/s. The porous structure has resulted because of balling effect. The available material to machine is less because of higher porosity. This has resulted in lesser machining time requirement for specimens laser processed at a scan speed of 10 mm/s compared to those laser processed at a scan speed of 2.5 mm/s.



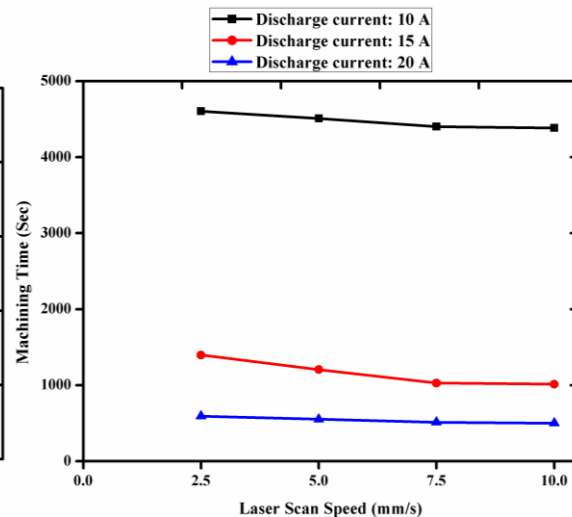
(a) For IN625



(b) For IN625-1 wt. % SiC (NiP-coated)



(c) For IN625-3 wt. % SiC (NiP-coated)

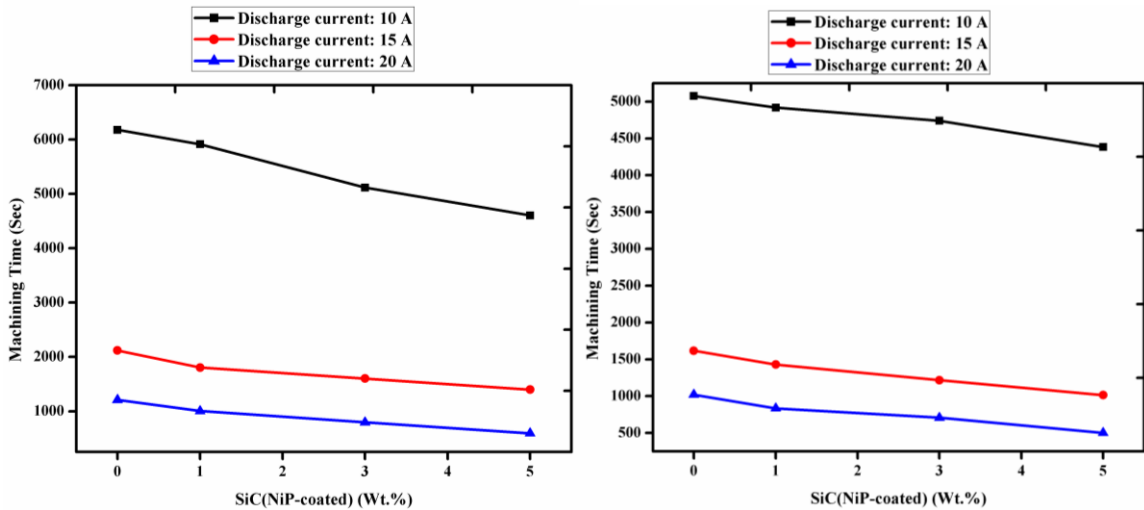


(d) For IN625-5 wt. % SiC (NiP-coated)

**Figure 5.33 Effect of Laser Scan Speed on Machining Time for IN625 and IN625-SiC (NiP-coated) Composites**

### 5.10.1.3 Effect of SiC (NiP-coated) Reinforcement

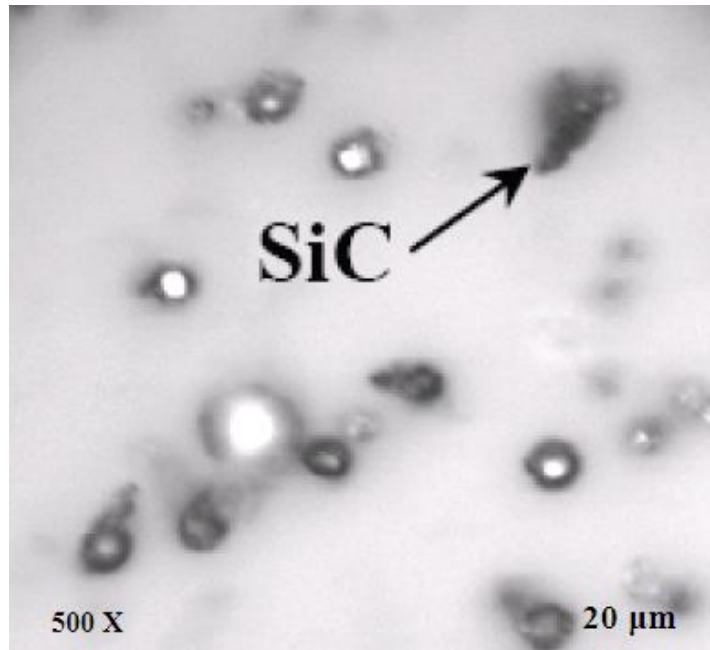
The variation of SiC (NiP-coated) reinforcement on machining time is shown in Figure 5.34 (a) and Figure 5.34 (b) for IN625 and IN625-SiC (NiP-coated) composites. The plots clearly reveal about the variation in machining time with the variation in weight percent of SiC (NiP-coated) reinforcement. The melting point of reinforcement is higher when compared to IN625 matrix. Reinforcement is having thermal conductivity of 114 W/m<sup>0</sup> K when compared to IN625 matrix with thermal conductivity 91 W/m<sup>0</sup> K. Because of high thermal conductivity of the reinforcement, the reinforcement SiC (NiP-coated) makes the heat to flow into the IN625 matrix. The heat dissipation results in increment in temperature of IN625 matrix. While machining the composites using WEDM melting and evaporation of IN625 matrix takes place. During evaporation process because of high melting point, the reinforcement particles get displaced from the IN625 matrix without melting. Further the debris of the WEDM machined IN625-SiC (NiP-coated) composites shown in the micrographs supports the views expressed above. The debris indicates the presence of IN625 in spherical form and the SiC (NiP-coated) in sharp irregular form.



(a) For a Laser Scan Speed of 2.5 mm/s

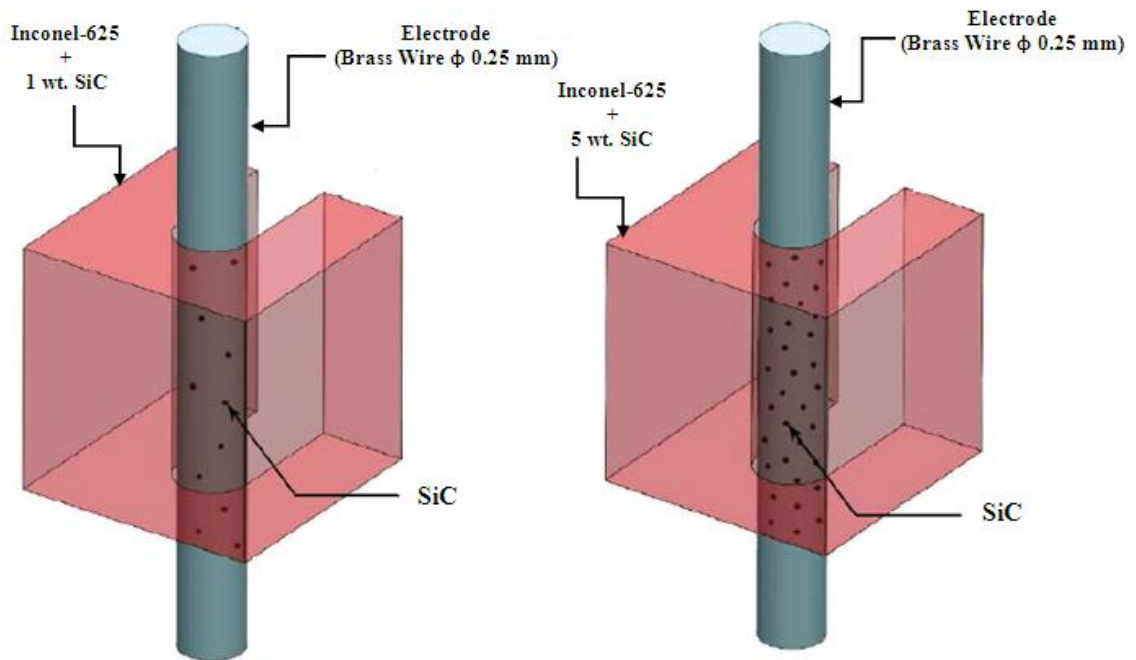
(b) For a Laser Scan Speed of 10 mm/s

**Figure 5.34 Effect of Weight Percentage of SiC (NiP-coated) Reinforcement on Machining Time for IN625 and IN625-SiC (NiP-coated) Composites**



**Figure 5.35 Optical Micrograph of WEDM Debris Showing Un-melt SiC particles and Solidified IN625**

The brass wire interaction with IN625-1 weight percentage SiC (NiP-coated) and IN625-5 weight percentage SiC (NiP-coated) composites at the time of WEDM is represented by CAD model in Figure 5.36 (a) and Figure 5.36 (b). The area of interaction is more for 1 weight percentage SiC (NiP-coated) composites when they are compared to 5 weight percentage SiC (NiP-coated) composites. As the machining time is directly proportional to the interaction area, it is IN625 matrix which has participated more in machining compared to reinforcement SiC (NiP-coated) particles. Hence a decrement in machining time is observed with increment in weight percent of NiP coated reinforcement.

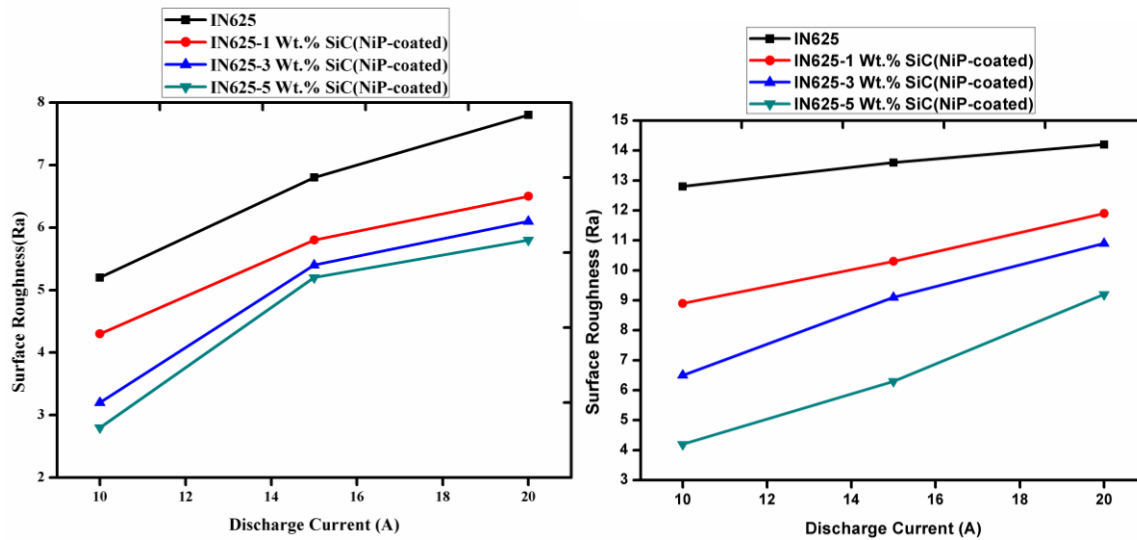


**Figure 5.36 Interaction of Brass Wire with IN625 - 1 and 5 Weight Percentage SiC (NiP-coated) Composites**

## 5.10.2 Surface Roughness (SR)

### 5.10.2.1 Effect of Discharge Current

The variation of surface roughness with variation of discharge current is shown in Figure 5.37 (a) and 5.37 (b) for IN625 and IN625-SiC (NiP-coated) composites. The plots clearly reveal that there is a variation in surface roughness with variation in discharge current. Increment in the surface roughness with increment in discharge current is observed due to discharge energy. The increment in discharge current leads to increment in discharge energy. The size of crater is large for higher discharge energy. Hence there is an increment in surface roughness with increment in discharge current.

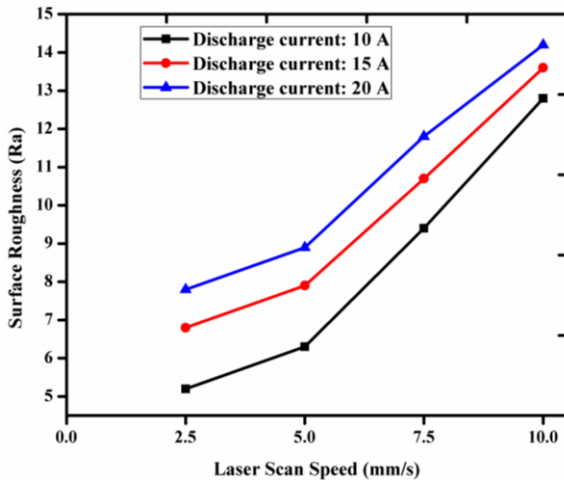


(a) For a Laser Scan Speed of 2.5 mm/s      (b) For a Laser Scan Speed of 10 mm/s

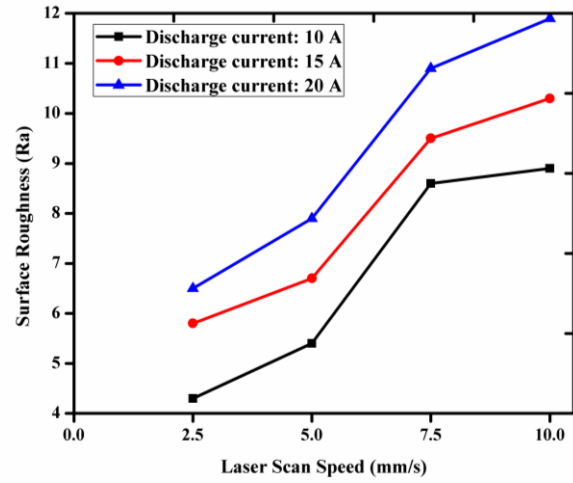
**Figure 5.37 Effect of Discharge Current on SR for IN625 and IN625-SiC (NiP-coated) Composites**

### 5.10.2.2 Effect of Scan Speed of Laser

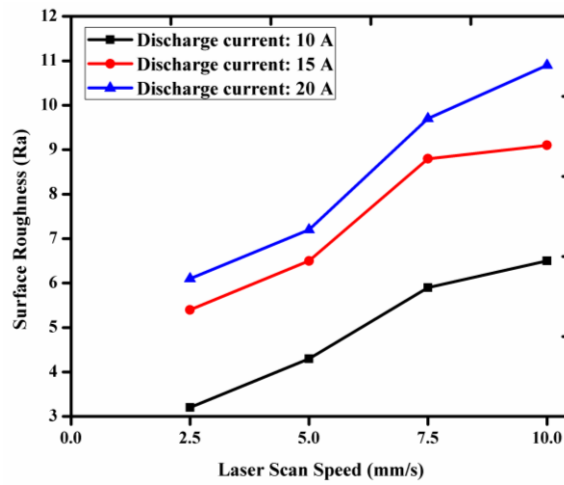
The effect of scan speed of laser on surface roughness is shown in Figure 5.38 (a) to Figure 5.38 (d) for IN625 and IN625-SiC (NiP-coated) composites. The plots clearly reveal about the variation of surface roughness with the variation of scan speed of laser. The increment in surface roughness with increment scan speed of laser is observed due to changes in porosity of the laser processed specimens at different scan speed of as per discussions done in the case of machining time. The change in porosity is because of balling effect and laser energy density. The density of IN625 and IN625-SiC (NiP-coated) composites is less at a scan speed of 10 mm/s because of balling effect and lesser energy density compared to those composites laser processed at scan speed of 2.5 mm/s. The higher balling effect at laser scan speed of 10 mm/s has resulted in higher surface roughness compared to surface roughness of the laser processed specimens at 2.5 mm/s.



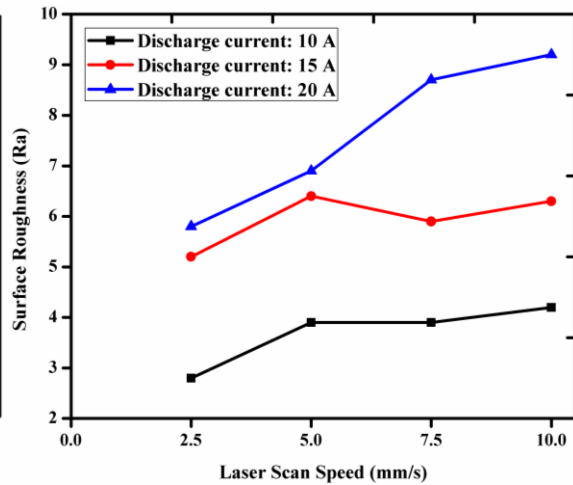
(a) For IN625



(b) For IN625-1 wt. % SiC (NiP-coated)



(c) For IN625-3 wt. % SiC (NiP-coated)



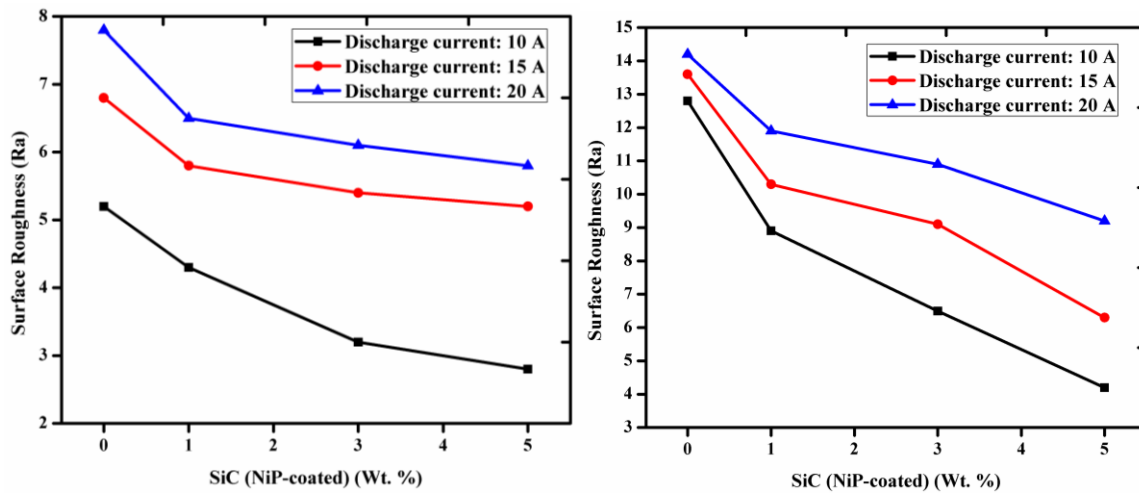
(d) For IN625-5 wt. % SiC (NiP-coated)

**Figure 5.38 Effect of Laser Scan Speed on SR for IN625 and IN625-SiC (NiP-coated) Composites**

### 5.10.2.3 Effect of SiC (NiP-coated) Reinforcement

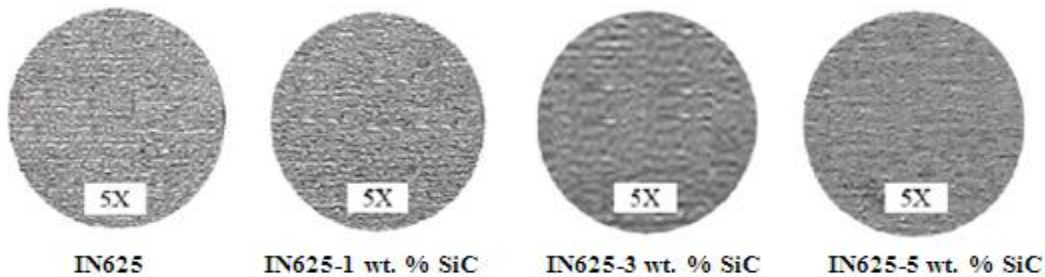
The variation of SiC (NiP-coated) reinforcement on machining time is shown in Figure 5.39 (a) and Figure 5.39 (b) for IN625 and IN625-SiC (NiP-coated) composites. The plots clearly reveal about the variation of surface roughness of the laser processed composites with variation in weight percent of NiP coated SiC particles. The increment in weight percent of NiP coated SiC results in improvement in surface finish due to

reduction in porosity. The high laser absorptivity of the NiP coated SiC particles reduces the porosity of the laser processed specimens with an increment in reinforcement weight percentage. Higher the reinforcement, results in higher laser absorption. The SEM of the machined surfaces of IN625-1 wt. % SiC (NiP-coated) and IN625-5 wt. % SiC (NiP-coated) shown in Figure 5.41 clearly reveal that surface of 5 wt. % SiC (NiP-coated) reinforced composites are smoother compared to surface of 1 wt. % SiC (NiP-coated) reinforced composites.



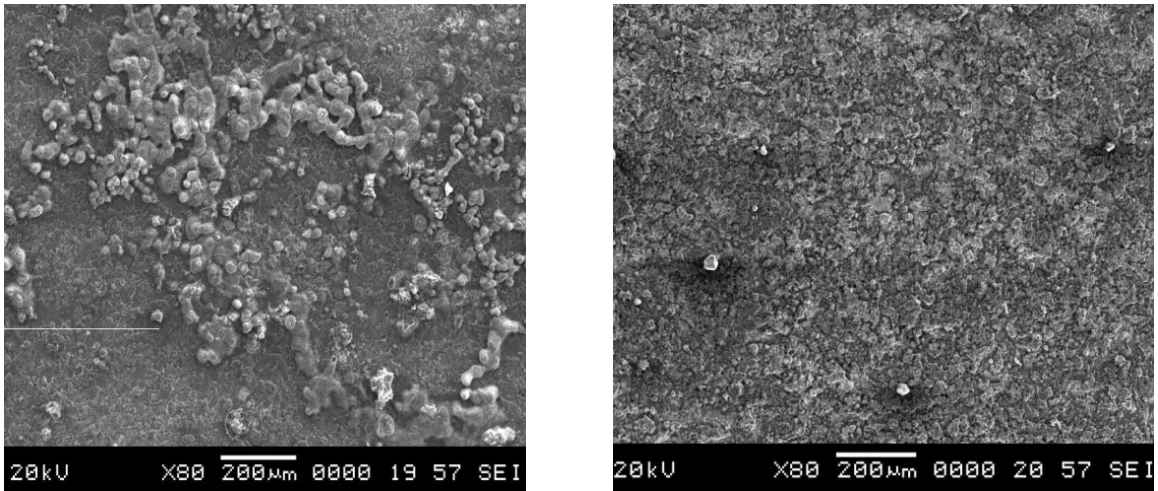
(a) For a Laser Scan Speed of 2.5 mm/s      (b) For a Laser Scan Speed of 10 mm/s

**Figure 5.39 Effect of Weight Percentage of SiC (NiP-coated) on SR of IN625 and IN625-SiC (NiP-coated) Composites**



**Figure 5.40 Optical Micrographs of Parts Sintered at a Laser Scan Speed of 2.5 mm/s**





**(a) IN625+1 Weight Percentage SiC (NiP-coated) (b) IN625+5 wt. % SiC (NiP-coated) Sintered at 2.5 mm/s**

**Figure 5.41 Scanning Electron Micrograph of Wire Electrical Discharge Machined IN625-SiC (NiP-coated) Composites at a Discharge Current of 20 A**

## CHAPTER 6

### CONCLUSIONS AND SCOPE FOR FUTURE WORK

#### 6.1 PREAMBLE

The experimental results were discussed in detail in the previous chapter. Studies on the processing and characterization of IN625-SiC (NiP-coated) metal matrix composites by laser based direct metal laser sintering and inferences drawn were also consolidated.

The various conclusions drawn from the present investigations are presented in this chapter under reinforcement coating and blending, micro-structure, physical properties, mechanical properties, corrosion resistance and machinability. The scope for future work is also presented at the end of this chapter.

#### 6.2 CONCLUSIONS

Deposition of IN625 with addition of variable wt. % of NiP coated SiC particulates using laser additive manufacturing (AM) process was investigated. The reinforcement coating and blending, micro-structure, density, micro-hardness, tensile properties, surface roughness, corrosion and machinability studies of the composites were studied. The following conclusions were drawn from the investigations carried out on IN625 and IN625 composites:

##### 6.2.1 Reinforcement Coating and Blending

- SiC reinforcement particles were successfully coated with NiP by electroless coating process and a homogeneous particulate mixture of IN625 and SiC (NiP-coated) was prepared using double cone blending equipment and IN625 and IN625-SiC (NiP-coated) composites for 1, 3 and 5 wt. % SiC (NiP-coated) were successfully produced by DMLS process by optimizing the laser scan speed.
- The encapsulation of NiP on SiC particles effectively avoids the formation of cracks or voids at the interface of metal/ceramic and ceramic particles clustering resulting in improved wetting and absorption of incident laser beam.
- The encapsulation of NiP on SiC particles helps in better flowability of the reinforcement particles during blending and laser processing due to increase in

SiC particle mass in the sense the density will be improved, with smooth surface, better spherical morphology and reduction in thermal shock characters during their exposure to laser beam and also there will be reduction in porosity.

### **6.2.2 Micro-structure**

- Metallographic studies clearly reveal uniform distribution of reinforcement and excellent bond between the IN625 matrix and SiC (NiP-coated) reinforcement due to encapsulation of NiP on SiC reinforcement particles.
- The thermal stresses developed during the process because of multiple reheating cycles, residual stress between the matrix and reinforcement, due to their difference in CTE generates high dislocations. The increment in dislocation density during laser processing results in grain refinement of IN625 matrix with fine microstructures and higher hardness is the result of these fine microstructures.
- Increase in weight percentage of NiP coated reinforcement results in more absorption of laser energy, more laser energy absorption leads to fine microstructure with dendrites, which again results in increased hardness because of C and Si atom introduction into the lattice of IN625.

### **6.2.3 Physical Properties**

- Density studies reveal that there was a decrease in density of IN625-SiC (NiP-coated) composites with increase in reinforcement and laser scan speed. The population of reinforcement per unit volume increases with addition of more weight percentage of NiP coated reinforcement. Therefore, the density of the composites decreases with increase in percentage of the reinforcement.
- Reduction in density with addition of NiP coated SiC weight percentage is significant in case of 5 wt. % of reinforcement, where a considerable 3.8 % reduction in density with IN625 is observed for a laser scan speed of 2.5 mm/s.
- The surface roughness of IN625 and IN625-SiC (NiP-coated) composites decreases with decrease in laser scan speed and increases with increase in laser scan speed. At lower laser scan speed, full melting of powders takes place,

resulting in reduced melt viscosity, balling effect and increased melt-cylinder diameter, leading to better connectivity and reduced inter-pore size results in better surface finish. At higher laser scan speed the low energy density results in partial melting and higher viscosity leading to balling effect. The balling effect results in poor surface finish.

- The surface roughness of IN625-SiC (NiP-coated) composites decreases with increase in wt. % SiC (NiP-coated) reinforcement. The increment in reinforcement results in increased absorption of laser which in turn results full melting of particulates without balling effect and good surface finish.

#### **6.2.4 Mechanical Properties**

- The higher hardness of SiC and addition of hard phase into IN625 matrix results in improvement in composite hardness with weight percentage increase of the SiC reinforcement. 13 to 33 % improvement in micro-hardness with the addition of 1 to 3 wt. % reinforcement into the matrix of IN625 for a laser scan speed of 2.5 mm/s was noticed.
- One more reason for micro-hardness improvement can be attributed to increased density of dislocation at the matrix-reinforcement interface. The increase in the dislocation density can be mainly attributed to the difference in the CTE of the matrix and the reinforcement.
- The significant improvement in the micro-hardness of the laser processed composites can also be attributed to excellent bonding between the reinforcing particle and the matrix.
- The increasing trend is observed for UTS, YS with addition of SiC (NiP-coated) reinforcement into IN625 matrix up to 3 wt. % and further addition has resulted in drastic reduction of UTS and YS. The % EL goes on decreasing with increase in wt. % of NiP-coated SiC particles. The decrement in UTS, YS and % EL is because of the brittle nature of the increased weight percentage of reinforcement.

### **6.2.5 Corrosion Resistance**

- The corrosion resistance of the IN625-SiC (NiP-coated) composites increases with increase in wt. % of SiC in IN625 matrix and decrease in laser scan speed. The better absorption of incident laser beam which increases with increase in weight percentage of reinforcement and higher densification and reduction in porosity of the composites results in increase in corrosion resistance of composites.
- At higher laser scan speed partial melting and higher balling effect results in high porosity composites and higher porosity results in decrease in corrosion resistance of composites.

### **6.2.6 Machinability**

- The machinability studies conducted using WEDM on the laser sintered IN625 and IN625-SiC (NiP-coated) composites clearly reveal that the machining time for IN625 and its composites decreases with increase in discharge current and machining time decreases with the increase in wt. % SiC of (NiP-coated). Similarly the surface roughness of the machined surface increases with increases in discharge current and decreases with increase in wt. % of SiC (NiP-coated).
- Increment in discharge current results in decrement in machining time due to higher energy availability at higher discharge currents and also a decrement in machining time was noticed for laser processed specimens at 10 mm/s compared to those processed at 2.5 mm/s because of higher porosity at higher scan speed of laser.
- Decrement in machining time with increment in weight percentage of NiP coated SiC particles because of heat flow from high thermal conductivity coated SiC reinforcement particles to low thermal conductivity IN625 matrix and higher laser absorption of coated SiC reinforcement particles.
- Increment in surface roughness with increment in discharge current was noticed because of higher discharge energy with larger crater size and Increment in surface roughness with increment in scan speed of laser was noticed because of higher porosity and balling effect.

### **6.3 SCOPE FOR FUTURE WORK**

In the present investigation the laser processing of nickel based IN625 and IN625-SiC (NiP-coated) composites were studied by analyzing their physical, mechanical, corrosion and machinability characteristics. The present work can be extended in number of directions as mentioned below:

- 1) Study can be extended to other nickel based alloys used in high temperature applications.
- 2) Investigations on the effect of morphology of matrix and reinforcement particles on laser processed parts may be conducted.
- 3) Process parameters can be optimized using statistical modeling and simulation softwares.
- 4) Solidification behavior of the laser processed parts may be analysed using solidification simulation softwares.
- 5) Machinability studies may be undertaken using other machine tools by employing parameter optimization techniques.

## APPENDICES

### APPENDIX A: Properties and Chemical Composition of IN625 and SiC

#### Properties of IN625

Density (g /cm <sup>3</sup> at 20 ° C)	8.44
Melting point (°C)	1350
Co-efficient of thermal expansion (10 <sup>-6</sup> / ° C)	12.8
Modulus of elasticity (GPa)	205.8

#### Chemical Composition of IN625 in Percentage (Powder Alloy Corp)

Ni	C	Fe	Mn	Si	Cr	Mo	Nb+Ta	Al	P	S	Co	Ti
58.0	0.10	5.0	0.50	0.50	20.0-	8.0-	3.15-	0.40	0.015	0.015	1.0	0.40
	max	max	max	max	23.0	10.0	4.15	max	max	max	max	max

#### Properties of SiC

Density (g / cm <sup>3</sup> )	3.2
Melting point (°C)	2830
Coefficient of thermal expansion (10 <sup>-6</sup> / ° C)	4.8
Modulus of elasticity (GPa)	414.2

#### Chemical Composition of SiC (Grindwell Norton)

SiC	Free C	Free Si	SiO <sub>2</sub>	Fe	Al	Ca	Mg
98.6	0.36	0.15	0.2	0.08	0.08	0.05	0.3

**APPENDIX B: Laser-based Particle Size Counter, Scanning Electron Microscope, Optical Microscope, X-ray Diffractometer and Their Salient Features**



**Particle Size Counter**

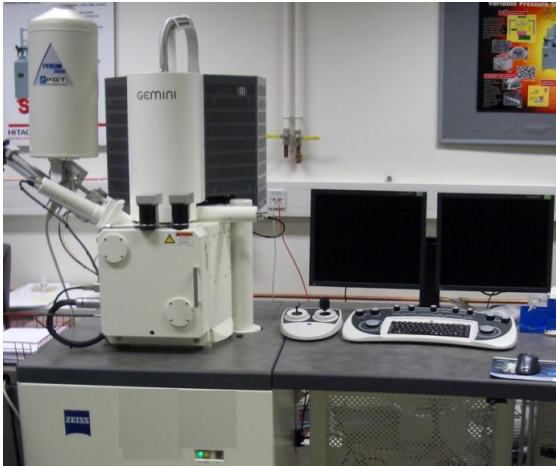
**Salient Features of Laser-based Particle Size Counter**

---

<b>Features</b>	<b>Description</b>
Make	HIAC/ROYCO, USA
Model	8000A Particle Counter
Sensor	HRLD-100 Laser-based light blocking sensor. Eight keyboard selectable channels for sizing flexibility Range: 1.2 to 100 microns.
Concentration limit	10,000 particles/ml.
Flow rate	60 ml/min.

---





**Scanning Electron Microscope**



**X-ray Diffractometer**

**Salient Features of SEM and XRD**

<b>Features</b>	<b>Description</b>
Make	Carl Zeiss, Germany
Model	Neon Crossbeam
Magnification	200, 500, 2K, and 5KX

<b>Features</b>	<b>Description</b>
Make	Bruker
Model	XRDD8ADVANCE
Scan Range	10 <sup>0</sup> -90 <sup>0</sup>

**Salient Features of Optical Microscope**

<b>Features</b>	<b>Description</b>
Make	Nikon, Japan
Model	OPTIPHOT-100S
Magnification	50, 100, 200,500 and 1000 X
Software	Clemex Vision 2.2

**APPENDIX C: Bath Composition of Electroless Nickel Phosphide Encapsulation and Equipments for Electroless Coating**

**Bath Composition for Electroless Nickel - Phosphide Deposition**

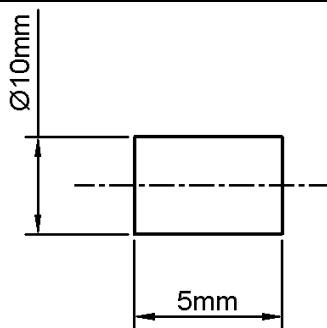

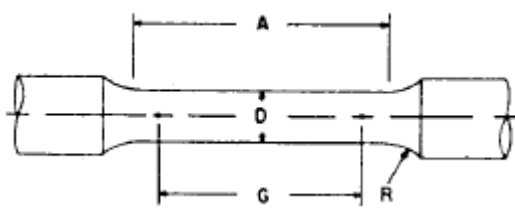
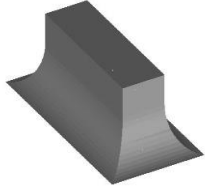
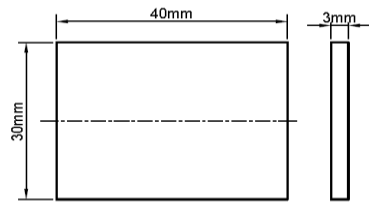

(Kang, et al., 2002)

Nickel Chloride, hexahydrate ( $\text{NiCl}_2 \cdot 6\text{H}_2\text{O}$ )	30 g/L
Sodium succinate, hexahydrate ( $\text{Na}_2\text{C}_4\text{H}_4\text{O}_4 \cdot 6\text{H}_2\text{O}$ )	10 g/L
Sodium Hypophosphite, monohydrate ( $\text{NaH}_2\text{PO}_2 \cdot \text{H}_2\text{O}$ )	20 g/L
Glycine ( $\text{H}_2\text{NCH}_2\text{COOH}$ )	10 g/L
Lead nitrate ( $\text{Pb}(\text{NO}_3)_2$ )	2 mg/L

**Equipments for Electroless Coating**

<b>Equipment</b>	<b>Make</b>	<b>Model</b>
Electronic Balance (Least count: 1mg)	Sartorius, Germany	BSA223S
pH meter	EQUIP-TRONICS	6Q-610
Magnetic Stirrer with Heater.	REMI	2MLH
Scanning Electron Microscope	Carl Zeiss, Germany	Neon Crossbeam System
X-ray Diffractometer	Brucker	XRDD8ADVANCE

**APPENDIX D: 2D and 3D Drawings of Test Specimens**

Test	Drawings of Test Specimens	
	2D	3D
Density / Microstructure / Microhardness / Machinability		
Tensile	 <p>Where D-Diameter=4.0+0.1mm Gauge Length-G=20+0.1mm Radius of the Fillet-R= 4mm Length of the Reduced Section-A= 20mm</p>	
Surface Roughness / Corrosion		

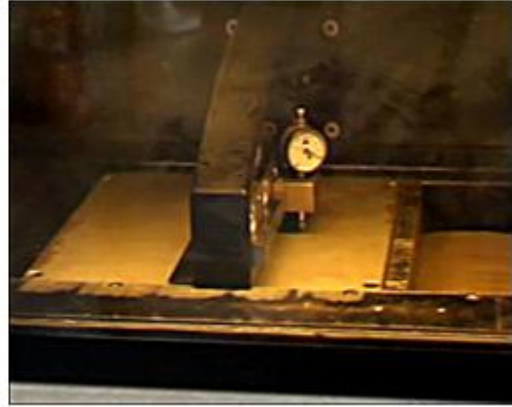
## APPENDIX E: EOSINT M250 DMLS Machine and Its Salient Features



(a) Exhaust Unit (b) EOSINT M250 DMLS Machine (c) Chiller & Compressor

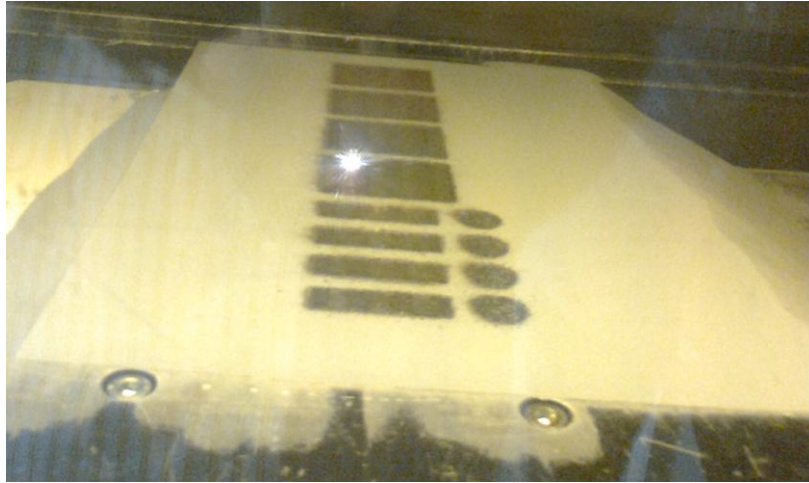
### Salient Features of EOSINT M250 DMLS Machine

Feature	Description
Make and Model	EOSINT M250 Xtended Machine, EOS Gmbh, Germany
Laser	CO <sub>2</sub> Laser, 240 W
Maximum Size of Built Part	250 x 250 x 150 mm
Software	PSW



**Mounting and Leveling of Base Plate in EOSINT M250 DMLS Machine**

**APPENDIX F: Preparation and Separation of Test Specimens from Base Plate using WEDM**



**Preparation of Test Specimens by Laser Sintering Process**



**Close up view of Separation of Test Specimens from Base Plate using WEDM**

**APPENDIX G: Density Measurement using Archimede's Principle**



**Weighing in Air**



**Weighing in Water**

## APPENDIX H: INSTRON-5569 Tensile Testing Machine Loaded with Specimen and Its Salient Features



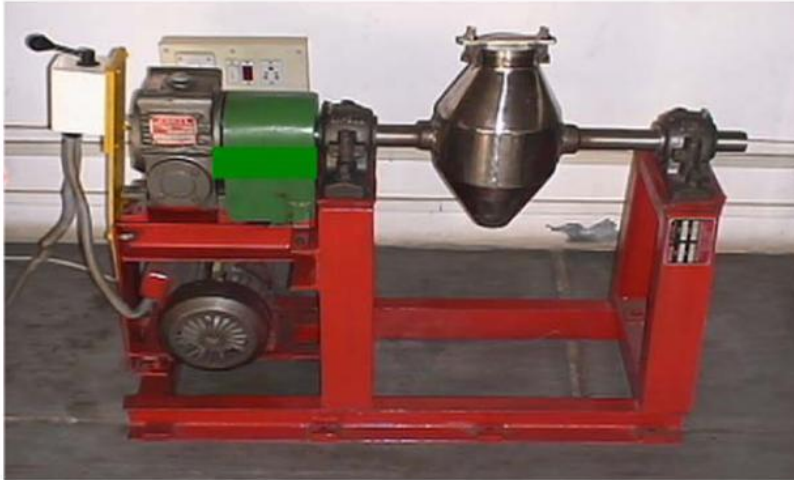
**INSTRON-5569 Loaded with Test Specimen**

### Salient Features of Tensile Testing Equipment INSTRON-5569

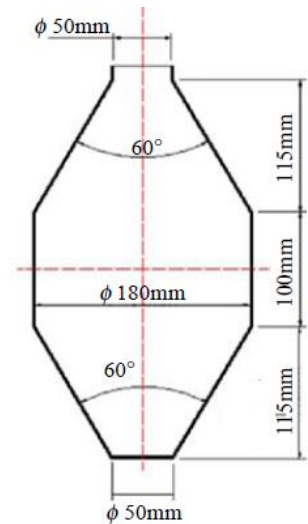
<b>Feature</b>	<b>Description</b>
Make	Instron, USA
Model	5569
Load Accuracy	+/- 1%, with strain rate 0.1 mm/min
Data Rate	10 Points / Sec
Load Range	Upto 10 KN



## APPENDIX I: Double Cone Blender with Schematic Diagram of Conical Container



**Double Cone Blender**



**Conical Container**

### Salient Features of Double Cone Blender

Feature	Description
Make	Hindustan Engineering Company, Calcutta, India
Model	DCB-LAB
RPM	45
Capacity	5.16 Liters

**APPENDIX J: Machining and Surface Preparation of Test Specimens for Micro-structure Studies**



**(a) Tool Room Lathe**



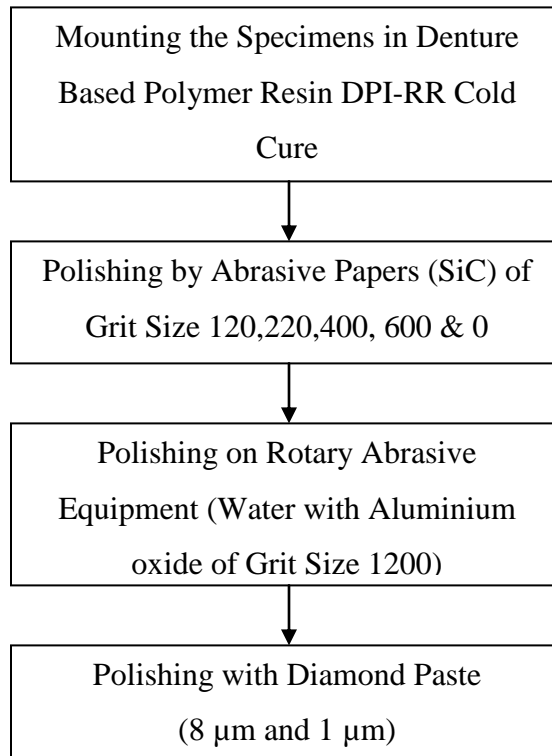
**(b) Close View**

**Machining of Test Specimens using Tool Room Lathe**



**Test Specimens Mounted using Denture Based Polymer**

### Steps for Surface Preparation



(a) Rotary Abrasive Polishing Equipment



**(b) Rotary Abrasive Polishing Equipment (c) Diamond Paste With Polishing Cloth**  
**Equipments for Surface Preparation**

## APPENDIX K: Confocal Microscope and Micro-hardness Tester with Salient Features



**Confocal Microscope**



**Micro-hardness Tester**

### Salient Features of Micro-hardness Tester

<b>Feature</b>	<b>Description</b>
Make	Clemex Technologies, Canada
Model	Clemex ST-2000
Test load	10, 50, 100, 200, 300, 500, 1000 & 2000 g
Dwell time	5 – 99 s
Magnification of microscope	25 – 400 X
Maximum measurement	100 x 50 mm

## APPENDIX L: Schaublin CNC Lathe for Machining of Tensile Test Specimens and Its Salient Features



**Schaublin CNC Lathe**

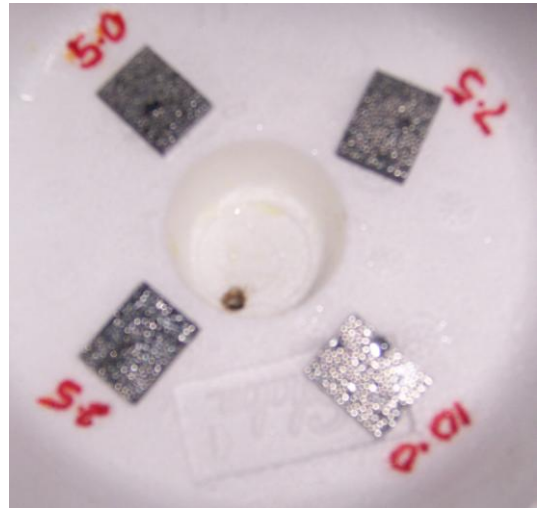
### **Salient Features of Schaublin CNC Lathe**

<b>Feature</b>	<b>Description</b>
Make and Model	Schaublin 125 CNC, Switzerland
Height of Centers	125 mm
Maximum Distance Between Centers	500 mm
Spindle Speeds	0-5000 rpm
Maximum Diameter of Chuck	150 mm
Transverse Travel X-Axis	180 mm
Longitudinal Travel Z-Axis	410 mm
Control System	GE Fanuc Series 20 T

**APPENDIX M: Salt Spray Apparatus and Its Salient Features for Corrosion Testing**



**(a) Salt Spray Chamber**



**(b) Close View of Specimens**

**Salt Spray Apparatus**

**Salient Features of Salt Spray Apparatus**

<b>Feature</b>	<b>Description</b>
Make	CM EnviroSystems
Model	SILVERFOG 450
Cabinet Capacity	450 Liters
Salt Solution Reservoir Capacity	80 Liters
Salt Spray Fallout Rate	1-2 ml/80 cm <sup>3</sup> /hr
Temperature Range Controller	35 <sup>0</sup> C ± 1

**APPENDIX N: Wire Electrical Discharge Machine (WEDM) used for Machinability Studies and Its Salient Features**



**WEDM (ROBOFIL 290) used for Machinability Studies**

**Salient Features of WEDM**

<b>Feature</b>	<b>Description</b>
Make	Charmilles Technologies, Switzerland
Model	ROBOFIL 290
Work Capacity	750 x 550 x 250 mm
Axis Travel X/Y/Z	350 x 250 x 256 mm
Maximum Taper Angle	30 <sup>0</sup> per 100 mm



## REFERENCES

- Adeqoyin, I., Mohamed and Lavernia, E.J. (1991). "Particulate reinforced MMCs-a review". *Journal of Material Science*, 26, 1137-1156.
- Agarwal, B.D., and Broutman, L.J. (1980). "Analysis and performance of fiber composites". *John Wiley & Sons*, New York, 3-12.
- Agarwala, M., Bourell, Beaman, Marcus, and Barlow. (1995). "Direct selective laser sintering of metals". *Rapid Prototyping Journal*, 1(1), 26-36.
- Agarwala, R.C., and Agarwala, V. (2003). "Electroless alloy/composite coatings: A review". *Sadhana*, 28, 475-493.
- Ahmad, M., Akhter, J.I., Iqbal, M., Akhtar, M., Ahmed, E., Shaikh, A., and Saeed, K. (2005). "Surface modification of Hastelloy C-276 by SiC addition and electron beam melting". *Journal of Nuclear Materials*, 336, 120-124.
- Ahmad, M., Ali, G., Ahmed, E., Haq, M. A., and Akhter, J. I. (2011). "Novel microstructural growth in the surface of Inconel 625 by the addition of SiC under electron beam melting". *Applied Surface Science*, 257, 7405-7410.
- Ahmed, N., Bakare, M.S., McCartney, D.G., Voisey, K.T. (2010). "The effects of microstructural features on the performance gap in corrosion resistance between bulk and HVOF sprayed Inconel 625". *Surface & Coatings Technology*, 204, 2294–2301.
- Allison, J.E., and Cole, G.S. (1993). "Metal matrix composites on the automotive industry: Opportunities and challenges". *Journal of Materials*, 45(1).
- Anna Bellini and Selcuk Guceri. (2003). "Mechanical characterization of parts fabricated using fused deposition modeling". *Rapid Prototyping Journal*, 9(4), 252-264.
- Ashish Srivastava, Amit Rai Dixit, and Sandeep Tiwari. (2014). "Experimental investigation of wire EDM process parameteres on aluminium metal matrix composite Al 2024/SiC". *International Journal of Advance Research and Innovation*, 2(2), 511-515.

Badrossamay, M., and Childs. (2007). “Further studies in selective laser melting of stainless and tool steel powders”. *Int. Journal of Machine Tools Manuf.*, 47, 779-784.

Bi, G., Sun, C.N., Nai, M.L., and Wei, J. (2013). “Micro-structure and mechanical properties of nano-TiC reinforced Inconel 625 deposited using LAAM”. *Physics Procedia*, 41, 828-834.

Bineli, A., Jardini, A., Peres, A., Bernardes, L., and Filho, R. (2011). “Microchannels fabrication in direct metal laser sintering”. 5<sup>th</sup> International Conference on Advanced Research in Virtual and Rapid Prototyping, Leiria, Portugal, 28<sup>th</sup> September – 1<sup>st</sup> October.

Borowski, T., Brojanowska, A., Kost, M., Garbacz, H., and Wierzchon, T. (2009). “Modifying the properties of the Inconel 625 nickel alloy by glow discharge assisted nitriding”. *Vacuum*, 83, 1489–1493.

Burak, D., Tekmen, C., Gavgali, M., and Cocen, U. (2011). “The Effect of electroless Ni coating of SiC particles on the corrosion behavior of A356 based squeeze cast composite”. *Journal of Mechanical Engineering*, 57(1), 11-20.

Calignano, F.; Manfredi, D.; Ambrosio, E.P.; Iuliano, L.; and Fino, P. (2014). “Influence of process parameters on surface roughness of aluminium parts produced by DMLS”. *Int. J. Adv. Manuf. Technol.*, 67, 2743-2751.

Changa, K., Huang, J., Yanb, C., Yeha, T., Chenb, F., and Kai, J. (2012). “Corrosion behavior of Alloy 625 in supercritical water environments”. *Progress in Nuclear Energy*, 57, 20-31.

Chatterjee, A.N., Sanjay Kumar, Saha, P., Mishra, P.K., Roy Choudhury, A. (2003). “An experimental design approach to selective laser sintering of low carbon steel”. *Journal of Materials Processing Technology*. 136, 151–157.

Chen, Y., Cao, M., Xu, Q., and Zhu, J. (2003). “Electroless nickel plating on silicon carbide nano particles”. *Journal of Surface and Coating Technology*, 172, 90-94.

Chester, T.S. (1991). “Non-metallic materials for gas turbine engines”. *Adv. Mater. Processes*, 139(6), 32-39.

- Cho, H., Bang, K.H., and Lee, B.W. (2010). "Influence of refractory ceramic coatings on high temperature properties of Inconel 617". *Surface & Coatings Technology*, 205, 409–413.
- Chung, W.S., Chang, S.Y., and Lin, S.J. (1996). *Journal of Plating and Surface finishing*, 83, 68.
- Clyne, T.W. (2000). "An introductory overview of MMC system, types and developments, in comprehensive composite materials". *Elsevier*, 3, 1-26.
- Cooper, D.E., Blundell, N., Maggs, S., and Gibbson, G.J. (2013). "Additive layer manufacture of Inconel 625 metal matrix composites, reinforcement material evaluation". *Journal of Materials Processing Technology*, 213, 2191-2200.
- Cooper, K.P., Slebodnick, P., and Thomas, E.D. (1996). "Seawater corrosion behavior of laser surface modified Inconel 625 alloy". *Materials Science and Engineering A*, 206, 138-149.
- Dai, H.B., Liu, H.X., and Wang, F.H. (2006). *Journal of Surface and Coating Technology*, 201, 2859.
- Das, S., Joseph J. Beaman, Martin Wohler, and David L. Bourell. (1998). "Direct metal laser sintering for high performance metal components". *Rapid Prototyping Journal*, 4(7), 112-117.
- Dhar, S., Purohit, R., Saini, N., Sharma, A. and Kumar, G.H. (2007). "Mathematical modeling of electrical discharge machining of cast Al-4Cu-6Si alloy-10 wt. % SiC composites". *Journal of Materials Processing Technology*, 194, 1(3), 24-29.
- Dhingra, A.K. (1986). "Metal replacement by composite", *Journal of Materials*, 38(3), 17.
- Dimov, Pham,D.T., Lacan, and Dotchev, K.D. (2001). "Rapid toling applications of the selective laser sintering process". *Assembly Automation*, 21(4), 296-302.

Dinda, G. P., Dasgupta, A. K., and Mazumder, J. (2009). "Laser aided direct metal deposition of Inconel 625 superalloy: Microstructural evolution and thermal stability". *Materials Science and Engineering: A*, 509(1-2), 98-104.

Dotter, R.T. (1984). "Blending and premixing of metal powders". *Metals Handbook*, 9<sup>th</sup> edition, 7, Powder Metallurgy, 186-189.

Dwivedi, A., Kumar, P. and Singh, I. (2008). "Experimental investigation and optimisation in EDM of Al 6063 SiCp metal matrix composite". *International Journal of Machining and Machinability of Materials*, 3(3), 293–308.

Dwivedi, D. K. (2000). "Effect of cutting parameters and heat treatment on specific power consumption in machining En-31". *Transaction in Indian Institute of Metals*, 54(4), 539-543.

Exner, H.E. (1980). "Solid-state sintering: Critical assessment of theoretical concepts and experimental methods". *Powder Metall.*, 4, 203-209.

Fisher, P, Locher, M, Romano, Weber, Kolossov, and Glardon, R. (2004). "Temperature measurements during selective laser sintering of titanium powder". *International Journal of Machine Tools and Manufacture*, 44, 1293-1296.

Fouchal, F., and Dickens, P. (2007). "Adaptive screen printing for rapid manufacturing". *Rapid Prototyping Journal*, 13(5), 284-290

Gaard, A., Krakhmalev, P., and Bergstrom, J. (2006). "Micro structural characterization and wear behavior of Fe-Ni-TiC MMC prepared by DMLS". *J. of Alloys Comp*, 421, 166-171.

George, P.M., Raghunath, B.K., Manocha, L.M. and Warriar, A.M. (2004). "EDM machining of carbon-carbon composite—a Taguchi approach". *Journal of Materials Processing Technology*, 145(1), 66-71.

German, R.M. (1992). "Emerging P/M technologies in the USA". *Int. J. Powder Metall.*, 28, 77-85.

- Ghosh, S.K., and Saha, P. (2011). “Crack and wear behavior of SiC particulate reinforced aluminium based metal matrix composite fabricated by direct metal laser sintering process”. *Materials and Design*, 32, 139–145.
- Ghosh, S.K., Bandyopadhyay, K., Saha, P. (2014). “Development of an in-situ multi-component reinforced Al-based metal matrix composite by direct metal laser sintering technique—Optimization of process parameters”. *Materials Characterization*, 93, 68-78.
- Gopalakannan, S., Senthilvelan, T., and Ranganathan, S. (2012). “Modeling and optimization of EDM process parameters on machining of Al 7075-B<sub>4</sub>C MMC using RSM”. *Elsevier Procedia Engineering* 38, 685-690.
- Gu, D., and Shen, Y. (2006). “WC–Co particulate reinforcing Cu matrix composites produced by direct laser sintering”. *Materials Letters*, 60, 3664–3668.
- Gu, D., and Shen, Y. (2008). “Processing conditions and micro-structural features of porous 316L stainless steel components by DMLS”. *Appl. Surf. Sci.*, 255, 1880-1887.
- Gu, D., and Shen, Y. (2009). “Balling phenomena in direct laser sintering of SS powder: Metallurgical mechanisms and control methods”. *Materials and Design*, 30(8), 2903-2910.
- Gu, D., Chang, F., and Dai, D. (2015). “Selective laser melting additive manufacturing of novel aluminium based composites with multiple reinforcing phases”. *Journal of Manufacturing Science and Engineering*, 201-222, (DOI 10.1007/978-3-662-46089-4\_7).
- Gu, D., Shen, Y., Fang, S., and Xiao, J. (2007). “Metallurgical mechanisms in direct laser sintering of Cu–CuSn–CuP mixed powder”. *Journal of Alloys and Compounds*, 438, 184–189.
- Gu, D., Shen, Y., Lu, Z. (2009). “Microstructural characteristics and formation mechanism of direct laser-sintered Cu-based alloys reinforced with Ni particles”. *Materials and Design*, 30, 2099–2107.

Gu, D.D., Meiners, W., Wissenbach, K., and Poprawe, R. (2012). "Laser additive manufacturing of metallic components: materials, processes and mechanisms". *International Materials Reviews*, 57(3), 133-164.

Guo, Z.N., Wang, X., Huang, Z.G. and Yue, T.M. (2002). "Experimental investigation into shaping particle-reinforced materials by WEDM-HS". *Journal of Materials Processing Technology*, 129, 1-3, 56-59.

Hattali, M.L., Valette, S., Ropital, F., and Mesrati, N. (2009). "Study of SiC–nickel alloy bonding for high temperature applications". *Journal of the European Ceramic Society*, 29(4), 813-819.

Ho, K.H., Newman, S.T., Rahimifard, S. and Allen, R.D. (2004). "State of the art in wire electrical discharge machining (WEDM)". *International Journal of Machine Tools and Manufacture*, 44, 12-13, 1247-1259.

Hopkinson, N., and Dickens, P. (2001). "Rapid prototyping for direct manufacture", *Rapid Prototyping Journal*, 7(4), 197-202.

Ibrahim, I.A., Mohamed, F.A., and Lavernia, E.J. (1991). "Particulate reinforced MMCs- A review". *Journal of Material Science*, 26, 1137-1156.

Kang, M., Man, J., Kimb, Kima, J.W., Kimc, Y.K., Chungd, H., and Yiea, J.E. (2002). "Simple and fast microwave-enhanced wet etching of SiC particles for electroless Ni-P plating". *Journal of Surface and Coatings Technology*, 161, 79-85.

Kathiresan, M. and Sornakumar, T. (2010). "EDM studies on aluminium alloy-silicon carbide composites developed by vortex technique and pressure die casting". *Journal of Minerals and Materials Characterization and Engineering*, 9, 1, 79-88.

Khaing, M.W., Fuh, and Lu. (2001). *Journal of Material Processing Technology*, 113, 269-272.

Kim, G.D., and Oh, Y.T. (2008). "A benchmark study of rapid prototyping process and machine: Qualitative comparisons of mechanical properties, accuracy, roughness, speed and material cost". Proc. Int Mech Engg, 222, Part B, *Journal of Engineering*

*Manufacture*, 19-24.

Ko-Ta Chiang. (2008). "Modelling and analysis of the effects of machining parameters on the performance characteristics in the EDM process of Al<sub>2</sub>O<sub>3</sub>+TiC mixed ceramic". *International Journal of Advanced Manufacturing Technology*, 37, 523-533.

Kruth, J.P. (1991). "Material increase manufacturing by rapid prototyping techniques". *CIRP Annals*, 40(2) 603-614.

Kruth, J.P., Levy, Froyen, Rombouts, and Merckels. (2003). *Annals of CIRP*, 52, 139-142.

Kruth, J.P., Levy, Klocke, and Childs. (2007). "Consolidation phenomena in laser and powder-bed based layered manufacturing". *Annals of CIRP*, 56(2), 730-759.

Kruth, J.P., Peeters, Smolderen, Bonse, Laoul, and Froyen. (1998). "Comparison between CO<sub>2</sub> and Nd: YAG lasers for use with selective laser sintering of steel-copper powders". *Int. Journal of CAD/CAM and Computer Graphics*, 13(4-6), 95-110.

Kumar, S. (2009). "Manufacturing of WC-Co moulds using SLS machine". *Journal of Materials Processing Technology*, 209, 3840-3848.

Leon, C.A., and Drew, R.A.L. (2000). "Preparation of nickel-coated powders as precursors to reinforce MMC's". *Journal of Material Science*, 35, 4763-4768.

Levy, G.N., Ralf Schindel, and Kruth, J.P. (2003). "Rapid manufacturing and rapid tooling with layer manufacturing technologies, state of the art and future perspective". *Annals of the CIRP*, 52(2), 589-609.

Li, L., Li, Z.Y., Wei, X.T., and Cheng, X. (2015). "Machining characteristics of Inconel 718 by sinking-EDM and wire-EDM". *Materials and Manufacturing Processes*, 30(8), 968-973.

Li, X.C., Stampfl, Fritz, and Prinz. (2000). "Mechanical and thermal expansion behavior of laser deposited metal matrix composites of Invar and TiC". *Mater. Sci. Eng., A* 282, 86-90.

- Li, Y., Bai, P., Wang, Y., Hub,J., Guo, Z. (2009). “Effect of TiC content on Ni/TiC composites by direct laser fabrication”. *Materials and Design*, 30, 1409–1412.
- Liu, G. W., Muolo, M. L., Valenza, F., and Passerone, A. (2010). “Survey on wetting of SiC by molten metals”. *Ceramics International*, 36(4), 1177-1188.
- Lloyd Ploof. (2008). “Electroless nickel composite coatings”. *Journal of Advanced Materials and Processes*, 36-38.
- Majumdar, J.D.,Kumar,A., and Li.L. (2008). “Direct laser cladding of SiC dispersed AISI 316L stainless steel”. *Trib. Int.*, 42(5), 750-753.
- Manfredi, D., Calignano, F., Krishnan, M., Canali, R., Ambrosio, E.P., and Atzeni,E. (2013). “From powders to dense metal parts: Characterization of a commercial AlSiMg alloy processed through direct metal laser sintering”. *Materials*, 6, 856-869.
- Manfredi,D., Calignano,F., Ambrosio,E.P., Krishnan,M., Canali,R., Biamino,S., Pavese,M., Etzeni, Iuliano,L., Fino,P., and Badini, C. (2013). “Direct Metal Laser Sintering: an additive manufacturing technology ready to produce lightweight structural parts for robotic applications”. *La Metallurgia*, Italiana, 1-10.
- Manfredi,D., Calignano,F., Ambrosio,E.P., Krishnan,M., Canali,R., Biamino,S., Pavese,M., Etzeni, Iuliano,L., Fino,P., and Badini, C. (2014). “Additive Manufacturing of Al Alloys and Aluminium Matrix Composites”. <http://dx.doi.org/10.5772/58534>.
- Manikandan, R., and Venkatesan,R. (2012). “Optimizing the Machining Parameters of Micro-EDM for Inconel 718”, *Journal of Applied Sciences*, 12, 971-977.
- Maria Grazia Violante, Luca Iuliano and Paolo Minetola. (2007). “Design and production of fixtures for freeform components using selective laser sintering”. *Rapid Prototyping Journal*, 13(1), 30-37.
- McKimpson, M.G., and Scott,T.E. (1989). “Processing and properties of MMCs containing discontinuous reinforcement”. *Mat. Sci. and Engg.*, 107A, 93-106.
- Miracle, D.B. (2005). “Metal matrix composites-From science to technological significance”. *Composites Science and Technology*, 65, 2526-2540.



- Moakher, M., Fernando, and Muzzio. (2000). "Experimentally validated computations of flow, mixing and segregation of non-cohesive grains in 3D tumbling blenders". *Powder Technol.*, 109, 58-71.
- Mognol, P, Rivette, Fegou and Lesprier, T. (2006). "A first approach to choose between HSM, EDM and DMLS processes in hybrid rapid tooling". *Int. Journal of Manufacturing Technology*, 29, 35-40.
- Muller, F. and Monaghan, J. (2000). "Non-conventional machining of particle reinforced metal matrix composite". *International Journal of Machine Tools and Manufacture*, 40(9), 1351-1366.
- Murali, K., Saha, P., Roy, S.K., and Kumar, S. (2004). "Direct laser sintering of iron-graphite powder mixture". *J. Mater. Processing Tech*, 136, 179-185.
- Murali, K., Chatterjee, A.N., Sahaa, H., Palaia, R., Kumar, S., Roy, S.K., Mishra, S., Roy Choudhury, A. (2003). "Direct selective laser sintering of iron-graphite powder mixture". *Journal of Materials Processing Technology*, 179-185.
- Muthamara, A., Janmanee, P. and Fukuzawa, Y. (2010). "A study of micro-EDM on silicon nitride using electrode materials". *International Transaction Journal of Engineering, Management and Applied Sciences and Technologies*, 1(1), 1-7.
- Nanimina, A.M., Abdul-Rani, A.M., Ahmad, F., Zainnuddin, A. and Lo, S.H.J. (2011). "Effects of electro-discharge machining on aluminum metal matrix composite", *Journal of Applied Sciences*, 11(9), 1668-1672.
- Niu, H.J., and Chang. (1999). "Selective laser sintering of gas and water atomised high speed steel powders". *Scr. Mater.*, 41(1), 25-30.
- Niu, H.J., and Chang. (2000). "Selective laser sintering of gas atomized M2 high speed steel powder". *J. Mater. Sci.*, 35, 31-38.
- Ozben, T., E.Kilickap, and O.Cakir. (2008): "Investigation of mechanical and machinability properties of SiC particle reinforced Al-MMC". *J. Mater. Process. Technol.*, 198, 220-225.

- Ozgun, O., Gulsoy, Yilmaz, R., Findik, F., (2013). "Injection molding of nickel based 625 superalloy: Sintering, heat treatment, microstructure and mechanical properties". *Journal of Alloys and Compounds*, 546, 192–207.
- Ozols, A., Pagnola, M., and Sirkin, H. (2006). *Journal of Surface and Coating Technology*, 200, 6821.
- Parveen Kumar Saini, Gurkirat Singh, and Taljeet Singh. (2014). "Study the Effect of Process Variables on Cutting Velocity during WEDM of Al/ZrO<sub>2</sub>-MMC". *International Journal of Engineering Science Invention Research & Development*, 1(4).
- Paul, B.K., and Voorakarnam, V. (2001). "Effect of layer thickness and orientation angle on surface roughness in laminated object manufacturing". *Journal of Manufacturing Processes*, 3, 2.
- Paul, C. P., Ganesh, P., Mishra, S. K., Bhargava, P., Negi, J., and Nath, A. K. (2007). "Investigating laser rapid manufacturing for Inconel-625 components". *Optics & Laser Technology*, 39(4), 800-805.
- Pham, D.T., and S.S.Dimov. (2001). "Rapid Manufacturing: The Technologies and Applications of Rapid Prototyping and Rapid Tooling". *Springer*, London.
- Planson, D., Locatelli, and Lanois. (1999). *Journal of Material Science Engineering B.*, 61(62), 497.
- Pogson, S.R., Fox, P., Sutcliffe, C.J., and Neill, W.O. (2003). "The production of copper parts using DMLS". *Rapid Prototyping Journal*, 9(5), 334-343.
- Powell, R.A. (1983). "Powder metallurgy; the age of maturity". *Design News*, 30(12), 41-50.
- Priyaranjan Sharma, P., Chakradhar, D., Narendranath, S. (2015). "Evaluation of WEDM performance characteristics of Inconel 706 for turbine disk application". *Materials & Design*. DOI:10.1016/j.matdes.2015.09.036.
- Rack, H.J. (1990). "Metal matrix composites". *Adv. Mater. Processes*, 137 (1), 37-39.

- Ramesh, C.S. (2009). "Microstructure and mechanical properties of NiP coated Si<sub>3</sub>N<sub>4</sub> reinforced Al6061 composites". *Material Science and Engineering: A*, 2, 25.
- Ramesh, C.S., Srinivas, Channabasappa, (2009). "Abrasive wear behaviour of laser sintered iron–SiC composites". *Wear*, 267, 1777–1783.
- Rodge, M. K., Sarpate, S. S., Sharma, S. B. (2013). "Investigation on Process Response and Parameters in Wire Electrical Discharge Machining of Inconel 625". *International Journal of Mechanical Engineering and Technology*, 4(1).
- Rossia, S., Defloriana, F., Venturini, F. (2004). "Improvement of surface finishing and corrosion resistance of prototypes produced by direct metal laser sintering". *Journal of Materials Processing Technology*, 148 301–309.
- Rozenek, M., Kozak, J., Dabrowski, L. and Lubkowski, K. (2001). "Electrical discharge machining characteristics of metal matrix composites". *Journal of Materials Processing Technology*, 109(3) 367-370.
- Ruffo, M, Tuck and Hague. (2007). "Make or buy analysis for rapid manufacturing", *Rapid Prototyping Journal*, 13(1), 23-29.
- Schwartz, M.M. (1984). "Composite materials handbook". (Eds.) B. Harold, Crawford, Elizabeth Richardson, *McGraw-Hill Book Company*, New York.
- Shellabear, M and Nyrhila, O. (2007). "Advances in materials and properties of direct metal laser-sintered parts". Paper presented in *LANE* conference.
- Simchi, A. (2006). "Direct Laser Sintering of metal powders: Mechanism, kinetics and microstructural features". *Mater. Sci. Eng. A*, 428, 148-158.
- Simchi, A., (2004). "The role of particle size on the laser sintering of iron powder". *Metallurgical and Materials Transactions B*, 35B, 937.
- Simchi, A., (2010). "Densification and microstructural evolution during co-sintering of Ni-base superalloy powders". *Metallurgical and Materials Transactions A*, 37 A, 2549-2557.

Simchi, A., and Asgharzadeh. (2004). "Densification and micro-structural evaluation during laser sintering of M2 high speed steel powder". *Mater. Sci. Technol.*, 20(11), 1462-1468.

Simchi, A., and Godlinski. (2008). "Effect of SiC particles on the laser sintering Al-7Si-0.3 Mg alloy". *Scr. Mater.*, 59, 199-202.

Simchi, A., and Pohl, H. (2003). "Effects of laser sintering processing parameters on the microstructure and densification of iron powder". *Materials and Engineering A* 359, 119-128.

Simchi, A., Petzoldt, and Pohl. (2001). "Direct metal laser sintering: Material considerations and mechanisms of particle bonding". *International Journal of Powder Metallurgy*, 37(2) 49-61.

Simchi, A., Petzoldt, F., Pohl, H., (2003). "On the development of direct metal laser sintering for rapid tooling. *Journal of Materials Processing Technology*, 141, 319–328.

Singh, G., Vohra,H., and Kaur,M. (2012). "Fabrication and Characterization of Aluminium Matrix Composites by High Velocity Oxy-Fuel Thermal Spraying". *Advanced Materials Research*, 585, 317-321.

Singh, H., Jit, N., Anand, K.T. (2014). "An overview of metal matrix composite: Processing and SiC based mechanical properties". *Chemical Business*, 28(2), 45.

Singh, P.N., Raghukandan, K., Rathinasabapathi, M. and Pai, B.C. (2004). "Electric discharge machining of Al-10%SiC as-cast metal matrix composites". *Journal of Materials Processing Technology*, 155-156, 1-3, 1653-1657.

Singh,S., Singh,R., and Singh, G. (2014). "Development of Aluminium MMC with hybrid reinforcement - A review", *Materials Science Forum*, 808,109-119.

Song, Y.A. (1997). "Experimental study of the basic process mechanism for direct selective laser sintering of low-melting metallic powder". *Annals of CIRP*, 45(1), 127-130.

- Srinivasa, C.K. (2009). "Friction and wear behavior of iron-silicon carbide composites". *Journal of Materials Processing Technology*, 5429-5436.
- Srinivasa, C.K. (2010). "Blending of iron and silicon carbide powders for producing metal matrix composites by laser sintering process". *Journal of Rapid prototyping*, 16(4), 258-267.
- Srinivasa,K., Vinod, R., and Shashikumar, P.V. (2012). "Machinability studies on laser sintered iron-silicon carbide MMCs using wire electrical discharge machining". *International Journal of Materials and Product Technology*, 43, 68-82.
- Storch, S., Nellessen, Schaefer, and Reiter. (2003). "Selective laser sintering: qualifying analysis of metal based powder systems for automotive applications". *Rapid Prototyping Journal*, 9(4), 240-251.
- Stucker, B. (2006). "Additive manufacturing technologies". *Springer*.
- Tan, X. Ren, K. Sridharan, T.R. Allen. (2008). "Corrosion behavior of Ni-base alloys for advanced high temperature water-cooled nuclear plants". *Corrosion Science*, 50, 3056–3062.
- Taya, M., and Arsenault,R.J. (1989). "Metal matrix composites–Thermo mechanical behaviour". New York, *Pergmon Press*, 238-243.
- Tiwari,R., Herman,H., Kowalsky.K., and Marantz,D.R. (1990). "Mechanical behaviour of thermal sprayed metal matrix composites". High performance composites for the 1990's, *TMS-New Jersey*, 195.
- Tuan, W.H., Wu, and Yang. (1995). *Journal of Material Science*, 30, 855.
- Upadhya, K. (1992). "Composite materials for aerospace applications, developments in ceramic and metal matrix composites". Kamaleshwar Upadhya, PA:*TMS publications*, 3-24.
- Urquhart, A.W. (1991). "Molten metals sire MMCs, CMCs". *Adv. Mater. Processes*, 140 (7), 25-29.

- Valente, T., and Galliano, F.P. (2000). "Corrosion resistance properties of reactive plasma-sprayed titanium composite coatings". *Surface Coating Technology*, 127, 86-92.
- Vaucher, S., Paraschivescu, Andre, and Beffort. (2002). "Selective laser sintering of aluminium- silicon carbide metal matrix composites". *Materials Week, ICM-Munich*, 30<sup>th</sup> Sep-10<sup>th</sup> Oct, (ISBN3-88355-314-X).
- Whittmore, O.J., and Varela, J.A. (1987). " Pore growth and shrinkage during sintering". 4<sup>th</sup> International Symposium on Science and Technology of Sintering, Tokyo, Japan, 4-6, November.
- Williams, J.D., and Carl R. Deckard. (1998). "Advances in modelling the effects of selecting parameters on the SLS process". *Rapid Prototyping Journal*, 4(2), 90-100.
- Wilson, M.J., and Shin, Y.C., (2012). "Microstructure and wear properties of laser deposited functionally graded Inconel 690 reinforced with TiC". *Surface and Coatings Technology*, 207,517-522.
- Yadroitsev, I., Bertrand, and Smurov. (2007). "Parametric analysis of the selective laser melting process". *Appl. Surf. Sci.*, 253, 8064-8069.
- Yan, B.H., Tsai, H.C., Huang, F.Y. and Lee, L.C. (2005). "Examination of wire electrical discharge machining of Al<sub>2</sub>O<sub>3</sub>/6061 Al composites". *International Journal of Machine Tools and Manufacture*, 45, 3, 251-259.
- Yao,H., Zhu,G.L., and Wang,Y.Z. (2011). "Preparation of Ni-Coated SiC Ceramic Composite Powder by Electroless Plating". *Applied Mechanics and Materials*, 117-119, 77-80.
- Yilbas, B.S., Khaled,M., and Gondal, M.A., (2001). "Electrochemical response of laser surface melted inconel 617 alloy". *Optics and Lasers in Engineering* 36, 269–276.
- Zahrani, M.E., Alfantazi, A.M. (2012). "Molten salt induced corrosion of Inconel 625 superalloy in PbSO<sub>4</sub>–Pb<sub>3</sub>O<sub>4</sub>–PbCl<sub>2</sub>–Fe<sub>2</sub>O<sub>3</sub>–Z". *Corrosion Science*, 65, 340–359.
- Zhan, Y., and Zhang, G. (2003). "The effect of interfacial modifying on the mechanical and wear properties of Cu/SiC composites". *Material Letters*, 57, 4583-4591.

Zhang, Y., Xi, M., Gao, S., and Shi, L., (2003). "Characterization of laser direct deposited metallic parts". *Journal of Materials Processing Technology*, 142, 582–585.

Zheng, B., Topping, T., Smugeresky, J.E., Zhou, Y., Biswas, A., Baker, D., and Lavernia, E.J., (2010). "The influence of Ni-coated TiC on laser-deposited Inconel-625 metal matrix composites". *Metallurgical and Materials Transactions A*, 41A, 568-573.

Zhu, H.H. (2005). "Micro-structural evolution in direct laser sintering of Cu-based metal powder". *Rapid Prototyping Journal*, 11(2), 64-71.

Zhu, S.M., Wang, L., Li, G.B., and Tjong, S.C., (1995). "Laser surface alloying of Incoloy 800H with silicon carbide: Microstructural aspects". *Materials Science and Engineering A*, 201, L5-L7.

Zou, G., Cao, M., Jin, H., Kang, Y., and Chen, Y. (2006). "Nickel layer deposition on SiC nano particles by simple electroless plating and its dielectric behaviours". *Journal of Powder Technology*, 168, 84-88.

## PUBLICATIONS

### INTERNATIONAL JOURNALS

- 1) Sateesh, N.H., Mohankumar, G.C., and Prasad Krishna, (2015): “Influence of Ni-P Coated SiC and Laser Scan Speed on Microstructure and Mechanical Properties of IN625 Metal Matrix Composites”, *Lasers in Manufacturing and Materials Processing, Springer Publications (Published)*. (DOI 10.1007/s40516-015-0014-3).
- 2) Sateesh, N.H., Mohankumar, G.C., and Prasad Krishna, (2014): “Effect of Heat Treatment on Coated Ceramics for Composite Formation by Laser Processing” *International Journal of Advances in Engineering Sciences*, 4(4), 14-18.
- 3) Sateesh, N.H., Mohankumar, G.C., and Prasad Krishna, (2014): “Effect of Process Parameters on Surface Roughness of Laser Sintered Inconel Superalloy”, *International Journal of Engineering and Scientific Research*, 5 (8), 232-236.
- 4) Sateesh, N.H., Mohankumar, G.C., and Prasad Krishna, (2015): “Effect of Process Parameters on Microstructure, Density, Micro-hardness and Surface Roughness of Laser Processed Inconel-625 Superalloy Composites”, *Ciencia E Tecnica.Vitivinicola, A Science and Technology Journal*, (Under Review).

### INTERNATIONAL CONFERENCE

- 1) Sateesh, N.H., Mohankumar, G.C., Prasad Krishna, Srinivasa, C.K., and Vinod, A.R., (2014): “Microstructure and Mechanical Characterization of Laser Sintered Inconel-625 Superalloy”, *Elsevier Procedia Material Science*, 5 (2014) 772–779, *International Conference on Advances in Manufacturing and Materials Engineering*, NITK, Surathkal, Karnataka, India.
- 2) Sateesh, N.H., Mohankumar, G.C., and Prasad Krishna, (2014): “Surface Roughness Studies on Laser Sintered Inconel-625”, *International Conference on Industrial, Mechanical and Production Engineering: Advancements and Current Trends*, MANIT, Bhopal, Madhya Pradesh, India.



## ACADEMIC CURRICULUM VITAE

<b>1. Name and Designation</b>	: <b>N. H. SATEESH,</b> Selection Grade Lecturer,
<b>2. Address for Communication</b>	: Veerabhadraswamy Nilaya, 10 <sup>th</sup> 'A' Cross, Gangothri Road, Gangothri Nagara, S.I.T. Extn., TUMKUR-572103 <b>Email:</b> <a href="mailto:sateeshnijagal@gmail.com">sateeshnijagal@gmail.com</a>
<b>3. Date of Birth</b>	: 1-05-1976
<b>4. Department (Organisation)</b>	: Department of Technical Education, Bangalore
<b>5. Field of Specialisation</b>	: Mechanical Engineering (G), Machine Design, Advanced Manufacturing

### 6. Academic Qualifications:

Degree	University / Institution	Division / Equivalent	Year	Specialisation
B.E. (Mech.)	Siddaganga Institute of Technology, Tumkur	Distinction	1997	Mechanical Engineering
M.E.	U.V.C.E, Bangalore	I	2006	Machine Design
Ph.D. (Pursuing under QIP-Poly)	N.I.T.K, Surathkal	Course Work – CGPA-8.75 Thesis on 'Processing and Characterization of Inconel 625-SiC Metal Matrix Composites by Direct Metal Laser Sintering'		

### 7. Academic Experience:

Sl. No.	Institution / Department	Period of Service	Designation
1	Govt. Polytechnic, Tumakuru.	Aug 2001 to Jul 2006	Lecturer
2	Govt. Polytechnic, Tumakuru.	Aug 2006 to Jul-17 2011	Senior Grade Lecturer
3	S.J.(Govt.) Polytechnic, Bengaluru	Jul-18 2011 to Aug 2011	Senior Grade Lecturer
4	S.J.(Govt.) Polytechnic, Bengaluru	Aug 2011 to Jul-17 2013	Selection Grade Lecturer
5	Karnataka (Govt.) Polytechnic, Mangaluru	Jul-18 2013 to Till date	Selection Grade Lecturer

I hereby declare that the entries in this Academic Curriculum Vitae are true to the best of my knowledge and belief.

Date:

Place: NITK, SURATHKAL

(N. H. SATEESH)